

Structural, Conformational and Reactivity studies on DNA
base pairs and Phospholipids using Density Functional
Theory (DFT)

Thesis Submitted to AcSIR For the Award of
the Degree of

DOCTOR OF PHILOSOPHY
In Chemistry



By

Deepti Mishra

Registration Number: 10CC13J26026

Under the guidance of

Dr. Sourav Pal

CSIR- National Chemical Laboratory

DECLARATION BY RESEARCH SCHOLAR

I hereby declare that the work incorporated in this thesis entitled **“Structural, Conformational and Reactivity studies on DNA base pairs and Phospholipids using Density Functional Theory (DFT)”** submitted by me for the degree of Doctor of Philosophy to the AcSIR is the record of the work I have carried out at the Physical Chemistry Division, National Chemical Laboratory, Pune – 411 008 from April 2011 to December 2013 under the supervision of Dr. Sourav Pal, is original and has not formed the basis of award of any degree or diploma. Such material as has been obtained from other sources has been duly acknowledged in this thesis.

Date:

Deepti Mishra

Physical Chemistry Division

CSIR- National Chemical Laboratory

Pune-411008

CERTIFICATE BY RESEARCH GUIDE

This is to certify that the work presented in the thesis entitled “Structural, Conformational and Reactivity studies on DNA base pairs and Phospholipids using Density Functional Theory (DFT)” by **DEEPTI MISHRA**, submitted for the degree of **Doctor of Philosophy in Chemistry** was carried out under our supervision at the Physical Chemistry Division, National Chemical Laboratory, Pune, 411008, India. All the materials from other sources have been duly acknowledged in the thesis.

Dr. Sourav Pal

(Research Guide)

Dr. Sailaja Krishnamurthy

(Research co-Guide)

Date:

Place: Physical and Materials Chemistry Division

CSIR- National Chemical Laboratory

Pune- 411008

Dedicated to

*My dear father and my beloved
husband*



For Sir

**Gururbrahma Gururvishnu: Gururdevo Maheshwara:
Gurussakshat Parabrahma Tasmai Shreegurave Nama:**

Acknowledgement

“My acknowledgement is a personal expression of self and soul in which my heartfelt thanks is given to all that I am grateful for receiving - into my life.”

~ Eleesha

I would like to express my deepest gratitude to my advisor, Dr. Sourav Pal, who has supported me throughout my thesis with patience and guided me by his immense knowledge. I thank him for allowing and giving me opportunity to work independently and add value to the research work. I was strongly motivated by his inspiring classroom lectures. I thank him for his ‘freedom to work’ attitude. Apart from the scientific discussions, we used to debate on many issues during the tea time. I learnt a lot from him. He has been a fantastic adviser, who taught me how to do research in an individualistic way. It is my great pleasure to thank my research guide, Dr. Pal for giving me opportunity to join his lab in NCL. I really appreciate his way of imagining things and his good sense of humour.

I owe a special debt to my co-supervisor Dr. Sailaja Krishnamurty for introducing me to the field of ab initio molecular dynamics. I thank Sailaja for her sincere and continuous support throughout my doctoral studies. It has been really fun to learn shell scripting, software installation under her guidance. I must acknowledge Sailaja for the enriching discussions which helped improve the quality of my work on many an occasion. I will always remember a conversation during which she said that science should be a passion and not a profession.

I am obliged to Director, NCL for providing me the infrastructure to carry out the work presented in this thesis. I am grateful to Indo-French project funding for my earlier Fellowship and also CSIR for awarding me the direct Senior Research Fellowship. I am thankful to DST for providing the timely financial

support to participate in X Girona Seminar. I cannot forget the Dept. of Bioinformatics Banasthali Vidyapith, where I took my first lessons in the field of research.

The present thesis work would have been difficult without the association of my labmates in NCL. I am really thankful to Dr. Nayana Vaval with whom I am most comfortable in lab. I always used to discuss my all problems and I always used to get the best solution from her. I can never forget her emotional support during these years. She will be there always in a list of my very good friends. I also had the fortune of interacting with the new scientists of our thriving group: Dr. Kumar Vanka, Dr. Neelanjana Sengupta, and Dr. Sudip Roy. My thanks go to my seniors Dr. Akhilesh and Dr. Prashant, for helping me with the basic computational chemistry and making me comfortable with basic linux commands during the initial phase of my research. Special thanks go to Rahul da, Saikat, Arijit da, Sumantra da, Tuhina, Himadri da and Bhakti for making me very comfortable in the group and treating me more as a friend than as a junior. Among my seniors Lallu and Subbu da owe special thanks for being very good friend and making me understand of what is right and what is wrong in life. The next cluster of names contains my batch mates and juniors. I had fun of attending course work with Sapna, Jitendera and Mudit. Sapna used to share her knowledge of chemistry for making me understand the basics. I had fun moments with all my juniors Sayali, Debarati, Achintya, Arya, Susanta, Kamalika, Anagha Manzoor, chotu Himadri, Turbasu, Sudip and Deepak. My special thanks goes to Sayali who was always helpful to me and without giving second thought I can always ask for any kind of help. During last year of my research I met Vidhika and Madhulita and we used to have fun time in my SA while cooking and watching TV serials. I should not forget to thank students in computer room Prathit (pandit ji), Jaya, Manoj, Jugal, Nisha, Sneha, Shantanu, Yuvraj, Amrita and Mrityunjay by making me comfortable in computer room while cracking jokes.

Apart from my labmates I earn three very good friends like Meenal, Rani and Swapna di. I can never forget their support and help and making me so comfortable in a new state by teaching Marathi.

I am very lucky to get kind and unwavering support from my both families. My in laws were always supporting these years and never gave any social and family

responsibility which can divert my interest from research. My parents made tremendous sacrifices to ensure that I had good education. I thank my Mommy and Daddy for your seamless patience, words of wisdom, and the independence that you have given me since my childhood. I also acknowledge my grandfather for his encouragement to complete this higher education. I thank my elder and younger brothers Rohit and Mohit for their sincere concern and good counsel. I should not forget to thank my sister in law Rashmi and my niece Tiya. Gratefully, I thank my husband, Atul, for understanding the importance that this Ph.D. holds for me, for motivating me in this crucial period of degree, for appreciating my aspirations, and for his unconditional encouragement and adjustments. I dedicate this thesis to my daddy and my beloved husband Atul. For this and more, I am forever in their debt. Atul you and our baby have been my inspiration in whatever I have done and achieved till now.

Date:

Deepti Mishra

Contents

	List of abbreviations	xi
	List of publications	xiv
	Abstract	xvi
1	Introduction	1
1.0	Introduction	1
1.1	Outline of the problem	4
1.2	Structural overview of Phospholipids	6
1.3	Structural overview of DNA bases and base pairs	12
1.4	Experimental and Theoretical Investigation on Structure and Conformation of a Phospholipid Molecule: A literature survey	14
1.5	Experimental and Theoretical Investigation on Structure, Reactivity of DNA base pairs: A literature survey	19
1.6	Scope of the thesis	22
1.7	Organization of the thesis	23
1.8	References	27
2	Theoretical Methods and Computational Details	35
2.1	The many-body problem	37
2.1.1	Born-Oppenheimer approximation	37
2.1.2	Hartree approximation	38

2.1.3	Hartree-Fock approximation	39
2.1.4	Beyond Hartree-Fock (Correlation energy)	41
2.2	Density functional theory	41
2.2.1	Thomas-Fermi theory	42
2.2.2	Hohenberg-Kohn theorems	43
2.2.3	Kohn-Sham equations	44
2.2.4.	Exchange-correlation functional	47
2.3.	Density based reactivity descriptors: Conceptual DFT	48
2.3.1	Local Reactivity Descriptors (LRDs)	50
2.3.3	HOMO-LUMO analysis	52
2.3.4	Pearson's definitions of Hardness and Softness	53
2.4.	Molecular Dynamics	54
2.4.1	Classical Molecular Dynamics	54
2.4.2	<i>Ab Initio</i> molecular dynamics	56
2.4.3	Parameter for analysis of BOMD trajectories	57
2.5	References	59
3	Molecular Conformations of Na-DiMyristoyl Phosphatidyl Glycerol (DMPG)	63
3.1	Introduction	65
3.2	Methodology: Conformational and Computational Details	69
3.3	Results and discussion	73
3.3.1	Conformational analysis of a DMPG molecule	73
3.3.2	Structural aspects, electronic properties of the lowest ten DMPG molecular conformations and their comparison with	80

	conformations in a single crystal	
3.3.3	Conformational Analysis in the presence of water molecules and hydration energy	91
3.4	Conclusions	95
3.5	Reference	96
4	Understanding the orientation of water molecules around the phosphate and attached functional groups in a phospholipid molecule	100
4.1	Introduction	102
4.2	Local Reactivity Descriptors	106
4.3	Methods and Computational Details	109
4.4	Results and Discussion	112
4.4.1	Hydration behaviour of neutral head groups	115
4.4.2	Hydration behaviour of charged head groups	127
4.4.3	Prediction of Hydration sites using Local Reactivity Descriptors	133
4.5	Conclusion	138
4.6	References	140
5	Ionization Potential and Structure Relaxation of Adenine, Thymine, Guanine and Cytosine Bases and Their Base Pairs: A quantification of reactive sites	146
5.1	Introduction	148
5.2	Theoretical Background	151
5.3	Computational Details	153

5.4	Results and Discussion	154
5.4.1	Geometry	154
5.4.2	Reactivity study of nucleobases and base pairs	158
5.4.3	Electron density of the base and base pair cations radical	164
5.5	Conclusion	167
5.6	References	168
6.	Role of Substituents on the Reactivity and Electron Density	173
	Profile of Diimine Ligands	
6.1	Introduction	175
6.2	Theoretical Background	178
6.3	Computational Details	182
6.4.	Discussion	185
6.4.1.	Global reactivity	185
6.4.2	Intra and inter-molecular reactivity trend	188
6.4.3.	Electron density analysis	196
6.4.4.	Reaction energies for Ru-ligand interaction	198
6.5.	Conclusion	202
6.6	References	204
7.	Conformational Specific Phospholipid Tail Dynamics	
	of anionic DMPG (dimyristoyl Phosphatidyl Glycerol)	210
	Molecule: Conclusions and Future Scope	
7.1.	Introduction	212
7.2.	Methodology and Computational Details	215
7.3.	Results and Discussion	217

7.3.1. Overall structural changes	217
7.3.2. Disorder parameter for the alkyl chains	221
7.4. Conclusion and Future Scope	222
7.5. References	223

List of Abbreviations

The following abbreviations, in alphabetical order, that have been used in this thesis:

AIMD	<i>Ab initio</i> molecular dynamics
BOMD	Born-Oppenheimer molecular dynamics
CPMD	Car-Parrinello molecular dynamics
DFT	Density functional theory
DMPC	Dimyristoyl Phosphatidyl Choline
DMPE	Dimyristoyl Phosphatidyl Ethanolamine
DMPG	Dimyristoyl Phosphatidyl Glycerol
DNA	Deoxyribose Nucleic Acid
FF	Fukui Function
FMO	Frontier Molecular Orbitals
GAMESS	General Atomic Molecular and Electronic Structural System
GGA	Generalized gradient approximation
HF	Hartree-Fock
HK	Hohenberg-Kohn
HOMO	Highest Occupied Molecular Orbital
KS	Kohn-Sham
LDA	Local density approximation
LUMO	Lowest Occupied Molecular Orbital
MD	Molecular dynamics
MOT	Molecular Orbital Theory
MP	Møller-Plesset
PES	Potential Energy Surface
RMS-BLF	Root mean square-Bond length fluctuations

List of Publications

This thesis is based on the following papers, which are referred to in the text by their Roman numerals:

- I. **Deepti Mishra** and Sourav Pal* (2009) Ionization potential and structure relaxation of adenine, thymine, guanine and cytosine bases and their base pairs: A quantification of reactive sites. *Journal of Molecular Structure: THEOCHEM* 902, 96–102
- II. **Deepti Mishra**, Sailaja Krishnamurthy* and Sourav Pal* (2011) Understanding Molecular Conformations of Na-DiMyristoyl-PhosphatidylGlycerol (DMPG) Using DFT based method *Molecular Simulation* Vol 37, Issue 11, 953-963.
- III. **Deepti Mishra**, Susanta Das, Sailaja Krishnamurthy* and Sourav Pal* (2013) Understanding the orientation of water molecules around the phosphate and attached functional groups in a phospholipid molecule: A DFT based study. *Molecular Simulation*, 39, 937-955.
- IV. Bhakti S Kulkarni, **Deepti Mishra** and Sourav Pal* (2013) Role of substituents on the reactivity and electron density profile of diimine ligands: A density functional theory based study. *Journal Of Chemical Sciences*, 125, 1247–1258.
- V. **Deepti Mishra**, Sailaja Krishnamurthy and Sourav Pal. Conformational Specific Phospholipid Tail Dynamics of anionic DMPG (dimyristoyl Phosphatidyl Glycerol) Molecule. Manuscript under preparation.

The following papers are co-authored by me but are not included in this thesis:

- Himadri Sekhar De, Sailaja Krishnamurty, **Deepti Mishra**, and Sourav Pal* (2011) Finite Temperature Behavior of Gas Phase Neutral Au_n ($3 \leq n \leq 10$) Clusters: A First Principles Investigation *J. Phys. Chem. C*, 115 (35), pp 17278–17285.
- Gowri Priya , Amol S. Kotmale , Rupesh L. Gawade , **Deepti Mishra** , Sourav Pal , Vedavadi G. Puranik , Pattuparambil R. Rajamohanan and Gangadhar J. Sanjayan* (2012) Helical folding in heterogeneous foldamers without inter-residual backbone hydrogen-bonding. *Chem. Commun.*, 48, 8922-8924.

Abstract

Several domains of modern computational science are converging on complex problems in the general field of systems biology. Predicting the properties and behaviour of complex biological systems by computer simulation from a fundamental, *ab initio* perspective has long been a vision of computational scientists. While methods for high level quantum mechanical (QM) calculations have been developed and proven to be very successful in calculating energies, equilibrium structures, vibrational frequencies, and more properties of small to medium sized molecules, the computational resources required for very large systems (e.g. a protein of many hundreds of atoms) is usually unattainable [1-3]. For these very large systems, more approximate modelling tools are often used such as molecular mechanics [4-5]. These more approximate methods greatly accelerate the speed at which energy calculations are performed, but they do not explicitly account for electronic structure. This can be a disadvantage, because there is a significant amount of information encoded in the electronic structure of a system. The understanding of structure of biomolecules at electronic level helps certainly in answering the conformational behaviour which is occurring mainly due to the electrostatic interactions at the molecular level.

Among the various bio molecules phospholipids are important components of biological membranes, and in order to understand the specific roles of different phospholipids for membrane structure and function, a detailed structural knowledge of the membrane constituents is necessary, particularly concerning the conformation and interactions of the polar lipid head groups at the

membrane surface. Molecular conformation dominating a bilayer is thus an outcome of balance of all these forces within and between the molecules. A complete insight about all these forces and hence their role in stabilizing various conformations is best obtained from a Quantum Mechanical (QM) methodology. The thesis work is organized in seven chapters including introduction. The chapter wise brief overview of the thesis is as follows:

Chapter 1 explains the detail structure and literature survey (Experimental and theoretical investigation) of both phospholipid molecule and DNA base pairs. The main and primary objectives of the thesis have been discussed in this chapter and these are:

- i. Characterisation of the conformational and structural landscapes of model biomolecules viz. DNA base pairs and phospholipids.
- ii. Characterisation of the balance of molecular interactions which govern their structures, particularly in hydrated environments.

At the end of the chapter the scope of the entire thesis is also discussed.

Chapter 2: This chapter is focussed to elaborate some of the theoretical approaches used to study the same. The methodology used in both cases is based on Density Functional Theory. Later, we also discuss the AIMD technique based on the DFT, to study the effect of temperature on single phospholipid molecule with various conformations. Finding the ground state geometry and the associated electrostatics with various bio molecules have been a central goal of many researchers. Both these methodologies will be elaborated in this chapter.

Chapter 3: In this chapter, we attempt to understand the various possible conformations available for an anionic lipid molecule DiMyristoyl-PhosphatidylGlycerol (DMPG) with Na as its charge compensating cation. Our study reveals a rich conformational space with two different types of glycerol body orientations, more commonly known as rotamers. We demonstrate that these conformations are an outcome of delicate balance of electrostatic and van der Waals forces along with intramolecular hydrogen bonds achieved by a critical combination of torsion angles.

Chapter 4: The adsorption of water molecules around a polar region (in particular around the phosphate moiety) in the phospholipid molecules is studied in this chapter. Phospholipid molecules with different functional groups are known to respond in varying fashion to the water molecules. The adsorption sites for water molecules are validated by density functional theory based reactivity descriptors viz., Fukui functions in PE model system.

Chapter 5: This chapter deals with Density Functional Theory (DFT) calculations to show relaxation in geometry of base pairs on cation radical formation. The changes in hydrogen bond length and angles show that in the cationic radical form the structure of the base pairs relaxes due to the distribution of charge. The reactive sites of bases have been analyzed using condensed Fukui functions in a relaxed and frozen core approximation. The effects of relaxation on the reactivity indices are also analyzed.

Chapter 6: In this chapter, we study the reactivity of diimines like 2, 2'-bipyridine, 1, 10-phenanthroline and 1, 2, 4-triazines using density based reactivity descriptors. We discuss the enhancement or diminution in the reactivity of these ligands as a function of two substituent groups, namely methyl (-CH₃) group and phenyl (-C₆H₅) group. In addition, the possible strength of interaction

of these ligands with metal ion is supported with actual reaction energies of Ru-L complexes.

Chapter 7: The last chapter of the thesis includes the Born Oppenheimer Molecular Dynamics of a DMPG (dimyristoyl Phosphatidyl Glycerol) phospholipid molecule having two different conformations. The present part of work has been dedicated to understand the melting process of the individual anionic phospholipid molecule, however with the preliminary results we cannot conclude anything about the melting and hence extend this chapter for our future work.

References

- [1] Szabo A, Ostlund NS. Modern Quantum Chemistry: Introduction to Advanced Electronic Structure Theory. 1st ed. Vol. 1. Dover Publications; Mineola, N.Y.: 1996. The Hartree Fock Approximation. pp. 108.
- [2] Levine IN. Quantum Chemistry. 6th ed. Vol. 1. Prentice Hall; Upper Saddle River, N.J.: 2008. Ab initio and Density Functional Treatments of Molecules. pp. 480.
- [3] Jensen F. Introduction to Computational Chemistry. 2nd ed. Vol. 1. Wiley; Chichester, England: 2006. Electronic Structure Methods: Independent-Particle Models. pp. 80.
- [4] Cramer CJ. Essentials of Computational Chemistry: Theories and Models. 2nd ed. Vol. 1. Wiley; Chichester, England: 2004. Molecular Mechanics. pp. 17.
- [5] Leach A. Molecular Modelling: Principles and Applications. 2nd ed. Vol. 1. Prentice Hall; Harlow, England: 2001. Empirical Force Field Models: Molecular Mechanics. pp. 165.

CHAPTER 1

Introduction

I don't believe you have to be better than everybody else. I believe you have to be better than you ever thought you could be.

[Ken Venturi](#)

1.0. Introduction

Several domains of modern computational science are converging on complex problems in the general field of systems biology. Predicting the properties and behaviour of complex biological systems by computer simulation from a fundamental, *ab initio* perspective has long been a vision of computational scientists. It has been recognized since several years that the key to achieve this goal is to utilize hierarchies of methods and time scales that connect macro- to nano-systems, i.e. a multiscale approach. Multiscale modelling and simulation has emerged as a new research area which has already had a significant impact on many scientific and engineering disciplines. Particular progress has been made in how to relate the molecular-scale chemistry to mesoscopic and macroscopic material and biomaterial properties. Based on large-scale atomistic and molecular modelling methods, hierarchical multi-scale modelling is capable of providing a bottom-up description of chemically complex materials and bio molecules. [1-5]. Despite the similarity of the strategy for different applications, *the necessary parameters included in the approach are problem and system dependent.*

Molecular shape, molecular conformation and molecular charge distribution play crucial roles in the selectivity and function of biologically active molecules. Molecular shape and conformation are controlled by a delicate balance between the forces operating through covalent bonds, *i.e.* those which determine their ‘skeletal’ structures, and the so-called ‘non-bonded interactions’, operating through space

between neighbouring groups of atoms or local charges within the molecules, or between the molecules and their local environment. Together all these determine their conformational landscapes and preferred architectures. Molecular shape and the interactive forces between the molecule and its neighbourhood also play a crucial role in the molecular transport and molecular recognition processes that are involved in almost all aspects of biological function. The ubiquitous hydrogen-bonded interactions, operating both within the molecules and externally with neighbouring molecules, are important. The subtle balance between intra- and inter-molecular hydrogen-bonded interactions in controlling biomolecular conformations, the delicate balance between hydrogen-bonded and other ‘non-bonded’ interactions, and the way in which co-operative interactions may control the specificity of molecular structure and function still remain unclear.

In the last few years, using a powerful combination of molecular electronic and/or vibrational spectroscopy, or microwave spectroscopy, coupled with *ab initio* computation, it has become possible to begin to address directly some of these fundamental biophysical questions. Conversion of the images into structural assignments has depended crucially on the support provided by high-level *ab initio* quantum chemical calculation. Indeed, it is the synergy between experiment and *ab initio* computation that has made all this possible. *Theory and experiment enjoy a symbiotic relationship—their interaction is a co-operative one.* In view of the same, computational biochemistry is an expanding field that relies heavily on the increasing efficiency of computers and clever algorithms to approach very large and

complex problems. While methods for high level quantum mechanical (QM) calculations have been developed and proven to be very successful in calculating energies, equilibrium structures, vibrational frequencies, and more properties of small to medium sized molecules, the computational resources required for very large systems (e.g. a protein of many hundreds of atoms) is usually unattainable [6-8]. For these very large systems, more approximate modelling tools are often used such as molecular mechanics [9-10]. These more approximate methods greatly accelerate the speed at which energy calculations are performed, but they do not explicitly account for electronic structure. This can be a disadvantage, because there is a significant amount of information encoded in the electronic structure of a system. The understanding of structure of biomolecules at electronic level helps certainly in answering the conformational behaviour which is occurring mainly due to the electrostatic interactions at the molecular level.

1.1. Outline of the problem

Among the various bio molecules, phospholipids are important components of biological membranes and in order to understand the specific roles of different phospholipids for membrane structure and function, a detailed structural knowledge of the membrane constituents is necessary, particularly concerning the conformation and interactions of the polar lipid head groups at the membrane surface. During recent years structural information with atomic resolution of a great number of complex membrane lipids has become available from X-ray single crystal analysis [11].

Especially regarding zwitterionic phosphoethanolamine lipids, the structures of a dozen of model compounds with varying numbers of N-methyl groups have been solved, comprising polar head groups and single chain and double chain lipids. When comparing these structures, it is surprising that in all of them the zwitterionic phosphoethanolammonium groups, despite the differences in the degree of N-methylation and hydration and variations in head group packing and intermolecular interactions, adopt very similar preferred conformations. This suggests that the conformation of the phosphoethanolamine group is governed by strong intramolecular interactions and that the varying crystal environment does not significantly affect the conformational preference of the phosphoammonium zwitterion. Therefore, it is necessary to give a clear consensus about their individual structural and dynamical properties in the gel and in the less ordered liquid-crystalline states. The effects of the intra and intermolecular electronic forces on the structure and energetic of these systems make the task nontrivial both experimentally and computationally. In view of the same the main objective of the present thesis is to understand the energy landscape which determines these preferred conformational features.

The main and primary objectives of the thesis include:

- i. Characterisation of the conformational and structural landscapes of model biomolecules viz. DNA base pairs and phospholipids.
- ii. Characterisation of the balance of molecular interactions which govern their structures, particularly in hydrated environments.

Therefore, the aim of the thesis necessitates describing a large area of a QM potential energy surface (PES), which will lead to different energy terms and different parameters. It is thus generally necessary either to proceed from step one, i.e. to fit force field parameters on an adequately selected set of QM (Quantum Mechanics) models, or, at least, test the available force field on the desired set of models and adjust if necessary, before proceeding to the next step. In addition to this using the bottom up methods which are more accurate and reliable one can predict the intra molecular interactions involved and capture the movements at the electronic level. For example many properties of the lipid bilayers (especially those related to phase transitions) can be attributed to the aggregation (intermolecular) interactions between phospholipid molecules and some properties (such as packing symmetry) can be directly attributed to the intrinsic (intra molecular) structural and dynamical characteristics of single (gas phase) phospholipid molecules.

In the present chapter we begin by giving the brief introduction and structural information of Phospholipids and DNA base pairs molecules in section 1.2 and 1.3 respectively. The associated motivational literature survey including both experimental and theoretical studies on phospholipids and base pairs are discussed in section 1.4 and 1.5 respectively. We have dedicated section 1.6 to discuss the scope of the thesis. The present section 1.1 outlines the problem of the present thesis.

1.2. Structural overview of Phospholipids

Phospholipids play an important role and are major class of bio molecules. Phospholipids are the fundamental building blocks of cellular membranes and are the major part of surfactant, the film that occupies the air/liquid interfaces in the lungs. The basic structure of the molecule consists of a polar or charged head group and a pair of non-polar fatty acid tails, connected via a glycerol linkage. This structure, which contains both polar and non-polar segments, is termed as amphiphilic and the word describes the tendency of these molecules to assemble at interfaces between polar and non-polar phases. Phosphoglycerides are the most common class of phospholipids whose structural backbone consists of a three-carbon alcohol with the formula $\text{CH}_2\text{OH}-\text{CHOH}-\text{CH}_2\text{OH}$, two fatty acid chains, each typically having an even number of carbon atoms between 14 and 20, attached (via a dual esterification) to the first and second carbons of the glycerol molecule, denoted as the sn1 and sn2 positions, respectively. The third hydroxyl group of glycerol, at position sn3, reacts with phosphoric acid to form phosphatidate.

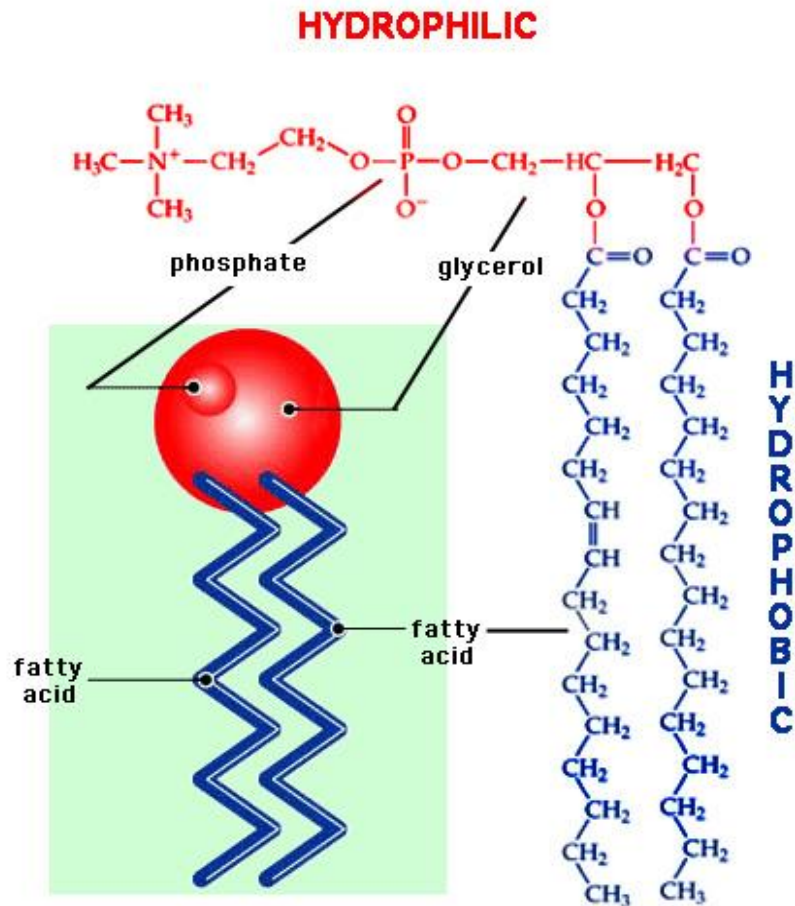
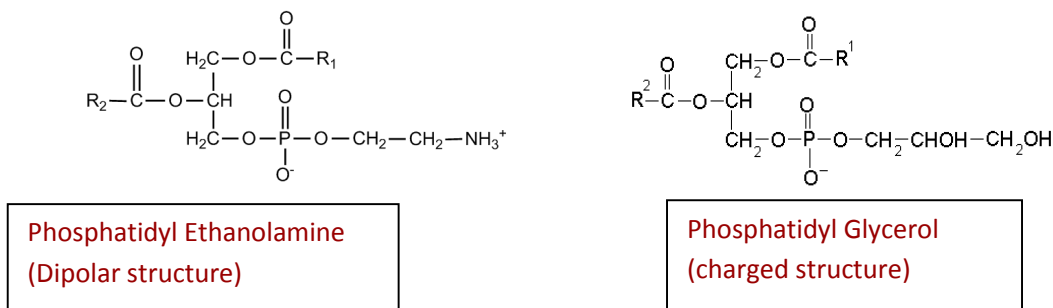


Figure 1.1. The Dipolar view of a phospholipid molecule.

Common phospholipids which are widely distributed in nature are produced by further reaction of the phosphate group in phosphatidate with an alcohol, such as serine, ethanolamine, choline, glycerol, or inositol. The structure of the head groups has not yet been fully characterized, but they will have large interactions with other molecules because of their charged groups. It is possible that lipids cause conformational changes in membrane proteins necessary for their function and that the interaction of drugs

with hydrated head groups which is a key step in passive diffusion through the membrane. Thus, there is an important need to understand the behaviour and structure of the head group layer. The resulting lipids may be charged, for example, phosphatidyl serine (PS), phosphatidyl inositol (PI), and phosphatidyl glycerol (PG); or dipolar (having separate positively and negatively charged regions), for example, phosphatidyl choline (PC), and phosphatidyl ethanolamine (PE).



Some of the types of phospholipids are:

- Phosphatidic acid (PA) (DMPA, DPPA, DSPA)
- Phosphatidylcholine (PC) (DDPC, DLPC, DMPC, DPPC, DSPC, DOPC, POPC, DEPC)

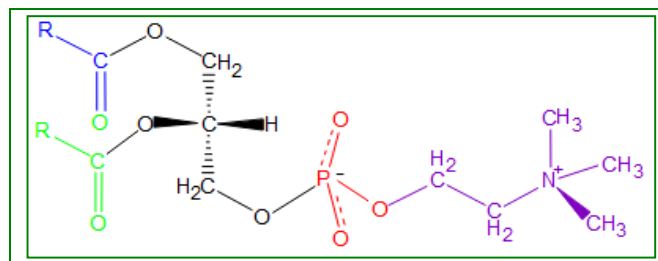
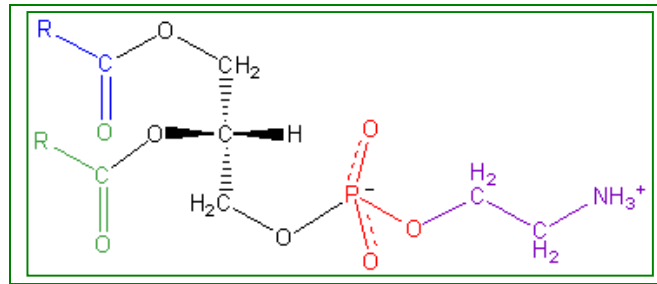


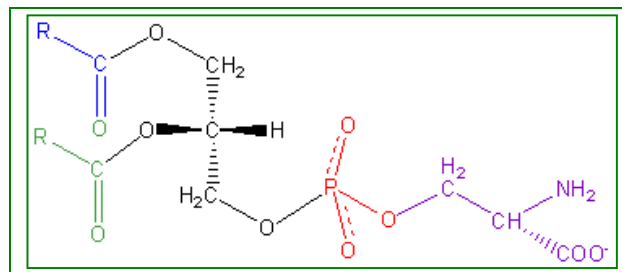
Figure 1.2 ,2-Dimyristoyl-*sn*-glycero-3-phosphocholine

- Phosphatidylglycerol (PG) (DMPG, DPPG, DSPG, POPG)

- Phosphatidylethanolamine (PE) (DMPE, DPPE, DSPE DOPE)

Figure 1.3 1,2-Dimyristoyl-*sn*-glycero-3-phosphoethanolamine

- Phosphatidylserine (PS) (DOPS)

Figure 1.4 1,2-Dimyristoyl-*sn*-glycero-3-phosphoserine

When many phospholipid molecules are placed in water, their hydrophilic heads tend to face water and the hydrophobic tails are forced to stick together, forming a bilayer. Each of the molecular forces acting within a phospholipid molecule further comprise of:

- (a) Electrostatic interactions (attractive and repulsive),
- (b) Hydrogen bonds,
- (c) Dispersive forces, and
- (d) Ionic bonds (in case of charged lipid molecules).

Molecular conformation dominating a bilayer is thus an outcome of balance of all these forces within and between the molecules. A complete insight about all these forces and hence their role in stabilizing various conformations is best obtained from a Quantum Mechanical (QM) methodology.

Due to the large size of phospholipid molecule QM studies have been limited to understanding the interactions of the hydrophilic polar head group so far. Early studies used methyl phosphate ions as models and applied semi empirical or Hartree Fock methods to analyze the structural and hydration properties. More recent studies have applied Density Functional Theory (DFT) based methodologies to the same effect with improved understanding on the hydration and electronic polarization around the head group and interaction of head group with model dust particles.

1.3. Structural overview of DNA bases and base pairs

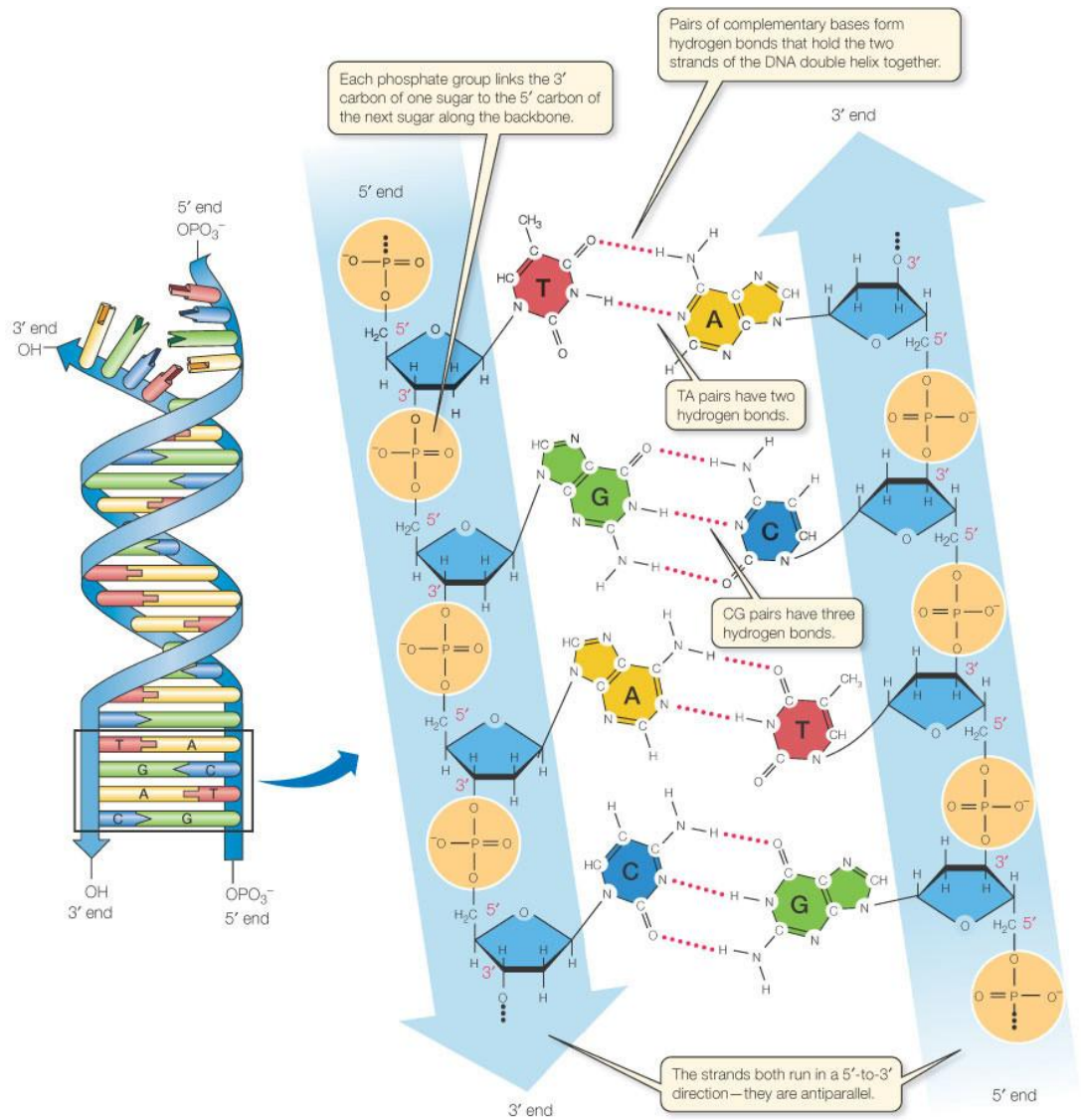


Figure 1.5. The famous helical model of DNA and its structural details.

The remarkable year of 1869 was a landmark year in genetic research; because it was the year in which Swiss physiological chemist Friedrich Miescher first identified nucleic acid which he termed as "nuclein" inside the nuclei of human white blood cells. The term "nuclein" was later changed to "nucleic acid" and eventually to "deoxyribonucleic acid," or "DNA". Discovery of DNA helical structure was always associated with the name of Watson and Crick [12]. They were the first scientists to formulate an accurate description of the complex double-helical structure of this molecule. Watson and Crick's work was based on the research of numerous scientists before them, including Friedrich Miescher, Phoebus Levene, and Erwin Chargaff [13-15].

As depicted in Figure 1.5 in the double-stranded DNA, the two strands run in opposite directions and the bases pairs up such that A (Adenine) always pairs with T (Thymine) and G (Guanine) always pairs with C (Cytosine). The A-T base-pair has 2 hydrogen bonds and the G-C base-pair has 3 hydrogen bonds. The G-C interaction is therefore stronger than A-T. These hydrogen bonds help in maintaining the structure and specificity of systems. In particular, the hydrogen bond determines the magnitude and the nature of the interactions of the biomolecules and is consequently responsible for the important unique properties of nucleic acids [12]. The stability of DNA and RNA structure is not only due to the H-bond base pairing, but also the base stacking, which is actually an interaction between π -orbital of the aromatic rings of the bases [16]. Due to the small size and existence of experimental data, these base pairs have been chosen as prototype of DNA structure in theoretical investigations. The

interesting information about their electronic structure and the weakly held molecular complexes can be obtained by quantum chemical treatment [17-21].

1.4. Experimental and Theoretical Investigation on Structure and Conformation of a Phospholipid Molecule: A literature survey

The crystal structures of several different lipids have been determined and provide an important reference for studying the conformation of lipids in bilayers [22-24]. The orientation of the glycerol backbone is parallel to the acyl chain axis in PC and PE, but perpendicular to this axis in the crystal structures of dilauroylglycerol (DLG) and 1,2-DPG [23,25]. The large polar headgroups in phospholipids dominate their interfacial chemistry, but it is not known how they influence the orientation or conformation of the glycerol backbone. An intuitive picture is that the large polar or charged headgroup effectively pulls the end of the glycerol chain away from hydrophobic interior of the bilayer, thereby orienting the backbone parallel to the acyl chain axis as seen in the crystal structures of PE and PC. In addition nuclear magnetic resonance (NMR) spectroscopy is a powerful experimental method for investigations of liquid crystals in general and lyotropic mesophases in particular. Deuterium (^2H) NMR has been employed extensively for studies of the molecular order, structure, and dynamics in lipid bilayers [26-32].

Solid-state ^{13}C NMR provides an approach for determining the interfacial conformation of membrane lipids in bilayer structures. Cornell (1981) originally observed that the carbonyl resonances of the sn-1 and sn-2 chains in

dipalmitoylphosphatidylcholine (DPPC) had distinct NMR frequencies and line shapes.

Consideration of biological membranes at the molecular level requires a detailed knowledge of the preferred conformations of phospholipids. Furthermore, conformational details of these “monomers” are of considerable importance in developing a reasonable model for the “macromolecular” structure of the membrane complex and in the understanding of lipid-protein interactions. In general, the typical short range intra molecular nonbonded interactions play an important role in determining the conformations of molecules. In phospholipids, these interactions appear to be the major factors in producing the energetically favoured conformations. Conformations of lipid molecules and their stability within a bilayer are influenced by two major forces viz., (a) intra molecular and (b) inter molecular ones. The phospholipid molecules, being made up from glycerol, two fatty acids and a phosphate group, have a polar head region and non-polar tail region. Hence, each of the molecular forces further comprise of (a) electrostatic interactions (attractive and repulsive), (b) hydrogen bonds, (c) dispersive forces, and (d) ionic bonds (in case of charged lipid molecules). Molecular conformation dominating a bilayer is thus an outcome of balance of all these forces within and between the molecules. Sundralingam et al noticed that the preferred conformations of phospholipids are majorly contributed by nonbonded interactions. Therefore, their results showed that intramolecular chain stacking not only stabilizes, but also restricts the favored conformations of phospholipids to a limited number of possibilities [33].

Considering all the experiment and theoretical investigations the most debated topics in the area of phospholipids is the kind of conformations that populate various lipid bilayers in the gel (non-melted state of the bilayer) and liquid crystalline (melted state of the bilayer) states. In view of this, various experimental techniques such as NMR [34-38] and X-ray [39] have been applied in the past. In addition to this, various conformations were also proposed theoretically based on these studies [39]. Theoretical methods, especially those based on molecular mechanics (MM) methods, were also applied rigorously to analyse the various possible conformational probabilities within a bilayer [40–50]. Interestingly, most of the theoretical simulations (especially the MM-based studies) begin with the conformations predicted by the old X-ray studies, and hence with more biased conformations. Thus, a clear consensus on the individual structure of lipid molecules and their role in controlling the dynamical properties of bilayer is still eluding. In this context, it is more meaningful and interesting to design bilayers with various possible conformations and analyse their stability–property relationship from a more fundamental aspect.

A complete insight about all these forces involved in deciding the conformational behaviour and also their role in stabilizing various conformations is best obtained from a Quantum Mechanical (QM) methodology. Several research groups have attempted to understand these aspects in recent years. However, due to the large size of phospholipid molecule QM studies have been limited to understanding the interactions of the polar head group so far. Early studies used methyl phosphate ions as models and applied semi-empirical or Hartree Fock methods

to analyze the structural [51-53] and hydration properties [54]. More recent studies have applied Density Functional Theory (DFT) based methodologies to the same effect with improved understanding on the hydration [55-56] and electronic polarization [57] around the head group and interaction of head group with model dust particles [58]. A more recent study has applied hybrid QM/MM method to study the hydration phenomena of dipalmitoylphosphatidylcholine head group [59].

The fluid-like nature of the lipid bilayers leads to the absence of high-resolution structures, except few crystal structures, i.e. non fluid phase. Measurements on hydrated bilayers are limited to data reproducing averaged properties of many molecules on a large time scale, for example, NMR measured order parameters, T1 relaxation times, neutron scattering density profiles, etc. This lack of experimental accurate structural data is also responsible for the eventual inaccuracy of the lipid force fields, which are generally optimized in order to reproduce experimentally measured properties. In fact, as recognized by experts, this situation is unfortunate due to the importance of the accuracy of the method in describing and understanding the detailed atomistic structure of biological membranes [60].

Importantly, the presence of different functional groups modifies the overall charge of a phospholipid molecule, making it zwitterionic, anionic or cationic in nature. The overall charge on the molecule modulates its molecular interactions with the components present in the aqueous phase resulting in different membrane responses towards the incoming ion, protein, drug molecule, etc. Hence, depending on the functional group in the molecule, its application is seen to vary, viz. drug delivery,

protein–lipid interaction, solvation and so on [61]. The presence of different functional groups at the polar region changes entirely the electrostatic interaction involved and hence the hydration behaviour too. X-ray and other experimental studies show that for an individual phospholipid molecule in the gas phase, the functional groups tend to orient towards the phosphate group due to involved intramolecular electrostatic interactions [62]. However, the molecule adopts an extended form in the presence of water and a neighbouring phospholipid molecule [63]. The effect of continuum solvation model has been studied on PE and PC model systems using Hartree Fock method [54]. However, the hydration study of different functional groups attached to the phosphate moiety using explicit water molecules with more accurate methods is still eluding. In addition to the head group, the tail region has also been taken into account in the more extended form of the model system to study the various conformations and their energetic profile as a result of intramolecular interactions involved in the phospholipid system [62-63]. However, in such cases, more extensively classical molecular dynamics methods have been used to study biological membrane properties. The force fields used in these classical molecular dynamics simulations to reproduce the experimental properties are parameterised using quantum mechanics calculations on small model molecules [43-47]. Molecular dynamics (MD) studies have been devoted to a large number of structural properties and has explored, till date, dihedral angle values [43-45], head group flexibility [48-49], tail orientation [46], phase changes [64-65], hydration effect [66–68], interaction with ions and molecules [69-70] and evaluation of local order parameter [71-72]. In

addition to this, recently, Parthasarathi et al. [73] have studied the significant interaction of mannose sugar with two different phospholipids using DFT. Parthasarathi et al. have shown the importance of the influence of tail on phospholipid interaction with other molecules.

1.5. Experimental and Theoretical Investigation on Structure, Reactivity of DNA base pairs: A literature survey

Redox properties of nucleic acid bases are important characteristics of DNA and are one of the key factors in the storage and transfer mechanism of the genetic information. Correct determination of the redox potentials, electron affinities (EAs), and ionization potentials (IPs) is of great interest for the understanding of thermodynamic and kinetic properties of DNA, possible radiation damage and repair, and oxidation reactions as well as excess electron transfer through DNA. It is known that base alterations and single-strand breaks are mediated by the one-electron deficient DNA base radicals. Therefore, there is a need to understand the chemical and physical mechanism of DNA oxidation. Unfortunately, limited experimental information is available for the redox potentials, EAs, and IPs of DNA bases and base pairs [74-77]. Only recently, the experimental oxidation potential of the guanine-cytosine base pair was obtained [78]. Experiments done by several groups prove that even very low energy electrons can break DNA by various mechanisms [79]. Electron attachment followed by single-strand break is one of the processes described [80]. The purpose of the present research is to explore the possibility of formation of stable

radicals with significant structural changes and also to understand the energy changes associated with such processes. This is an important subject not only because attachment of electrons to DNA base pairs or radical formation (due to high-energy electron impact and/or ionizing radiation) would lead to strand breaks and therefore interrupt the information flow. Conversely, to the advantage of living things, such processes may break up mutant and potentially dangerous tumour cells. Rearrangement of the radicals to a deformed structure will incorporate increased strain in the rigid DNA strand. The resultant H and base pair radicals may be quenched by thiols in biological systems [81]. If not repaired quickly, the damaged DNA mutates, and it may ultimately cause cell death.

Yet little is known about the possible outcome of damage to the base pairs in terms of energetics and possible structural changes that can lead to strand breakage and therefore loss of genetic information. Furthermore, experimentally provided values are diverse; therefore, correct theoretical determination of highly accurate redox properties of DNA is important.

Due to the small size and existence of some experimental data, these base pairs have been chosen as prototype of DNA structure in theoretical investigations. The interesting information about their electronic structure and the weakly held molecular complexes can be obtained by quantum chemical treatment [17-21].

A spontaneous DNA mutation induced by proton transfer in the Guanine, Cytosine base pairs is a motivation to study electron transfer in DNA bases [82]. Ab initio calculations were applied to study nucleic acid bases and their hydrogen bonded

and stacked complexes. H-bonding of bases [83] was first investigated by the ab initio methods in 1986–1988. A real breakthrough in the quality of ab initio studies of bases and base pairs occurred around 1994–1995, when the first high level ab initio calculation with consistent treatment of electron correlation effects became feasible [84]. Lesions in DNA are caused by electrons with high and low energy resulting in cancer cell formation. So, the mechanisms of primary and secondary damage to purine and pyrimidine base pairs have been under intense investigations in recent years [85–96]. It has also been demonstrated recently that even very low energy electrons can induce strand breaks in DNA [80, 88, 97–99]. The structures and energetic of the closed shell [95,100, 101], H-abstracted and deprotonated A–T and G–C base pairs and bases have been explored. This signifies the change in the conformation of the native structure when it is exposed to the outside environment with UV or some chemical agents involving electron transfer. Electron correlation is necessary to obtain accurate charge distribution and dipole moments [102]. Effect of base stacking on the acid-base properties of adenine cation radical as well as studies of deprotonation states of guanine cation radical using both ESR and DFT have also been reported [103–104]. Advanced ab initio calculations for calculating stacking energy in the gaseous environment provide a benchmark for the experimental studies to give reference data for the magnitude and conformation of bases and base pairs [105]. It has been found that upon excitation of base cation radicals in DNA and in model systems, hole transfer from base to sugar occurs resulting in sugar radical formation and strand break formation [106]. Effect of base sequence on deprotonation of guanine cation radical

has found that the positive charge in guanine radical in oligonucleotide is delocalized over the extended p-orbitals of DNA bases [107]. Quantification of reactive sites for individual bases has already been done in the presence of water as medium and it shows the changes in reactivity descriptors of the bases in the presence of water [108]. Fukui functions represent the descriptors of reactivity [109]. From a practical point of view, quantitative knowledge of the geometry and energy of interaction is particularly important for the development and validation of the studies for the design of artificial receptor molecules. The reactive atoms of base pairs, as derived from Fukui functions, indicate the location of electrophilic and nucleophilic attack in DNA [110].

1.6. Scope of the thesis

The present thesis supports the existence and importance of intramolecular interactions in biomolecules. Therefore the level of calculations while simulating should be based on the objective of the simulation. Although the intermolecular interaction certainly important for the simulation as we simulate e.g the DNA strand, a big protein molecule, a phospholipid bilayer but one should not neglect the role of intramolecular interactions. The intramolecular forces are predominant in the determination of the phospholipid molecular structures. The fact that DMPC molecules retain their individual structure within assemblies has already been suggested in various experimental studies. Optimized dimeric structures, built from various DMPC conformers, show indeed that the substantial intermolecular

electrostatic interactions between the monomers do not modify the individual monomer geometries.

In addition to the role of electrostatic intramolecular interactions for the determination of the conformational and structural changes the same also defines some of the important biophysical properties like phase transition. Therefore, the main phase transition would be driven by intrinsic structural changes within the lipid molecules. Intermolecular interactions will, of course, influence the detailed dynamics in the bilayer, once the transformation has occurred within the molecules.

In addition to the phospholipid molecule studies we will also be addressing various structural parameters of DNA base pairs in the ionic form and quantification of the reaction energies using *ab initio* calculations. The other aspect of the present thesis is to quantify the reactive sites for DNA base pairs and phospholipid molecules. The scope of the present thesis also covers the study of the role of substituents towards the enhancement and/or diminution of the reactivity of 2, 2' bipyridine and its analogues with Ruthenium metal using density based reactivity descriptors.

1.7. References

- [1] Buehler M J, Dodson J, van Duin A C T, Meulbroek P, Goddard III W A, Mater Res Soc Symp Proc 894 (2006) 327.
- [2] Chu J W, Izveko S, Voth G A, *Mol Simul*, 32(2006) 211.
- [3] Lyubartsev A P, *Eur Biophys J* 35(2005) 53.
- [4] Weinan E, Engquist B, *Notices of the AMS*, 50 (2003) 1062.
- [5] Lyubartsev A P, Karttunen M, Vattulainen I, Laaksonen A, *Soft Materials*, 1 (2002) 121.
- [6] Szabo A, Ostlund NS. *Modern Quantum Chemistry: Introduction to Advanced Electronic Structure Theory*. 1st ed. Vol. 1. Dover Publications; Mineola, N.Y.: 1996. The Hartree Fock Approximation. pp. 108.
- [7] Levine IN. *Quantum Chemistry*. 6th ed. Vol. 1. Prentice Hall; Upper Saddle River, N.J.: 2008. Ab initio and Density Functional Treatments of Molecules. pp. 480.
- [8] Jensen F. *Introduction to Computational Chemistry*. 2nd ed. Vol. 1. Wiley; Chichester, England: 2006. Electronic Structure Methods: Independent-Particle Models. pp. 80.
- [9] Cramer CJ. *Essentials of Computational Chemistry: Theories and Models*. 2nd ed. Vol. 1. Wiley; Chichester, England: 2004. Molecular Mechanics. pp. 17.
- [10] Leach A. *Molecular Modelling: Principles and Applications*. 2nd ed. Vol. 1. Prentice Hall; Harlow, England: 2001. Empirical Force Field Models: Molecular Mechanics. pp. 165.

- [11] Pascher I, Lundmark M, Nyholm P G, Sundell S, *Biochim Biophys Acta* 1113 (1992) 339.
- [12] Watson J D, Crick F H C, *Nature* 171 (1953) 737.
- [13] Wolf G, *Chemical Heritage* 21 (2003) 10-11, 37.
- [14] Levene P A, *Journal of Biological Chemistry* 40 (1919) 415.
- [15] Chargaff E, *Experientia* 6 (1950) 201.
- [16] Hanlon S, *Biochem Biophys Res Commun* 23 (1966) 861.
- [17] (a) Hobza P, Sponer J, *Chem Rev* 99 (1999) 3247; (b) Sponer J, Leszczynski J, Hobza P, *J Biomol Struct Dynam* 14 (1996) 117.
- [18] Sponer J, Leszczynski J, Hobza P, *J Phys Chem* 100 (1996) 1965.
- [19] (a) Guerra C F, Bickelhaupt F M, *Angew Chem Int Ed Engl* 38 (1999) 2942; (b) Gould I R, Kollman P A, *J Am Chem Soc* 116 (1994) 2493; (c) Hutter M, Clark T, *J Am Chem Soc* 118 (1996) 7574; (d) Goddard III W A, *J Phys Chem B* 101 (1997) 4851.
- [20] Kawahara S, Wada T, Kawauchi S, Uchimaru T, Sekino M, *J Phys Chem A* 103 (1999) 8516.
- [21] Yanson I K, Teplitsky A B, Sukhodub L R, *Biopolymers* 18 (1979) 1149.
- [22] Hitchcock P B, Mason R, Thomas K M, Shipley G G, *Proc Natl Acad Sci USA* 71 (1974) 3036.
- [23] Pascher I, Sundell S, Hauser H, *J Mol Biol* 153, (1981) 79 1-806.
- [24] Hauser H, Pascher I, Pearson R H, Sundell S, *Biochim Biophys Acta* 650 (1981) 21.

- [25] Dorset D L, Pangborn W A, Chem Phys Lipids 48 (1988) 19.
- [26] Davis J H, Adv Magn Reson 13 (1989)195.
- [27] Seelig J Q, Rev Biophys 10 (1977) 353.
- [28] Bonev B B, Chan W C, Bycroft B W, Roberts G C K, Watts A, Biochemistry 39 (2000) 11425.
- [29] Lehnert R, Eibl H J, Müller K, J Phys Chem B 108 (2004) 12141.
- [30] Shaikh S R, Cherezov V, Caffrey M, Soni S P, LoCasio D, Stillwell W, Wassall S R, J Am Chem Soc 128 (2006) 5375.
- [31] Aussenac F, Lavigne B, Dufourc E J, Langmuir 21 (2005) 7129.
- [32] Aussenac F, Laguerre M, Schmitter J. M, Dufourc E J, Langmuir 19, (2003) 10468.
- [33] McAlister J, Yathindra N, Sundaralingam M, Biochemistry 2(6) (1973) 1189.
- [34] Hauser H, Guyer W, Pascher I, Skrabal P, Sundell S, Biochemistry 19 (1980) 366.
- [35] Hauser H, Pascher I, Sundell S, Biochemistry 27 (1988) 9166.
- [36] Hong M, Schmidt-Rohr K, Zimmermann H, Biochemistry 35 (1996) 8335.
- [37] Bruzik K S, Harwood J S, J Am Chem Soc 119 (1997) 6629.
- [38] Aussenac F, Laguerre M, Schmitter J-M, Dufourc E J, Langmuir 19 (2003) 10468.
- [39] Pearson R H, Pascher I, Nature 281 (1979) 499.

- [40] Jeffery K, Richard M V, Alfredo J F, Joseph W O C, Douglas J T, Carlos M R, Igor V, MacKerell A D, Richard W P, *J Phys Chem B* *114*, (2010) 7830.
- [41] Henin J, Shinoda W, Klein M L, *J Phys Chem B* *113* (2009) 6958.
- [42] Lopez Cascales J J, Berendsen H J C, Garcia de la Torre J, *J Phys Chem* *100* (1996) 8621.
- [43] Weiner S J, Kollman P A, Nguyen D T, Case D A, *J Comput Chem* *7* (1986) 230.
- [44] Duan Y, Wu C, Chowdhury S, Lee M C, Xiong G M, Zhang W, Yang R, Cieplak P, Luo R, Lee T, Caldwell J, Wang J M, Kollman P, *J Comput Chem* *24* (2003) 1999.
- [45] Kaminski G A, Friesner R A, Tirado-Rives J, Jorgensen W L, *J Phys Chem B* *105* (2001) 6474.
- [46] Feller S E, MacKerell AD Jr., *J Phys Chem B* *104* (2000) 7510.
- [47] Akutsu H, Nagamori T, *Biochemistry* *30* (1991) 4510.
- [48] Vanderkooi G, *Biochemistry* *30* (1991) 10760.
- [49] Stauch T R, *Mol Simul* *10* (1993) 335.
- [50] Marrink S J, Mark A E, *Biophys J*, *87* (2004) 3894.
- [51] Florian J, Baumruk V, Strajbl M, Bednarova L, Stepanek J, *J Phys Chem* *100* (1996) 1559.
- [52] Liang C, Ewig C S, Stouch T R, Hagler A T, *J Am Chem Soc* *115* (1993) 1537.
- [53] Pullman B, Pullman A, Berthod H, Gresh N, *Phys Lett* *33*, (1975) 11.

- [54] Landin J, Pascher I, Cremer D, J Phys Chem A 101 (1997) 2996.
- [55] Pohle W, Gauger R R, Bohl M, Mrazkova E, Hobza P, Biopolymers 74 (2004) 27.
- [56] Mrazkova E, Hobza P, Bohl M, Gauger D R, Pohle W, J. Phys. Chem. B 109 (2005) 15126.
- [57] I-Feng K, Douglas J T, J Phys Chem B 105 (2001) 5827.
- [58] Snyder J A, Madura J D, J Phys Chem B 112 (2008) 7095.
- [59] Yin J, Zhao Y P, J colloid and interface science 329 (2009) 410.
- [60] MacKerell A D, J Comput Chem 25 (2004) 1584.
- [61] Kinnunen P K J, Chem and Phys of Lipids 57 (1991) 375.
- [62] Krishnamurty S, Stefanov M, Mineva T, Begu S, Devoisselle J M, Goursot A, Zhu R, Salahub D R, J Phys Chem B 112 (2008) 13433.
- [63] Mishra D, Pal S, Krishnamurthy S, Mol Simul 37 (2011) 953.
- [64] Egberts E, Marrink S J, Berendsen H J C, Eur Biophys J 22 (1994) 423.
- [65] Marrink S J, Berger O, Tieleman P, Jahnig F, Biophys J 74 (1998) 931.
- [66] Murzyn K, Zhao W, Karttunen M, Kurziel M, Rog T, Biointerphases 1 (2006) 98.
- [67] Rog T, Murzyn K, Pasenkiewicz-Gierula M, Chem Phys Lett 352 (2002) 323.
- [68] Pandey P R, Roy S, J Phys Chem B 115 (2011) 3155.
- [69] Vanderkoi G, Biophys J 66 (1994) 1457.
- [70] Chanda J, Bandyopadhyay S, Langmuir 22 (2006) 3775.

- [71] Högberg C J, Lyubartsev A, *J Phys Chem B* 110 (2006) 14326.
- [72] Thaning J, Högberg C J, Stevensson B, Lyubartsev A, Maliniak A, *J Phys Chem B* 111 (2007) 13638.
- [73] Pathasarathi R, Jianhui T, Redondo A, Gnankaran S, *J Phys Chem A* 115 (2011) 12826.
- [74] Seidel C A M, Schulz A, Sauer M H M, *J Phys Chem* 100 (1996) 5541.
- [75] Faraggi M, Broitman F, Trent J B, Klapper M H, *J Phys chem* 100 (1996) 14751.
- [76] Steenken S, Jovanovic S V, *J Am Chem Soc* 119 (1997) 617.
- [77] Fukuzumi S, Miyao H, Ohkubo K, Suenobu T, *J Phys Chem A* 109 (2005) 3285.
- [78] Caruso T, Carotenuto M, Vasca E, Peluso A, *J Am Chem Soc* 127 (2005) 15040.
- [79] Collins G P, *Sci Am* 289(3) (2003) 26.
- [80] Berdys J, Anusiewicz I, Skurski P, Simons J, *J Am Chem Soc* 126 (2004) 6441.
- [81] Steenken S, *Chem Rev* 89 (1989) 503.
- [82] Hanna M W, Lippert J L (Ed.), *Molecular complexes*, R Foester, London:Elek Vol.1; S. Scheiner (Ed.), *Molecular Interactions*, 1997.
- [83] Hobza P, Sandorfy C, *J Am Chem Soc* 109 (1987) 1302 .
- [84] Colson A O, Sevilla M D, *Int J Radiat Biol* 67 (1995) 627.
- [85] Bera P P, Schaefer H F, *Proc Natl Acad Sci USA* 102 (2005) 6698.

- [86] Abdoul-Carime H, Gohlke S, Illenberger E, Phys Rev Lett 92 (2004) 168103.
- [87] Ptasinska S, Denifl S, Scheier P, Illenberger E, Mark T D, Angew Chem Int Ed 44 (2005) 6941.
- [88] Boudaiffa B, Cloutier P, Hunting D, Huels M A, Sanche L, Med Sci 16 (2000) 1281.
- [89] Evangelista F A, Paul A, Schaefer H F, J Phys Chem A 108 (2004) 3565.
- [90] Kumar A, Knapp-Mohammady M, Mishra P C, Suhai S, J Comput Chem 25 (2004) 1047.
- [91] Li X F, Sevilla M D, Sanche L, J Phys Chem B 108 (2004) 19013.
- [92] Liu B, Hvelplund P, Nielsen S B, Tomita S, J Chem Phys 121 (2004) 4175.
- [93] Luo Q, Li J, Li Q S, Kim S, Wheeler S E, Xie Y M, Schaefer H F Phys Chem Chem Phys 7 (2005) 861.
- [94] Luo Q, Li Q S, Xie Y M, Schaefer H F, Collect Czech Chem Commun 70 (2005) 826.
- [95] Profeta L T M, Larkin J D, Schaefer H F, Mol Phys 101 (2003) 3277.
- [96] Richardson N A, Wesolowski S S, Schaefer H F, J Phys Chem B 107 (2003) 848.
- [97] Sanche L, Phys Scripta 68 (2003) C108.
- [98] Boudaiffa B, Cloutier P, Hunting D, Huels M A, Sanche L, Science 287 (2000) 1658.
- [99] Li X F, Sevilla M D, Sanche L, J Am Chem Soc 125 (2003) 13668.

- [100] Richardson N A, Wesolowski S S, Schaefer H F, J Am Chem Soc 124 (2002) 10163.
- [101] Li X F, Cai Z L, Sevilla M D, J Phys Chem A 106 (2002) 9345.
- [102] Nowak M J, Lapinski L, Kwiatkowski J S, Leszczynski J (ed.) in *Computational Chemistry: Reviews of Current Trends* Leszczynski J. World Scientific press, Singapore 2 (1997) 140.
- [103] Adhikary A, Kumar A, Khanduri D, Sevilla M D, J Am Chem Soc 130 (2008) 10282.
- [104] Adhikary A, Kumar A, Becker D, Sevilla M D, J Phys Chem B 110(2006) 24171.
- [105] Hobza P, Sponer J, J Am Chem Soc 124 (2002) 11802.
- [106] Kumar A, Sevilla M D, J Phys Chem B 110 (2006) 24181.
- [107] Kobayashi K, Yamagami R, Tagawa S, J Phys Chem B 112 (2008) 10752.
- [108] Sivanesan D, Subramanian V, Unni Nair B, J Mol Str (Theochem) 544 (2001) 123.
- [109] Fukui K, Science 218 (1982) 747.
- [110] Mishra D, Pal S, J. Mol. Str (Theochem) 902 (2009) 96.

CHAPTER 2

Theoretical Methods and Computational Details

*He who loves practice without **theory**
is like the sailor who boards ship
without a rudder and compass
and never knows where to be cast.*

-Leonardo da Vinci

Abstract

As discussed in chapter 1, the aim of the thesis is to address the structure, conformation and electrostatics involved in two major biomolecules viz. phospholipids and DNA base pairs. This present chapter is focussed to elaborate some of the theoretical approaches used to study the same. The methodology used in both cases is based on Density Functional Theory. Later, we also discuss the AIMD technique based on the DFT, to study the effect of temperature on single phospholipid molecule with various conformations. Finding the ground state geometry and the associated electrostatics with various bio molecules have been a central goal of many researchers. Both these methodologies will be elaborated in this chapter.

In the last decade, various quantum mechanical methods have been implemented to treat the electronic structure of molecules, clusters and solids. We begin Section 2.1 with a brief introduction to the many-body problem by discussing the Born-Oppenheimer approximation, Hartree approximation, Hartree-Fock theory, and methods beyond Hartree-Fock. In Section 2.2 we provide a summary of density functional theory which is as an alternative route for performing such calculations. Special attention is given to the Hohenberg-Kohn theorems, Kohn-Sham equations, and the different exchange-correlations functionals. In section 2.3 we briefly focus on density based reactivity descriptors used thoroughly in the present piece of work to determine essential reactivity centres of the discussed biomolecules. In Section 2.4 a description of the concepts of molecular dynamics and special mention have been given to the *ab initio* molecular dynamics are laid in the same section.

2.1. The many-body problem

Any given system composed of N electrons and M nuclei can be determined by solving the Schrödinger equation. The *time-independent Schrödinger equation* [1] has the form

$$H\Psi = E\Psi \quad (2.1.1)$$

where Ψ is the wavefunction of the system, E is the energy eigenvalue and H is the Hamiltonian operator. H is the sum of the kinetic energy T and potential energy V operators and can be written as

$$H = -\sum_{i=1}^N \frac{\hbar^2}{2m} \nabla_i^2 - \sum_{A=1}^M \frac{\hbar^2}{2M_A} \nabla_A^2 + \frac{1}{2} \sum_{i \neq j}^N \frac{e^2}{r_{ij}} + \frac{1}{2} \sum_{A \neq B}^M \frac{Z_A Z_B e^2}{R_{AB}} - \sum_{i=1}^N \sum_{A=1}^M \frac{Z_A e^2}{r_{iA}} \quad (2.1.2)$$

In the above equation the first two terms are the kinetic energies of N electrons with masses m and M nuclei with masses M_A , the third term is the electrostatic repulsion between electrons separated by r_{ij} , fourth term is the electrostatic repulsion between nuclei separated by R_{AB} and the last term is the Coulombic attraction between electrons and nuclei r_{iA} distance apart.

2.1.1. Born-Oppenheimer approximation

Since nuclei have much larger masses their velocities are consequently smaller compared to electrons. The *Born-Oppenheimer approximation* [2] assumes that the nuclei are fixed which amounts to removing the second term in Equation (2.1.2). Due to the above approximation, the fourth term is a constant

and is included in the total energy after calculating the wavefunction. These simplifications result in the electronic Hamiltonian operator (H_e):

$$H_e = -\sum_{i=1}^N \frac{1}{2} \nabla_i^2 + \sum_{i \neq j}^N \frac{1}{r_{ij}} - \sum_{i=1}^N \sum_{A=1}^M \frac{Z_A e^2}{r_{iA}} \quad (2.1.3)$$

The conceptual and numerical problems related to the electron-electron interactions (second term) in Equation (2.1.3) are the most challenging to deal with. An elementary scheme would be to set the corresponding terms to zero implying that the N electrons move completely independent of each other. Then the total wavefunction Ψ becomes a product of N one-electron wavefunctions ψ_i .

$$\Psi = \psi_1(r_1)\psi_2(r_2)\dots\psi_N(r_N) \quad (2.1.4)$$

However such a Hamiltonian is very archaic and hence electron-electron interactions must be calculated.

2.1.2. Hartree approximation

To have the similarity model of electron-electron interactions, under the Hartree approximation each electron is thought of as moving in a field built by all other electrons. The electron-electron interactions then depend only on the positions of the electron under consideration which moves in an electronic sea made by the rest of the electrons. The second term in Equation (2.1.3) can therefore be approximated as a sum of one-electron potentials v_i where ψ_i is the orbital for the i^{th} electron.

$$\sum_{i \neq j}^N \frac{1}{r_{ij}} \approx \sum_{i=1}^N v_i(r_i) = \sum_{i=1}^N \int \frac{\rho(r_j) - |\psi_i(r_j)|^2}{|r_i - r_j|} dr_j \quad (2.1.5)$$

The solution of Hartree approximation needs to be derived self-consistently because calculation of ψ_i depends on $\sum_{i \neq j}^N \frac{1}{r_{ij}}$ which in turn is defined in terms of ψ_i .

The total wavefunction is still expressed as the *Hartree product* as given in Equation (2.1.4). However it is not antisymmetric with respect to exchange of electrons and does not account for the Pauli's exclusion principle. In order to bring in the Pauli's exclusion principle one has to go beyond the Hartree method.

2.1.3. Hartree-Fock approximation

In the *Hartree-Fock (HF) approximation* [3] the orthonormal spin orbitals that minimize the total energy is given by

$$E[\Psi] = \frac{\langle \Psi | H | \Psi \rangle}{\langle \Psi | \Psi \rangle} \quad (2.1.6)$$

for the above determinant form of Ψ_{HF} are found. The normalization integral

$\langle \Psi_{HF} | \Psi_{HF} \rangle$ is equal to 1 and energy is given by the formula

$$E_{HF} = \langle \Psi_{HF} | H | \Psi_{HF} \rangle = \sum_{i=1}^N H_i + \frac{1}{2} \sum_{i,j=1}^N (J_{ij} - K_{ij}) \quad (2.1.7)$$

where

$$H_i = \int \psi_i^*(x) \left[-\frac{1}{2} \nabla^2 + v(x) \right] \psi_i(x) dx \quad (2.1.8)$$

$$J_{ij} = \iint \psi_i(x_1) \psi_i^*(x_1) \frac{1}{r_{12}} \psi_j^*(x_2) \psi_j(x_2) dx_1 dx_2 \quad (2.1.9)$$

$$K_{ij} = \iint \psi_i(x_1)\psi_j^*(x_1)\frac{1}{r_{12}}\psi_i(x_2)\psi_j^*(x_2)dx_1dx_2 \quad (2.1.10)$$

J_{ij} are called as *Coulomb integrals* and K_{ij} are called *exchange integrals*.

Minimization of equation (2.1.7) subject to the orthogonalization conditions gives the HF differential equations

$$F\Psi_i(x) = \sum_{j=1}^N \varepsilon_{ij}\psi_j(x) \quad (2.1.11)$$

where

$$F = -\frac{1}{2}\nabla^2 + v + g = -\frac{1}{2}\nabla^2 + v + j - k \quad (2.1.12)$$

and j and k are the Coulomb and exchange operators respectively. In the HF scheme the one-electron effective potential has the form $v + g$, where v is the potential of an electron in the external field and g is equal to sum of Coulomb potential, taking into account the repulsion of the other electrons, and the exchange potential, which has no classical interpretation and is caused by the antisymmetrization of the one-electron functions in the expressions for ψ . The Coulomb and exchange potentials for each ψ_i depend on the solutions ψ_j of all the other equations with $j \neq i$. Therefore the HF equations form a system of interrelated equations that is solved by the *self consistency method*.

Even if the HF equations are correctly solved, the method eventually turns out to be theoretically incomplete. Despite the correct treatment of electronic exchange within the HF theory, electronic correlation is totally missing. Consequently the *correlation energy* may be defined as the difference between

the correct energy and that of the HF solution i.e. $E_{\text{corr}} \equiv E - E_{\text{HF}}$. Therefore, for including correlation one has to go beyond the HF theory.

2.1.4. Beyond Hartree-Fock (Correlation energy)

Some instances of the different methods that take correlation effects into account are the Møller-Plesset (MP) perturbation theory [4], configuration interaction (CI) [5] and coupled cluster (CC) [6]. In perturbation theory the difference between the exact Hamiltonian and sum of one electron operators is introduced as a perturbation to the unperturbed HF solution. Correlation corrections can be derived to a chosen order. Another way to include correlation is to work with a multi-determinant wavefunction instead of the single-determinant wave function. This approach is used in CI and CC methods. Treatment of exchange and correlation follows another route in the density functional theory which is covered in the next section.

2.2. Density functional theory

The *density functional theory* (DFT) [7] allows one to move away from the N electron wavefunction Ψ and its associated Schrödinger equation and replace them by the much simpler electron density $\rho(r)$ and its corresponding calculation scheme. The history of using electron density as the basic variable began with the pioneering work of Thomas and Fermi.

2.2.1. Thomas-Fermi theory

Thomas [8] and Fermi [9] proposed in 1927 that statistical considerations can be used to estimate the distribution of electrons in an atom. In this method the kinetic energy is approximated as an explicit functional of density, idealized as non-interacting electrons in a homogeneous gas with a density equal to the local density at the given point. Neglecting the exchange and correlation terms, the *Thomas-Fermi (TF) total energy* of an atom with a nuclear charge Z in terms of electron density is given by

$$E_{TF}[\rho(r)] = C_F \int \rho^{5/3}(r) dr - Z \int \frac{\rho(r)}{r} dr + \frac{1}{2} \iint \frac{\rho(r)\rho(r')}{|r-r'|} \quad (2.2.1)$$

where the Fermi coefficient $C_F = 2.871$. Assuming that for the ground state of an atom the electron density minimizes the energy functional $E_{TF}[\rho(r)]$ under the constraint

$$N = N[\rho(r)] = \int \rho(r) dr \quad (2.2.2)$$

Applying the method of Lagrange multipliers to incorporate the constraint, the ground-state electron density must satisfy the variational principle

$$\delta\{E_{TF}[\rho] - \mu_{TF}(\int \rho(r) dr - N)\} = 0 \quad (2.2.3)$$

which yields

$$\mu_{TF} = \frac{\delta E_{TF}[\rho]}{\delta \rho(r)} = \frac{5}{3} C_F \rho^{2/3}(r) - \left[\frac{Z}{r} - \int \frac{\rho(r_2)}{|r-r_2|} dr_2 \right] \quad (2.2.4)$$

Hence, the TF theory involves solving the Equation (2.2.4) under the constraint (2.2.2) and inserting the resulting electron density in Equation (2.2.1) to yield the total energy.

The TF theory though allows the explicit calculation of an atom's total energy, its accuracy is low. The errors for the total energies of atoms are relatively large and still more for molecules which are unstable within the TF theory. Due to these reasons, this method was considered as an oversimplified model.

2.2.2. Hohenberg-Kohn theorems

The modern formulation of density functional theory originated with the fundamental theorems of Hohenberg and Kohn [10]. The *first Hohenberg-Kohn (HK) theorem* states that: *The external potential $v(r)$ is determined, within a trivial additive constant, by the electron density $[\rho(r)]$.* Since $[\rho(r)]$ determines the number of electrons, it follows that $[\rho(r)]$ also determines the ground-state wavefunction Ψ and all other properties such as kinetic energy $T[\rho(r)]$, potential energy $V[\rho(r)]$ and total energy $E[\rho(r)]$ of the system. Hence the ground state expectation value of any observable, including the total energy, is a unique functional of the ground-state electron density $[\rho(r)]$.

$$E[\rho] = T[\rho] + V_{ne}[\rho] + V_{ee}[\rho] = \int \rho(r)v(r)dr + F_{HK}[\rho] \quad (2.2.5)$$

where $F_{HK}[\rho] = T[\rho] + V_{ee}[\rho]$ (2.2.6)

The *second HK theorem* states that: For a trial density $\tilde{\rho}(r)$ such that $\tilde{\rho}(r) \geq 0$ and

$$\int \tilde{\rho}(r) dr = N$$

$$E_0 \leq E_v[\tilde{\rho}] \quad (2.2.7)$$

This provides a variational principle such that the search for the lowest-energy wavefunction $\Psi_0(r)$ can be replaced by a search for the lowest energy electron density $[\rho_0(r)]$ and the ground-state energy E_0 is given as the minimum of the functional $E_v[\rho_0(r)]$.

The classical part of the electron-electron interaction $V_{ee}[\rho_0(r)]$ in Equation (2.2.6) is the Coulomb potential energy

$$J[\rho] = \frac{1}{2} \iint \frac{\rho(r_1)\rho(r_2)}{|r_2 - r_1|} dr_1 dr_2 \quad (2.2.8)$$

In the TF theory $V_{ee}[\rho(r)]$ is replaced by $J[\rho(r)]$ and kinetic energy $T[\rho(r)]$ is taken from the theory of a non-interacting uniform electron gas. This constitutes a direct approach for calculating $T[\rho(r)]$ and therefore the total energy if the electron density is known but only approximately. It would however be preferable to correctly calculate as $T[\rho(r)]$ it forms the leading part of the total energy. Kohn and Sham proposed introducing orbitals into the problem allowing more accurate computation of $T[\rho(r)]$ with a small residual correction that is handled separately.

2.2.3. Kohn-Sham equations

For a system of non-interacting electrons the kinetic energy is

$$T_0 = \sum_{i=1}^N n_i \langle \psi_i | -\frac{1}{2} \nabla^2 | \psi_i \rangle \quad (2.2.9)$$

and the electron density is

$$\rho(r) = \sum_{i=1}^N n_i |\psi_i(x)|^2 \quad (2.2.10)$$

with x including both space and spin coordinates. Here ψ_i and n_i are the natural spin orbitals and their occupation numbers respectively. Using orbitals to calculate the kinetic energy is an indirect though accurate approach.

Kohn and Sham [11] replaced the interacting many-body problem by a corresponding noninteracting particle system with the same density in an appropriate external potential. The total energy functional is then expressed in atomic units as

$$E[\rho(r)] = T_0[\rho(r)] + \frac{1}{2} \iint \frac{\rho(r)\rho(r')}{|r-r'|} dr dr' + E_{xc}[\rho(r)] + \int \rho(r)v(r)dr \quad (2.2.11)$$

In the above equation the first term is the kinetic energy functional of the system of noninteracting electrons with the same density, the second term is the classical Coulomb energy for the electron-electron interaction, the third term is energy functional incorporating all the many-body effects of exchange and correlation and the last term is the attractive Coulomb potential provided by the fixed nuclei.

The construction of the *Kohn-Sham (KS) functional* is based on the assumption that the exact ground state density can be represented by the ground state density of an auxiliary system of noninteracting particles. The solution of the

KS auxiliary system can be viewed as the minimization problem of the KS functional with respect to the density. This leads to N KS equations

$$\left[-\frac{1}{2}\nabla^2 + v_{eff}(\mathbf{r}) \right] \psi_i(\mathbf{r}) = \varepsilon_i \psi_i(\mathbf{r}) \quad (2.2.12)$$

$$\rho(\mathbf{r}) = \sum_i^N \sum_s |\psi_i(\mathbf{r}, s)|^2 \quad (2.2.13)$$

Here ε_i are eigenvalues, ψ_i are KS orbitals and v_{eff} is the effective potential

$$v_{eff}(\mathbf{r}) = v(\mathbf{r}) + \int \frac{\rho(\mathbf{r}')}{|\mathbf{r} - \mathbf{r}'|} d\mathbf{r}' + v_{XC}(\mathbf{r}) \quad (2.2.14)$$

that is the sum of potential from the nuclei, a Hartree-style potential and the potential for exchange and correlation. The latter is defined as

$$v_{XC}(\mathbf{r}) = \frac{\partial E_{XC}[\rho(\mathbf{r})]}{\partial \rho(\mathbf{r})} \quad (2.2.15)$$

In Equation (2.2.14) $v_{eff}(\mathbf{r})$ depends on $[\rho(\mathbf{r})]$. Hence the KS Equations (2.2.12), (2.2.13) and (2.2.14) have to be solved self-consistently. Therefore, in a DFT calculation one begins with a guess for $[\rho(\mathbf{r})]$ for constructing $v_{eff}(\mathbf{r})$ from Equation (2.2.14). After the first iteration we get a new electron density from which the Hartree and exchange-correlation potentials are generated to yield a new potential. This process is repeated until self-consistency is achieved.

2.2.4. Exchange-correlation functional

In the KS equations while the kinetic energy is incorporated correctly, a challenge in DFT is the search for a good approximation of the exchange-correlation functional $E_{XC}[\rho(r)]$. One of the many approaches is the *local density approximation (LDA)* [11]. The LDA exchange-correlation energy functional is given as

$$E_{XC}^{LDA}[\rho] = \int \rho(r) \varepsilon_{XC}[\rho(r)] dr \quad (2.2.16)$$

Where $E_{XC}[\rho(r)]$ is the exchange-correlation energy per particle of a uniform electron gas of density $[\rho(r)]$. The exchange part of $E_{XC}[\rho(r)]$ can be expressed analytically by that of a homogeneous electron gas.

$$\varepsilon_X[\rho(r)] = -C_X \rho(r)^{1/3}, \quad C_X = \frac{3}{4} \left(\frac{3}{\pi} \right)^{1/3} \quad (2.2.17)$$

The correlation part may be obtained from perturbation theory or from Quantum Monte Carlo method. The corresponding exchange-correlation potential and KS equation then become

$$v_{XC}^{LDA}(r) = \frac{\delta E_{XC}^{LDA}}{\delta \rho(r)} = \varepsilon_{XC}[\rho(r)] + \rho(r) \frac{\partial \varepsilon_{XC}[\rho(r)]}{\partial \rho} \quad (2.2.18)$$

$$\left[-\frac{1}{2} \nabla^2 + v(r) + \int \frac{\rho(r')}{|r-r'|} dr' + v_{XC}^{LDA}(r) \right] \psi_i(r) = \varepsilon_i \psi_i(r) \quad (2.2.19)$$

The self-consistent solution of Equation (2.2.19) defines the *LDA method*. Application of LDA amounts to assuming that the exchange-correlation energy for a non-uniform system can be obtained by applying uniform electron gas

results to infinitesimal portions of the non-uniform electron distribution and then summing over all individual contributions.

LDA is expected to work for systems with slowly varying electron densities. However it was failure for even semiconductors and insulators due to large cancellations in the exchange part. Hence further improvements are called for. A route to bring about this improvement is to take into account the gradient of the electron density. The idea is to include $\partial\rho(r)/\partial r$ as well as $\rho(r)$ to describe the exchange hole. This is implemented via the method of *generalized gradient approximation* (GGA) in which the exchange-correlation energy functional is written as

$$E_{XC}^{GGA}[\rho(r)] = \int \rho(r) F[\rho(r), \nabla\rho(r)] dr \quad (2.2.20)$$

In 1986 the exchange part of E_{XC}^{GGA} was proposed by Perdew and Wang (PW86) [12] and another correction was developed by Becke in 1988 (B88) [13]. Gradient corrections to the correlation part were proposed in 1986 by Perdew (P86) [14], in 1991 by Perdew and Wang (PW91) [15], in 1988 by Lee, Yang and Parr (LYP) [16] and in 1996 by Perdew, Burke and Ernzerhof (PBE) [17]. In all our density functional calculations the PW91 GGA functional and B3LYP GGA functional has been employed.

2.3. Density based reactivity descriptors: Conceptual DFT

Based on the famous Hohenberg and Kohn theorems [10], DFT provided a sound basis for the development of computational strategies for obtaining information about the energetics, structure, and properties of (atoms and) molecules at much lower costs than traditional *ab initio* wave function

techniques. On the other hand, a second branch of DFT has developed since the late 1970s, called “**conceptual DFT**” by its protagonist, R. G. Parr [18]. A breakthrough in the dissemination of this approach was the publication in 1989 of Parr and Yang’s 'Density Functional Theory of Atoms and Molecules' [7], which not only promoted “conceptual DFT” but, certainly due to its inspiring style, attracted the attention of many chemists. Many of such chemical phenomena can be understood and predicted by some theoretical quantities that have a direct relationship with the characteristic sets of important chemical properties. These quantities are, in general, called descriptors. The reactivity descriptors are very much pertinent to the reactivity of the molecular systems and are intended to provide a qualitative and semi-quantitative measure of the extent to which a particular site will be affected in a given condition. In the last two centuries, there have been several attempts to explain the nature of bonding and reactivity of molecular systems based on some intuitive ideas, models and empirical rules in terms of the reactivity descriptors [19-21]. In particular, the concept of the highest occupied molecular orbital (HOMO) and lowest unoccupied molecular orbital (LUMO) developed by Fukui (frontier molecular orbital theory) [22], Mulliken's donor acceptor concept (overlap and orientation principle) [23] and Pearson's hardness and softness concept (Hard-Soft Acid-Base principle) [24]. These descriptors or principles have made a profound impact on our understanding of the experimental observations at the microscopic level in an elegant way. Formulation and concept of some of these reactivity descriptors is summarized as follows.

2.3.1. Local Reactivity Descriptors (LRDs)

Density based response functions, called local and global reactivity descriptors (LRD and GRD), are derived from density function theory (DFT) [25]. Within the framework of density functional theory, Parr and co-workers have introduced several important chemical tools [26]. DFT has provided the theoretical basis for the concepts like electronic chemical potential, electro negativity, and hardness, collectively known as global chemical reactivity descriptor [27]. Fukui function [28] can be interpreted either as the change of electron density $\rho(r)$ at each point r when the total number of electrons is changed or as the sensitivity of chemical potential of a system to an external perturbation at a particular point r .

Therefore, the expression of Fukui function can be written as:

$$f(r) = (\partial\rho(r)/\partial N)_{v(r)} = (\partial\mu/\partial v(r))_N \quad (2.3.1)$$

The equation (2.3.1) involves the N -discontinuity problem [29-30] leading to the introduction of both right- and left-hand derivatives.

$$f^+(r) = (\partial\rho(r)/\partial N)_{v(r)}^+ \quad (2.3.2)$$

For a nucleophilic attack

and

$$f^-(r) = (\partial\rho(r)/\partial N)_{v(r)}^- \quad (2.3.3)$$

For an electrophilic attack,

The finite difference method, using the electron densities of N_0 , N_{0+1} , N_{0-1} defines

$$f^+(r) \approx \rho_{N_0+1}(r) - \rho_{N_0}(r) \quad (2.3.4 \text{ a})$$

$$f^{-}(r) \approx \rho_{N_o}(r) - \rho_{N_o-1}(r) \quad (2.3.4 \text{ b})$$

$$f^o(r) \approx \frac{1}{2}(\rho_{N_o+1}(r) - \rho_{N_o-1}(r)) \quad (2.3.4 \text{ c})$$

In order to describe the site reactivity or site selectivity, Yang *et al.* [31] proposed atom condensed Fukui function, based on the idea of electronic population around an atom in a molecule, similar to the procedure followed in population analysis technique. The condensed Fukui function for an atom k undergoing nucleophilic, electrophilic or radical attack can be defined respectively as

$$f_k^{+} \approx q_k^{N_o+1} - q_k^{N_o} \quad (2.3.5 \text{ a})$$

$$f_k^{-} \approx q_k^{N_o} - q_k^{N_o-1} \quad (2.3.5 \text{ b})$$

$$f_k^o \approx \frac{1}{2}(q_k^{N_o+1} - q_k^{N_o-1}) \quad (2.3.5 \text{ c})$$

where q_k is the electronic population of the k^{th} atom of a particular species.

The first and second partial derivatives of $E[\rho]$ with respect to the number of electron N under the constant external potential $v(r)$ are defined as the chemical potential μ and the global hardness η of the system respectively [27].

$$\mu = \left(\frac{\partial E}{\partial N} \right)_{v(r)} \quad \eta = \frac{1}{2} \left(\frac{\partial^2 E}{\partial N^2} \right)_{v(r)} \quad (2.3.6)$$

The inverse of the hardness is expressed as the global softness,

$$S = 1/2\eta \quad (2.3.7)$$

The global descriptor of hardness has been an indicator of overall stability of the system. When the two molecules interact, particular site, which is the most reactive site of the molecules are involved for the bond formation. So reaction

between two reactants is always local. That's why the site-selectivity of a chemical system cannot be studied using the global descriptors of reactivity. For this, appropriate local descriptors need to be defined. An appropriate definition of local softness $s(r)$ is given by [31],

$$s(r) = \left(\frac{\partial \rho(r)}{\partial \mu} \right)_{v(r)} \quad (2.3.8)$$

such that

$$\int s(r) dr = S \quad (2.3.9)$$

Rewriting Equation (2.3.8) and the definition of global softness, we can write

$$s(r) = \left(\frac{\partial \rho(r)}{\partial N} \right)_{v(r)} \left(\frac{\partial N}{\partial \mu} \right)_{v(r)} \quad (2.3.10)$$

$$= f(r) S \quad (2.3.11)$$

The condensed local softness, s_k^+ and s_k^- are defined accordingly for nucleophilic and electrophilic attack, respectively.

2.3.3. HOMO-LUMO analysis

Since the derivative of 2.3.1 is not known exactly, there are various different strategies to calculate, in an approximate way, the Fukui function. Two different finite-difference approaches can be followed. Separate calculations of $(N_0 + 1)$ and $(N_0 - 1)$ electrons simply by relaxation of orbitals from the neutral system. This approach has been known as the 'relaxed orbital' approach. On the contrary, assuming that the shape of molecular orbitals does not change when a small amount of charge is added or subtracted, Yang *et. al.* calculated the derivative of 2.3.1 as, governing electrophilic attack,

$$f^{-}(\vec{r}) \approx \rho_{HOMO}(\vec{r}) \quad (2.3.12)$$

Governing nucleophilic attack,

$$f^{+}(\vec{r}) \approx \rho_{LUMO}(\vec{r}) \quad (2.3.13)$$

And governing radical attack,

$$f^0(\vec{r}) \approx \frac{1}{2}[\rho_{HOMO}(\vec{r}) + \rho_{LUMO}(\vec{r})] \quad (2.3.14)$$

known as the ‘frozen orbital’ approximation, where $d\rho$ is same as $d\rho_{valance}$. Under frozen orbital approximation atom-condensed Fukui functions will be nothing but the respective atomic population of HOMO or LUMO orbitals. FMO theory predicts that the preferable electrophilic reaction in a molecule will take place at the site where the relative density of the HOMO is high and the position, which has a relatively high LUMO density, is preferable for the nucleophilic reaction.

2.3.4. Pearson’s definitions of Hardness and Softness

The general idea of classifying reagents with respect to their chemical behaviour stimulated further research on the physical properties of the complexes. Among all, the work contributed by Pearson is considered to be one of the most important works and it has been found to be very useful for correlating and better understanding of a very large amount of chemical information in terms of the hard and soft parameters. Later on these concepts were coined as HASB principle around 1963. He has actually classified the molecular systems in terms of the hard-soft acid-base in a general way: Hard acid: acceptors or nucleophiles, Soft acid: Low positive charge, Hard base: donors or electrophiles, Soft base: Low electronegativity. HSAB principle says that there is an extra stabilization if hard

acids bind to coordinate with hard bases and soft acids bind to coordinate with soft bases. A more interesting idea is the one that relates the hard-hard and soft-soft character, respectively, to ionic and covalent interaction [32-33]. A simple explanation for hard-hard interactions is by considering them to be primarily electrostatic or ionic interactions.

2.4. Molecular Dynamics

Molecular properties are very sensitive to the environment and the temperature. The effects of a finite temperature can be incorporated by means of the statistical mechanics methods. The representative samplings of the system are generated at finite temperature known as simulation. There are two major techniques for generating an ensemble namely Monte Carlo (MC) and molecular dynamics (MD). However, time-dependent phenomenon can be studied with molecular dynamic simulations. The method generates a series of time-correlated points in phase space (a trajectory) by propagating a starting set of coordinates and velocities according to Newton's second equation by a series of finite time steps.

2.4.1. Classical Molecular Dynamics

The basic principle of classical molecular dynamic is that the nuclear motion in a molecular system is treated by the classical equations of motion. The forces on atoms are derived from classical potential such as Lennard-Jones, Buckingham, etc. These classical potentials do not describe the electronic motion and hence, classical MD becomes computationally much cheap. Here the successive configurations of the system are generated by integrating the Newton's

equation of motion. Thus the time correlation of positions and velocities of the atoms in the system can be explained. Hence, MD is a deterministic approach, in which the state of the system at any future time can be predicted from its current state [34].

The trajectory is obtained by solving the differential equations involved in the Newton's second law. Given a set of atoms of masses M_I at position R_I one can write

$$F_I = M_I \ddot{R}_I \quad (2.4.1)$$

Where F_I is the force on atom I, which is related to the potential $U(R_I)$ as

$$F_I = -\frac{\partial U(R_I)}{\partial R_I} \quad (2.4.2)$$

Velocity-Verlet algorithm is the most commonly used time integration algorithm in molecular dynamics methods to solve the above equations [34]. The basic idea is to write two third-order Taylor expansions for the position $R_I(t)$, one forward and one backward in time. Adding these two equations gives a recipe for predicting the position a time step Δt later from the current and previous positions, and the current acceleration.

Acceleration can be calculated from force or equivalently, the potential. Velocities are needed to calculate kinetic energy, it can be calculated as

$$V_I(t) = \frac{R_I(t + \Delta t) - R_I(t - \Delta t)}{2\Delta t} \quad (2.4.3)$$

The velocities, forces and instantaneous values of all properties obtained after every Δt step is stored. This time ordered information can be used to calculate time correlation function, and thus can be used to calculate the transport

properties such as diffusion coefficient, viscosity coefficient, etc. The temperature dependent properties can also be calculated from the equipartition law.

$$\frac{3}{2}NK_B T = \left\langle \sum_{i=1,N} \frac{1}{2} m_i v_i^2 \right\rangle \quad (2.4.4)$$

In classical MD it is difficult to account for the local atomic properties such as, chemical bonding, including the chemical reactions which form and break bonds in a quantum mechanical fashion. On the other hand, quantum dynamics of the nuclear motion of a large molecular system becomes highly computationally expensive. These difficulties can be accomplished by the use of *ab initio* MD (AIMD).

2.4.2. *Ab Initio* molecular dynamics

In AIMD, the motion of the individual atoms is simulated using forces which are calculated quantum mechanically [35-36]. The nuclei are much heavier than the electrons, thus should be moved classically using the Newton's equation of motion under the electronic potential derived from quantum mechanical approach. In 1985, in a seminal paper, Car and Parrinello initiated the field of AIMD by combining the conventional MD technique with the DFT and were termed to be CPMD [37]. Thus the study of formation and breaking of chemical bonds became possible, in contrast to the conventional MD. A number of other techniques have been developed which are based on minimization of the electronic orbitals to their ground state at each time step. These techniques were referred to as BOMD [38].

Born-Oppenheimer molecular dynamics

It is the most commonly applied approach to AIMD. The BOMD simulation solving the static electronic structure problem is solved in each molecular dynamics step, given the set of fixed nuclear positions at that instance of time [38]. Where the time-independent Schrödinger equation is solved and simultaneously nuclei are propagating through classical molecular dynamics. The electronic problem is solved using DFT for obtaining the ground state eigenvalue. For an interacting system of electrons with classical nuclei fixed at positions $\{R_N\}$, the total ground state energy can be found by minimizing the KS energy functional with respect to basis subject the orthonormality constrain. The corresponding Lagrangian for BOMD is given as

$$\mathcal{L}_{BO}(R^N, \dot{R}_N) = \sum_{I=1}^N \frac{1}{2} M_I \dot{R}_I^2 - \min_{\{\phi_i\}} E^{KS}[\{\phi_i\}, R^N] \quad (2.4.5)$$

Equations of motion are given as

$$M_I \ddot{R}_I = -\nabla_I \left[\min_{\{\phi_i\}} E^{KS}[\{\phi_i\}, R^N] \right] \quad (2.4.6)$$

The equation of motion ensures that the minimization of the electronic energy is done at each MD step.

2.4.3. Parameter for analysis of BOMD trajectories

The insight of the cluster system and the motion of atoms within it is understood and analyzed through two traditional thermodynamic parameters viz.

RMS and MSD [39] in the work presented in this thesis. For the sake of completeness we briefly discuss these properties below:

Root-Mean Square BLF (Bond Length Fluctuation)

The parameter root-mean squared bond-length fluctuation (RMS-BLF or δ_{RMS}) are computed for trajectory at each temperature for individual clusters.

The parameter δ_{RMS} is a measure of the fluctuations in the bond lengths averaged over all the atoms and over the total time span. It is defined as:

$$\delta_{rms} = \frac{2}{N(N-1)} \sum_{i < j} \frac{\sqrt{\langle R_{ij}^2 \rangle_t - \langle R_{ij} \rangle_t^2}}{\langle R_{ij} \rangle_t} \quad (2.4.7)$$

where, N is the number of particles in the system, r_{ij} is the distance between the i^{th} and j^{th} particle in the system and $\langle \dots \rangle_t$ denotes a time average over the entire trajectory.

2.5. References

- [1] Schrödinger E, Ann Phys 79 (1926) 361.
- [2] Born M, Oppenheimer J R, Ann Phys 84 (1927) 457.
- [3] Roothaan C C J, Rev Mod Phys 23 (1951) 69.
- [4] Møller C , Plesset M S, Phys Rev 46 (1934) 618.
- [5] Sherrill C D, Schaefer H F, Adv Quantum Chem 34 (1999) 143.
- [6] Bartlett R J, J Phys Chem 93 (1989) 1697.
- [7] Parr R G, Yang W, *Density functional theory of atoms and molecules*, Clarendon Press, New York 1989.
- [8] Thomas L H, *Proc. Cambr Phil Soc* 23 (1927) 542.
- [9] Fermi E, Z Phys 48 (1928) 73.
- [10] Hohenberg P, Kohn W, Phys Rev 136 (1964) 864.
- [11] Kohn W, Sham L J, Phys Rev 140 (1965) 1133.
- [12] Perdew J P, Wang Y, Phys Rev B 33, (1986) 8800.
- [13] Becke A D, Phys Rev A 38 (1988) 3098.
- [14] Perdew J P, Phys Rev B 33 (1986) 8822.
- [15] Perdew J P, Wang Y, Phys Rev B 45 (1992) 13244.
- [16] Lee C, Yang W, Parr R G, Phys Rev B 37 (1988) 785.
- [17] Perdew J P, Burke S, Ernzerhof M, Phys Rev Lett 77 (1996) 3865.
- [18] Parr R G, Yang W, Annu Rev Phys Chem 46 (1995) 701.
- [19] (a) Pauling L, *The Nature of Chemical Bond and Structure of Molecule and Crystals*; Oxford and IBH: New Delhi, 1967. (b) Pal S, Chandrakumar K R S, J. Am. Chem. Soc. 2000, 122, 4145. (c) Chandrakumar K R S, Pal

- S, *J. Phys. Chem. A* 2002, 106, 5737. (d) Chandrakumar K R S, Pal S, *J Phys Chem A* 105 (2001) 4541. (e) Ghosh S K, *Chem Phys Lett* 172 (1990) 77.
- [20] (a) Mc Weeny R, *Coulson`s Valence*, Oxford University Press , Oxford, 1979. (b) Roy R K, Krishnamuthy S, Geerlings P, Pal S, *J Phys Chem A* 102 (1998) 3746. (c) Roy R K, Pal S, Hirao K, *J Chem Phys* 110 (1999) 8236. (d) Chattaraj P K, Maiti B, Sarkar U, *J Phys Chem A* 107(2003) 4973. (e) Chattaraj P K, *J Phys Chem A* 105 (2001) 511. (f) Parthasarathi R, Padmanabhan J, Elango M, Subramanian V, Chattaraj P K, *Chem Phys. Lett* 394 (2004) 225.
- [21] (a) Maksic Z B, *Theoretical Models of Chemical Bonding: The Concept of the Chemical Bond*; Ed.; Springer-Verlag: Berlin, 1990. (b) Krishnamurthy S, Roy R K, Vetrival R, Iwata S, Pal S, *J Phys Chem A* 101 (1997) 7253. (c) Parr R G, Chattaraj P. K, *J Am Chem Soc* 113 (1991) 1854 (d) Garza J, Vargas R, Cedillo A, Galván M, Chattaraj P K, *Theor Chem Acc* 115 (2006) 257.
- [22] K. Fukui, *Theory of Orientation and Stereo Selection*; Springer-Verlag, Berlin 1975.
- [23] (a) Mulliken R S, *J Am Chem Soc* 74 (1952) 811. (b) Orgel L E, Mulliken R S, *J Am Chem Soc* 79 (1957) 4839; (c) Tsubomura R S, Mulliken H, *J Am Chem Soc* 82 (1960) 5966.
- [24] (a) Pearson R G, *Hard and Soft Acids and Bases*, Dowden, Hutchinson, and Ross, Stroudsburg, PA, 1973; (b) Pearson R G, *Chemical Hardness: Applications from Molecules to Solids*; Wiley-VCH Verlag GMBH: Weinheim; 1997.

- [25] Parr, R. G.; Yang W. Oxford University Press, New York 1989.
- [26] Parr R G, Yang W, J Am Chem Soc 106 (1984) 4049-4050.
- [27] (a) Pearson R G, J Am Chem Soc 85 (1963) 3533-3539 (b) Sen K D, Chemical Hardness Struct. Bonding (Ed); Springer-Verlag: Berlin 1993 80, (c) Parr R G, J Am Chem Soc 105 (1983) 7512 (d) Parr R G, Donnelley R A, Levy M, Palke W E, J Chem Phy. 68 (1978) 3801-3808 (e) Pearson R, J Am Chem Soc 107 (1985) 6801.
- [28] Lis L J, McAlister M, Fuller N, Rand R P, Parsegian V A, Biophys J 37 (1982) 667.
- [29] Perdew J P, Parr R G, Levy M, Balduz J, L Phys Rev Lett 49 (1982) 1691.
- [30] Zhang Y, Yang W, Theor Chem Acc 103 (2000) 346-351.
- [31] (a) Yang Y, Parr R G, Proc Natl Acad Sci USA, 82 (1985) 6723. (b) Yang W, Mortier W J, J Am Chem Soc 108 (1986) 5708.
- [32] Huheey J E, Inorganic Chemistry: Principles of Structure and Reactivity; Harper and Row: New York, 1983.
- [33] Klopman G, Chemical Reactivity and Reaction Path, Wiley, New York, 1974.
- [34] Allen M P, Tildesley D J, Computer Simulation of Liquids. Clarendon Press,
- [35] Payne M C, Teter M P, Allan D C, Arias T A, Joannopoulos J D, Rev. Mod. Phys. 64 (1992) 1045.
- [36] Tuckerman M E, Ungar P J, von Rosenvinge T, Klein M L, J Phys Chem 100 (1996) 12878.
- [37] Car R, Parrinello M, Phys Rev Lett 55 (1985) 2471.

- [38] Marx D, Hutter J, Ab Initio Molecular Dynamics: Theory and Implementation published in Modern Methods and Algorithms of Quantum Chemistry, Edited by J. Grotendorst, NIC series **3** (2000).
- [39] (a) Kanhere D G, Vichare A, Blundell S A, Reviews in Modern Quantum Chemistry, edited by K. D. Sen, World Scientific, Singapore, 2001. (b) Berry RS, Haberland H, Clusters of Atoms and Molecules I, edited by H. Haberland Springer-Verlag, Berlin, 1994.

CHAPTER 3

Molecular Conformations of Na- DiMyristoyl PhosphatidylGlycerol (DMPG)

Abstract

Molecular conformations comprising a lipid bilayer determine the physico-chemical properties of the latter. In the present work, we attempt to understand the various possible conformations available for an anionic lipid molecule DiMyristoyl-PhosphatidylGlycerol (DMPG) with Na as its charge compensating cation. Our study reveals a rich conformational space with two different types of glycerol body orientations, more commonly known as rotamers. Interestingly, this is in agreement with the molecular conformations proposed earlier by NMR studies on lipid monomer solutions. We demonstrate that these conformations are an outcome of delicate balance of electrostatic and van der Waals forces along with intramolecular hydrogen bonds achieved by a critical combination of torsion angles. Na^+ ions are seen to interact predominantly with the oxygen atoms of the glycerol groups in tail and head along with that of phosphate oxygen atoms leading to a cage like orientation of lipid molecule around the Na^+ . Following the conformational analysis, we attempt to evaluate the electronic properties of few low lying conformations. The study shows that though the water molecules screen the $\text{Na-O}_{\text{lipid}}$ interactions, they do not dramatically modify the $\text{Na-O}_{\text{lipid}}$ bond distances. The lipid conformation retains the cage like structure around the Na^+ in the presence of water molecules. Some amount of charge transfer from the water molecules to Na ion is noted. The water molecules modify the phosphate-tail glycerol group interactions leading to a more stable $\text{Na-DMPG-H}_2\text{O}$ and $\text{Na-DMPG-4H}_2\text{O}$ complexes.

3.1. Introduction

Phospholipids are the third most important biological constituents after nucleic acids and proteins. As bilayers, they are the building blocks of cell membranes, thereby controlling specific transport between the cell and other biological constituents. In this context, physico (phase transition temperature) and chemical (composition, structure of the lipid molecules within the bilayer) properties of phospholipid bilayers are fundamental to the sustenance of the life [1]. One of the most debated topics in the area of phospholipids is the kind of conformations that populate various lipid bilayers in the gel (non-melted state of the bilayer) and liquid crystalline (melted state of the bilayer) states. For this purpose, various experimental techniques such as NMR [2-6] and X-ray [7] has been applied in the past. Various conformations were proposed based on these studies, [7] with some of them being confirmed by later, by experimental methods [2-3], while some others being debated upon [4-6]. Theoretical methods, especially those based on Molecular Mechanics (MM) methods, were also applied vigorously to analyze the various possible conformational probabilities within a bilayer [8-18]. Interestingly, most of the theoretical simulations (specially the MM based studies) begin with the conformations predicted by the old X-ray studies and hence, with more biased conformations. Thus, a clear consensus on the individual structure of lipid molecules and their role in controlling the dynamical properties of bilayer is still eluding. In this context, it is more meaningful and interesting to design bilayers with various possible conformations and analyze their stability-property relationship from a more fundamental aspect. This could eventually help in designing bilayers with functional

properties. The first step towards this is to have a database of various possible conformations that a lipid molecule can orient into along its synthesis during different enzyme catalyzed reactions. This is governed by various forces present within a molecule.

The phospholipid molecules synthesized from glycerol, two fatty acids and a phosphate group has a polar head region and a non-polar tail region (see Fig1). Hence, each of the molecular forces further comprises (a) electrostatic interactions (attractive and repulsive), (b) hydrogen bonds, (c) dispersive forces, and (d) ionic bonds (in case of charged lipid molecules). Molecular conformation dominating a bilayer is thus an outcome of the balance of all these forces within and between the molecules. A complete insight about all these forces and hence their role in stabilizing various conformations is best obtained from a Quantum Mechanical (QM) methodology. Several research groups have attempted to understand these aspects in recent years. However, due to the large size of phospholipid molecule QM studies have been limited to understanding the interactions of the polar head group so far. Early studies used methylphosphate ions as models and applied semi-empirical or Hartree Fock methods to analyze the structural [19-21] and hydration properties [22]. More recent studies have applied Density Functional Theory (DFT) based methodologies to the same effect with improved understanding on the hydration [23-24] and electronic polarization [25] around the head group and interaction of the head group with the model dust particles [26]. Another recent study has applied hybrid QM/MM method to study the hydration phenomena of dipalmitoylphosphatidylcholine head group. [27]

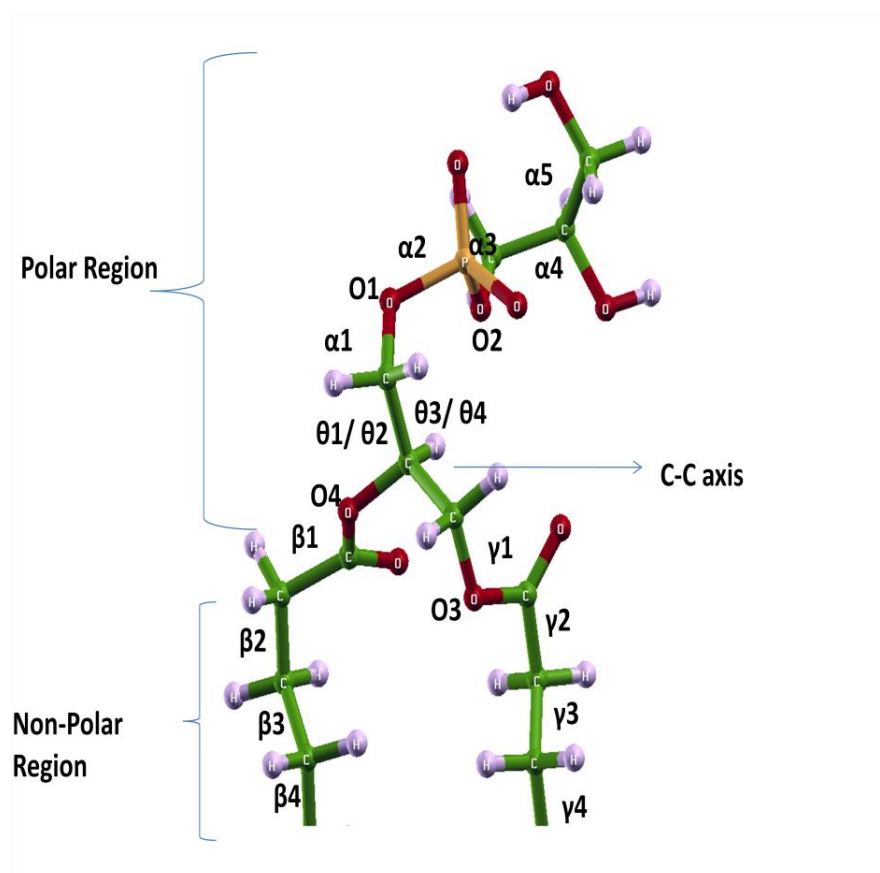


Figure 3.1. Standard torsion angle nomenclature with a phospholipid molecule. The figure also indicates the polar and non-polar regions of the molecule. Torsion angles α_1 - α_5 comprise of head; θ_1 , θ_2 , θ_3 , θ_4 comprise of neck region; and β_1 - β_4 , γ_1 - γ_4 comprise of body region. α_5 , α_4 , α_3 , α_2 , α_1 angles correspond to C-C-C-O2, C-C-O2-P, C-O2-P-O1, O2-P-O1-C, and P-O1-C-C respectively. θ_1 , θ_2 angles correspond to O1-C-C-C and O1-C-C-O4 respectively. θ_3 , θ_4 correspond to C-C-C-O3, and O4-C-C-O3 respectively. Thus, θ_1 , θ_2 torsion are interlinked. Similarly, θ_3 , θ_4 torsion angles are interlocked with each other.

DFT based conformational analysis on complete phospholipid molecules have been much more limited and still at its incipient stage with one of the works applying

semi-empirical methods on dimyristoyl phosphatidylcholine (DMPC) and its interaction with dipyridamole [28]. One of the recent studies applying DFT with empirical dispersion effects [29] on a DMPC molecule has brought out the richness of the conformational space of phospholipid molecules. The various conformers and their IR spectra were in good agreement with the experimental data obtained for DMPC bilayers highlighting that the DMPC molecules preserve their individual molecular structures in various assemblies. Another recent study [30] has further revealed that various conformations in phospholipids have their origin in the “de novo” synthesis and originate from the different conformational structures of glycerol (G) and glycerol 3-phosphate (G3P). Further it is noteworthy, that even the physical properties such as phase transition temperature of lipid molecule are driven by the characteristic conformations composing a bilayer [31- 32]. In short, conformations in various lipid bilayers are more molecular in origin, and the molecular conformations constituting a bilayer determine its physical properties.

Thus, motivated from the above mentioned work, which clearly bring out the importance of molecular conformations, we in this present chapter, attempt to analyze the molecular conformations of a negatively charged phospholipid molecule (DiMyristoyl-PhosphatidylGlycerol, DMPG, with 14 alkyl groups in the chain) and Na^+ as its charge compensating cation (Na-DMPG). PhosphatidylGlycerol's, (PG's) with various charge compensating cations participate in signal transduction [33-34] and hence in combination with other lipid molecules, constitutes 20-25% of the plasma membrane of some systems. It is also the precursor of surfactant and is present in the amniotic fluid of newborn. Hence, due to its importance, we attempt to have a

detailed understanding on the intra-molecular forces influencing the conformations of a DMPG molecule. The molecular conformations obtained in this study will be used for designing and building anionic bilayers. Such an exercise should finally help in bringing about a fundamental understanding on the physico-chemical properties of bilayers and eventually design them with specific applications. The present chapter is a first step towards that where we evaluate the various possible conformations that are available in the molecular phase space of DMPG.

3.2. Methodology: Conformational and Computational Details

Various important torsion angles of a lipid molecule and their standard nomenclature are given in Figure 3.1. The figure also indicates the polar and non-polar regions of the molecule. We have further classified the various regions of the DMPG molecule as follows: torsional angles α_1 - α_5 is grouped as head of the molecule; torsion angles θ_1/θ_2 , θ_3/θ_4 comprise neck region; and β_1 - β_4 , γ_1 - γ_4 comprise body region and remaining part of the alkyl chains known as tails. This classification helps in delineating various molecular conformations obtained in our study as will be discussed in the later sections. Na^+ was considered as the charge compensating cation.

Several initial conformations were conceived based on the above classification: (a) conformations generated by variation in the torsion angles within head, neck, body and tail region each, and (b) orientation of each portion with respect to each other such as head with respect to neck and neck with respect to body etc. This was done by systematically varying the α_1 - α_5 , θ_1/θ_2 , θ_3/θ_4 , and β_1 - β_4 , γ_1 - γ_4 within an interval of 30 degrees. While doing so, some of the conformations resulted in complicated structures

with atoms overlapping one another. However, some 60 starting conformations with various orientations of phosphate, glycerol groups were obtained. We note that the various bond lengths (such as P=O, P-O, C-C, C-H etc.) and bond angles (such as O-P-O, O=P=O, C-C-C and C-C-H etc.) were not varied during the process of generating various conformations. The bond length and bond angles have limited flexibility within the tetrahedral symmetry and it is the variation in the torsion angles that leads wide range of conformations. However, the bond lengths and bond angles undergo marginal variation for a given set of dihedral/torsion angles during the geometry optimization of the molecular conformation. Hence, only explicit variation in the dihedral angles was considered while generating various conformations. All the generated conformations were optimized using DFT method described below. Sodium ion has been included for charge compensation of the molecule in all of the above conformations. For each of the conformation, the position of Na^+ was varied in four ways. In the first position Na^+ was made to interact simultaneously with the oxygen atoms of the phosphate group, the oxygen atoms of head and tail groups as demonstrated in Figure 3.2 (position shown as (I)). In the second case, Na^+ is positioned such that it interacts with the oxygen atoms of the phosphate group and the oxygen atoms of the glycerol group in the head (position “II” in Figure 3.2). In the third case (position “III” in Figure 3.2), the Na ion interacts exclusively with the oxygen atoms of the phosphate group. In the fourth case, the head glycerol group is raised up with Na^+ interacting with the oxygen atoms of the phosphate group and those in the acyl chain only (position IV not shown in figure). Thus, on the whole, we had roughly 200 conformations of DMPG molecule to start with. In addition, we also

have generated two conformations proposed to be present in the crystal structure of DMPG by Pascher and co-workers [35]. Following the optimization of all the above conformations, the lowest energy conformation obtained was considered for understanding the role and position of water molecules on the optimized lowest energy conformer. One to four water molecules were systematically placed around the sodium atom while simultaneously interacting with both phosphate and glycerol groups of the head region.

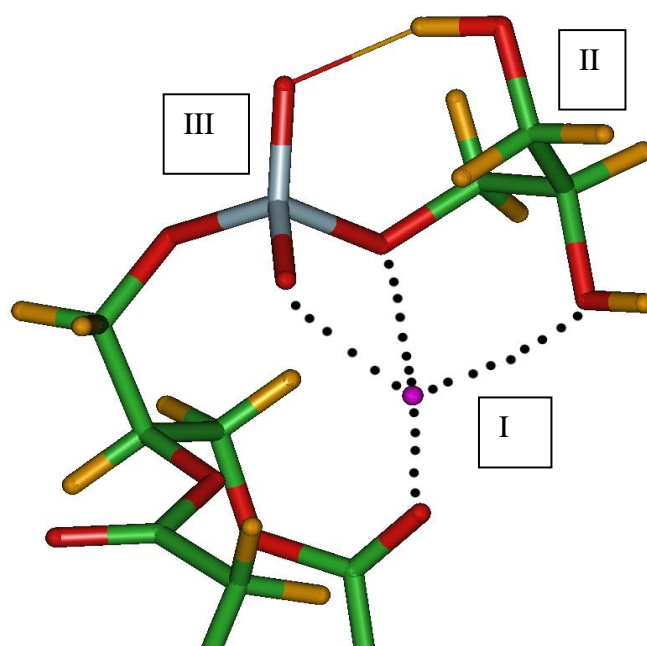


Figure 3.2. A pictorial demonstration of Na-O bonds within the DMPG molecule. The conformation represented below has the charge compensating Na^+ ion (shown in violet color) interacting with the oxygen atoms of glycerol group in the tail, glycerol group in the head as well as with those in the phosphate group (I). The other possible positions of Na^+ correspond to “II” and “III”.

“II” corresponds to the case Na^+ interacts with phosphate group and the glycerol group in the head only and “III” corresponds to the case when Na^+ is interacting exclusively with phosphate groups. It may be noted that the oxygen atoms in cases of “II” and “III” are oriented towards the Na^+ and are slightly differently positioned than

demonstrated later.

All the conformations of DMPG molecule and its charge compensating ion were optimized in the absence and in the presence of water molecules using deMon2k program.[36] The calculations were performed using a Generalized Gradient Approximation (GGA) of PBE exchange functional [37] and LYP correlation functional.[38] This functional was augmented by a damped empirical correction for dispersion-like interactions[39]. The empirical damped dispersion corrections have been included for all the atoms present in the system. This dispersion correction value has been derived using empirical based methods by this equation [39].

$$E_{disp} = -\sum_{i=1}^N \sum_{j=1}^{N-1} (C_6^{ij} / r_{ij}^6) f_{damp}(r_{ij}) \quad (3.1)$$

This describes the sum of all possible contributions of the i,j atom pair in the N atomic system and r_{ij} is the distance between the pair of atoms. This is necessary to account for the stabilizing van der Waals interactions between the alkyl chains [39]. All the atoms were described using double zeta plus valence polarization (DZVP) basis sets [40]. A2 auxillary function was used for fitting the density. The exchange correlation functional was numerically integrated on an adaptive grid with an accuracy of 10^{-5} [41]. The Coulomb energy was calculated by the variational fitting procedure proposed by Dunlap, Connolly and Sabin [42]. A quasi-Newton method in internal redundant coordinates with analytical energy gradients was used for optimizing the systems [43]. The structure was considered to be optimized once the Cartesian gradient and displacement vectors reached a threshold of 10^{-4} and 10^{-3} respectively.

3.3. Results and Discussion

3.3.1. Conformational analysis of a DMPG molecule

Geometric optimization of various DMPG conformations generated by us resulted in nearly 50 distinct local minima lying in the energy range of 0-60 kcal/mol. These minima differ with respect to each other through various aspects such as geometrical parameters (i.e torsional angles in head, neck and body), position of Na ion (as described in the Section 2), presence of intra molecular hydrogen bonds etc. In order to delineate various conformations and group them in a clearer way, we chose to classify them first based on the way the head and the two carbonyl groups (of tails) are arranged with respect to each other. In other words, it depends upon which of the the hydrogen atoms along the C-C axis shown in Figure 3.1, are replaced by the oxygen atoms of the carbonyl chain and head group atoms. Thus, three types of conformations are possible based on the various permutations of the hydrogen atoms being replaced by other alkyl chains. Figure 3(a) gives two of the three possible conformations (known as rotamers). Rotamer A is characterized by a combination of $\theta_3/\theta_4=180/60$, while rotamer B is characterised by $\theta_3/\theta_4=+60/-60$ respectively. This description was first introduced by Hauser and co-workers so as to classify various DMPG molecular conformations in solution [3] and by Pascher and coworkers in crystal structure [35]. Another rotamer with $\theta_3/\theta_4=60/180$ leads to a state where the two acyl chains are no longer in parallel position (figure not shown).

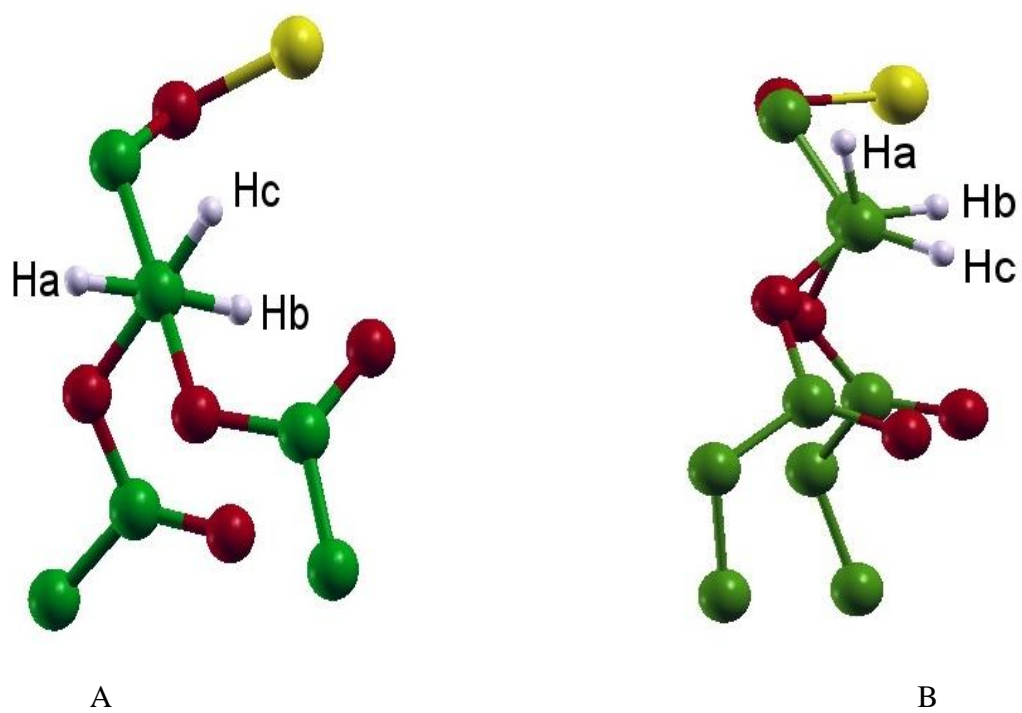


Figure 3.3 (a). Pictorial demonstration of the two possible rotamers (A & B) within a lipid molecule.

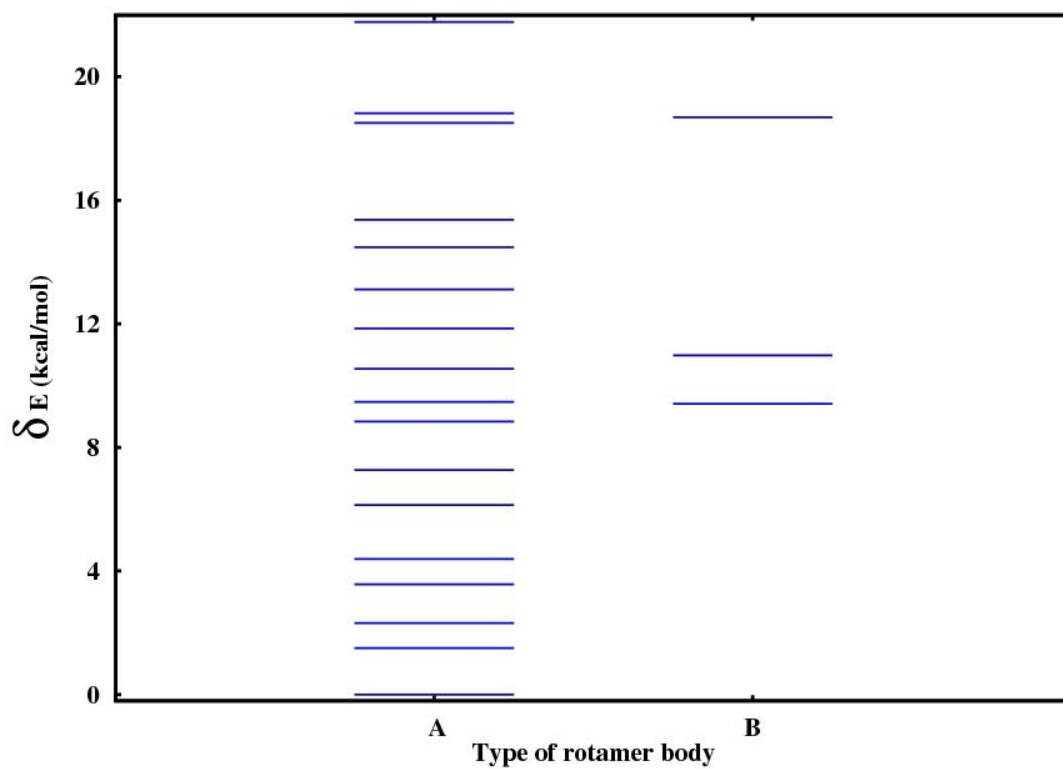


Figure 3.3(b). The energetics of various rotamer conformations as obtained from our DFT study on DMPG molecule. The lowest energy conformation is rotamer A and is referenced as 0.0 kcal/mol

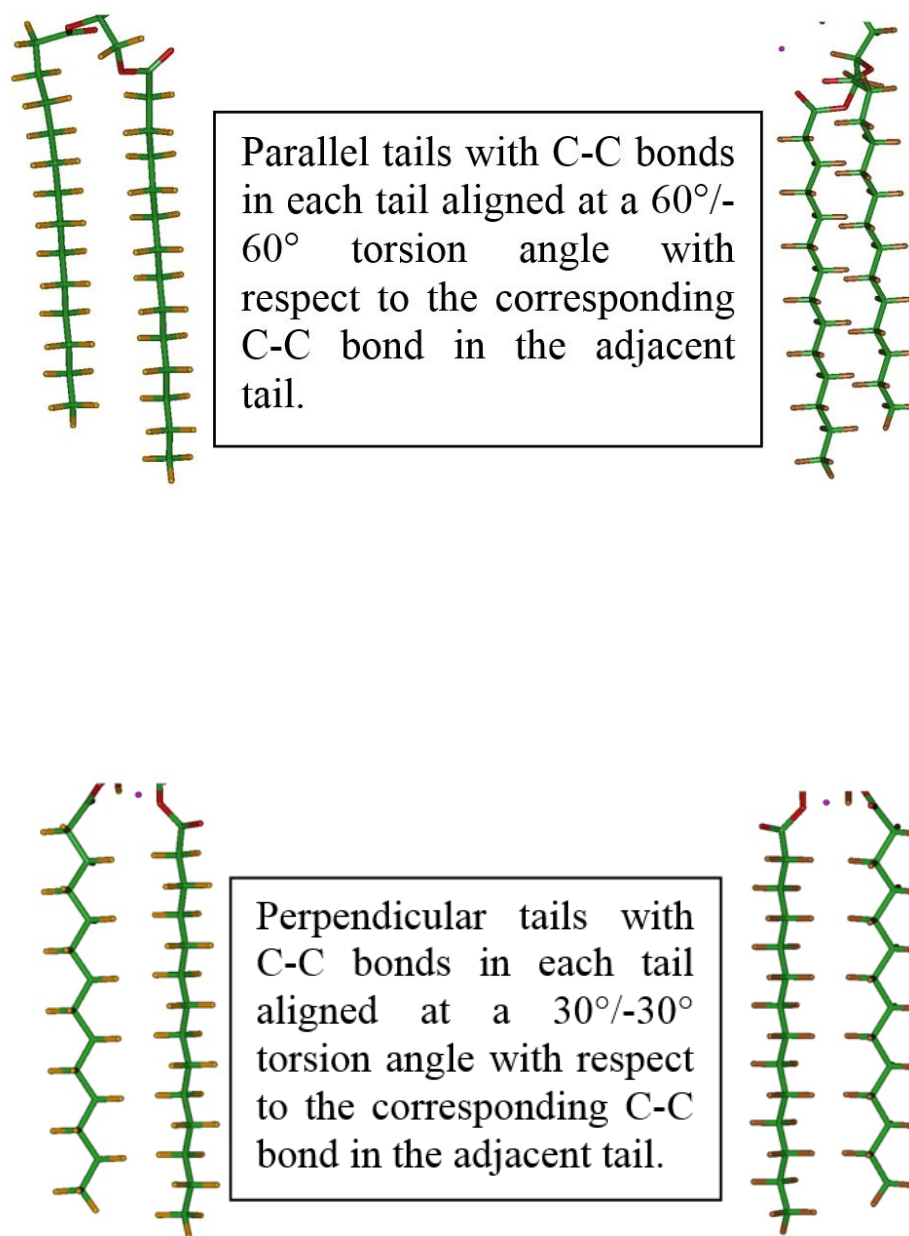


Figure 3.3(c). Parallel and perpendicular alignment of the tails shown in two different perspectives respectively.

It is analyzed that 90% of the distinct local minima obtained in our calculations of DMPG are of rotamer A type. Figure 3.3(b) depicts the potential energy distribution of various rotamers upto 20 kcal/mol. It is interesting to note that in the case of (a) single crystal structure, (b) micellar dispersion (lipid molecules in critical micellar concentration), as well as (c) monomeric solutions (lipid molecules dispersed in concentrations lower than critical micellar concentrations) rotamer A is the dominant conformation. The same is observed for the conformational space of DMPG. Rotamer C conformations are found to be lying at the higher end of the potential energy surface (nearly 60kcal/mol) with respect to the lowest energy conformation. Further analysis revealed that within each rotamer, there is a possibility for the glycerol head to be oriented towards the unsaturated oxygen atom in either gamma or beta chain. Thus, rotamer A conformations are further classified as A_β , A_γ and rotamer B conformation are classified as B_β , B_γ . A preliminary analysis of all the conformations obtained after DFT optimization shows that a higher percentage of them are orientated towards the gamma chain as compared to the beta chains as shown in Table 3.1 (a). This is due to the presence of C-C axis shown in Figure 3.1, which lowers the steric constraints when the head is oriented towards the gamma chain. Above all these, the acyl chains have a possibility to orient themselves parallel to each other (the relative torsion angle between the two corresponding CH_2 groups in acyl chains is 60 degrees in this case, see Figure 3.3 (c)) with lower interacyl chain distance of 4.24 Å. The other mutual orientation of tails is perpendicular to each other with the greater interacyl distance of 5.09 Å. This alignment is demonstrated in Figure 3.3(c). Considering this orientation of the tails, the conformations can be nomenclatured as $A_\beta(\parallel)$, $A_\gamma(\parallel)$, $A_\beta(\perp)$, $A_\gamma(\perp)$,

$B_{\beta}(\parallel)$, $B_{\gamma}(\parallel)$, $B_{\beta}(\perp)$, $B_{\gamma}(\perp)$. These lipid molecular orientations were briefly reported in the NMR study of lipid molecules dispersed in organic solvents as well as in water, in concentrations below critical micellar concentration (when lipid molecules are nearly in monomeric state), thereby validating the presence of such rich conformational space available for a lipid molecule.

Table 3.1(a). Distribution of conformations with glycerol head oriented towards the carbonyl groups in the tail.

<i>Orientation</i>	<i>Boltzman Distribution ratio</i>
Head towards the beta chain	0.131
Head towards the gamma chain	0.868

Table 3.1(b). Various types of intra-molecular hydrogen bonds possible in a DMPG molecule and their possible distribution within our scanned conformations.

<i>H--bond</i>	<i>Percentage</i>
CHOH—O=C beta chain	0%
CH ₂ OH—O=C beta chain	0%
CHOH—O=C gamma chain	20%
CH ₂ OH—O=C gamma chain	0%
CH ₂ OH—phosphate group	73%
CHOH—phosphate group	6%

In other words, there are several conformational orientations of the lipid molecules based on the orientation of the head, neck and body. For each of this conformation, we could have different positioning of sodium ions and intramolecular hydrogen bonds. Table 3.1 (b) elaborates the various types of intramolecular hydrogen bonds possible within a given conformation and their distribution within our scanned conformations. A detailed combination of all the above possible orientations leads to a complicated potential energy surface of the lipid conformation. In the next section, we analyze the lowest ten conformations as obtained from our DFT study with reference to the above classification of the conformations, their energetics and electronic properties.

3.3.2. Structural aspects, electronic properties of the lowest ten DMPG molecular conformations and their comparison with conformations in a single crystal

The position of Na^+ (or rather ion-lipid bridges) is widely debated in the literature [9, 44]. Some of the reports propose the ions to interact more with the phosphate group while others propose an ion-ester carbonyl interaction. Hence, to answer these questions, we have adopted four different positions of Na ion as discussed in Section 2. The ΔE values of all the studied conformations were seen to spread within a relative energy range of nearly 60 kcal/mol. DMPG molecule has four oxygen atoms in the phosphate region, two in the glycerol head group and four in the ester tail region (totaling to 10 oxygen atoms within the polar region of the molecule). During the optimization of all studied conformations, we note a strain in the entire structure with all the oxygen atoms attempting to bond with the charge compensating Na^+ ion. This leads to the presence of several Na-O bonds with the structure as shown in Figure 3.2. The Na-O bond distances in Na-O dimer are typically about 2.56 Å. On the other hand, Na-O bond distances in hydrated cation studies as seen to vary between 2.4 to 2.8 Å [45]. In our case of DMPG molecule, we notice Na-O bond distances varying from 2.25 Å to 2.6 Å in the first sphere followed by Na-O bond distances of 3.10-3.5 Å. In the present case, we have chosen 2.40 Å as a cut off for the ionic bond.[see ref. 45] Bond distances between 2.4 to 2.76 Å have been considered as a co-ordinate Na-O bond. Following this, classification of the type of bonds, we note a clear correlation between the relative stability of the conformation and number of ionic Na-O bonds. This is clearly brought out in Figure 3.4 which gives the relative

energies of various conformations versus the number of Na-O ionic bonds. Most of the conformations with 4 Na-O ionic bonds lie in the lower energy range and the conformations with lower number of Na-O bonds are higher in energy on an average.

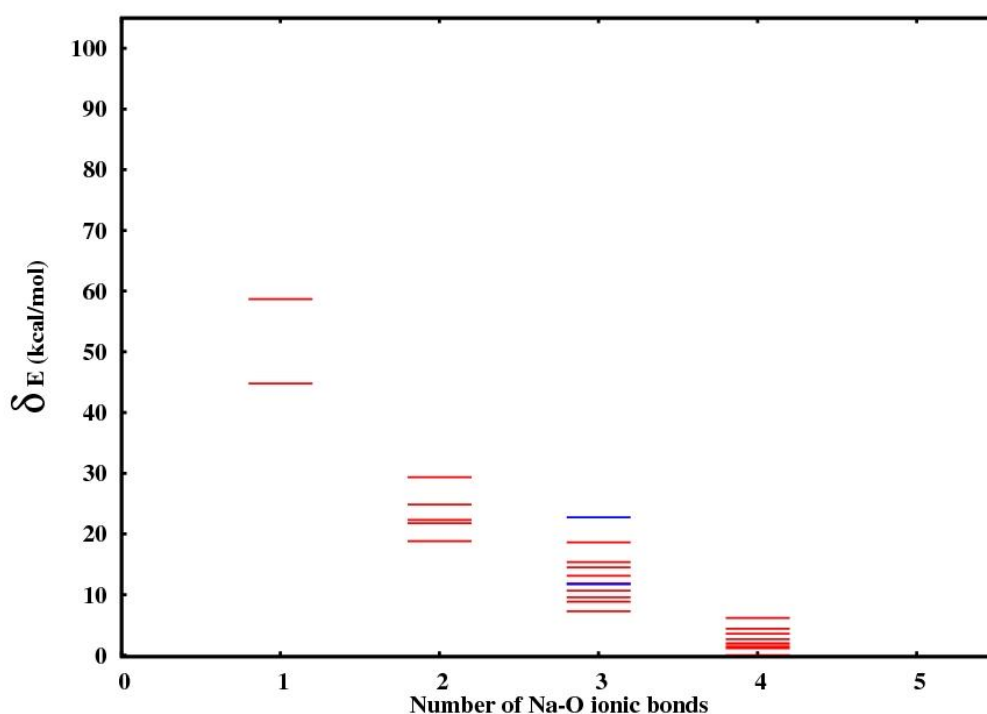


Figure 3.4. Relative energy of various conformations versus the number of Na-O bonds. Blue lines given the energetics of the fully optimized conformations of experimentally proposed geometries while red lines represent the conformations generated from DFT.

While greater number of Na-O ionic bonds is a necessary condition for the better stability of a DMPG molecular conformation, it is not the sufficient condition. In other

words, it appears that higher coordination of Na with O_{lipid} (oxygen atoms of lipid molecule) atom is not the only criterion, determining its overall stability. Other factors that are contributing to the stability of a conformation of a DMPG molecule are: (i) presence of a hydrogen bond within the molecule, (ii) electrostatic repulsion between the phosphate group and the two ester groups within the molecule, (iii) electrostatic repulsion between the two ester groups of the molecule, (iv) electrostatic repulsion between the oxygen atoms of the glycerol group in the head and phosphate group. A balance of all these forces is determined by the torsion angles within a given conformation. In order to explain this statement in detail, we have given in Table 3.2 the structural and energy details of lowest ten conformations obtained by our study of DMPG molecule.

Table 3.2. Electronic and structural properties of the ten lowest energy conformations of DMPG molecule. Average bond and inter atomic distances are given in Å. Energy values are given in kcal/mol.

Conformations	ΔE	No. of Ionic Na-O bonds	No. of coordinate Na-O bonds	No. of Hydrogen bonds	<Ionic Na-O bond distance >	<Distance between P and C _{ester} atoms >	O=C..C=O inter atomic distance
A γ ()	0.00	4	0	1	2.322	5.178	3.673
A β ()	1.19	4	0	1	2.350	4.913	3.954
A β (\perp)	1.44	4	1	1	2.341	5.191	3.634
A β (\perp)	1.88	4	0	1	2.327	5.465	3.895
A β (\perp)	2.00	4	0	1	2.347	4.935	3.993
A γ (\perp)	2.63	4	0	1	2.322	5.495	3.770
A β (\perp)	3.57	4	0	1	2.340	4.951	3.671
A β (\perp)	4.39	3	1	0	2.321	5.425	3.649
A β (\perp)	6.14	3	1	1	2.311	5.141	4.276
A γ ()	7.27	3	0	0	2.326	5.439	3.334

DMPG(A) Fully Optimized	22.74	3	0	0	2.293	6.110	4.780
DMPG(B) Fully Optimized	11.69 9	2	2	0	2.251	5.660	4.400
DMPG(A) Torsion angles fixed to the values as given in Ref. 35	34.30	2	0	0	2.210	6.337	4.564
DMPG(B) Torsion angles fixed to the values given in Ref. 35	34.38	2	0	0	2.220	6.195	3.955

We note that seven of the ten lowest energy conformations have four ionic Na-O bonds and rest of the six oxygen atoms make a coordinate bond with the Na^+ . The average Na-O bond distance (ionic) in the lowest energy conformation is 2.32 Å. The next two low lying conformations have the same number of Na-O bonds as well as similar average Na-O bond distances. However, a closer examination of the Na-O bond distances shows that the four Na-O distances are 2.24, 2.33, 2.33, and 2.39 Å in the ground state geometry, while in the first excited conformation they are 2.31, 2.34, 2.34, and 2.35 Å respectively. In both these conformations, Na^+ is simultaneously coordinated to oxygen atoms of the phosphate group, and the head and tail glycerol groups. The inter atomic distances between the negatively charged C=O groups and phosphate groups are 5.27, 5.09 Å and 5.25, 4.58 Å respectively in the ground state conformation and the first excited state respectively. The slightly longer individual Na-O bond distances and shorter P-C distances result in higher strain within the conformations and consequently slightly higher energy of the first excited state conformation and second excited state. In the fourth and fifth excited state, though Na atom is coordinated to four oxygen atoms, it is coordinated to only the atoms of the tail glycerol group and those in the phosphate group (thus, no atoms from the head glycerol group are involved in the Na-O bonding). Similarly, such minor differences in the positioning of the various charged groups in the structure results in energetically non-degenerate conformations in DMPG. It may be recalled that in one of the previous works, DMPC molecule was seen to have nearly 14 ground state conformations.

Thus, interestingly, the first four lowest energy conformations in DMPG molecule have charge compensating Na ion at “I” position (connecting the oxygen

atoms of the three polar negative regions of the molecule, viz., the phosphate group, the glycerol group in the head and one of the glycerol groups of the tail). Na ion is also present in position IV in the low energy conformations such as fourth and fifth excited state. However, it is ~ 15 kcal/mol and above that we note Na^+ is at positions II and 22 kcal/mol and above Na^+ at positions III. These results are consistent with the earlier reports which suggest that the presence of glycerol groups in the tails strongly influences the position of Na^+ ions in various lipid bilayers.[46,47] Zhao et al in their recent work [44] have proposed that nearly 70% of Na^+ – lipid interactions involve the ester carbonyls (glycerol groups) in the tails. Rest of the 30% of lipid- Na^+ ion interactions involves the phosphate groups of the lipid bilayer. In fact recent literature propose a dynamic movement of ions [47] within the lipid bilayer where the Na^+ ions diffuse from the head group to the glycerol group and back.

It is interesting to compare the energetic and the structural orientations of the above conformations with those proposed by the experimental studies. One of the very few reports available on the experimentally studied molecular conformations of DMPG is an X-ray based study in 1987 by Pascher and co-workers [35]. Through single crystal analysis, they proposed two independent molecules namely DMPG (A) and DMPG(B) to coexist in the crystalline structure. Generation of these two conformation from the given atomic fractional coordinates reveal that both these conformations have perpendicular orientations of tails. Interestingly, the head group in both these conformations is not oriented towards either of the unsaturated oxygen atoms in the tail glycerol groups (see Figure 3.5). The Na ion in both these conformations interacts with one of the oxygen atoms of the phosphate group and one

of the oxygen atoms of the head glycerol group. Optimization of both these conformations results in a considerable change of some of the dihedral angles from the proposed experimental values as shown in the Table 3 (underlined values). The fully relaxed geometry with starting conformation as DMPG (B) lies about 12 kcal/mol above the ground state geometry, while the fully relaxed conformation with DMPG (A) as starting geometry lies about 23 kcal/mol above the ground state conformation. In the former, the Na ion moves considerably to interact with oxygen atoms of the phosphate group as well as the oxygen atoms of the glycerol group in beta acyl chain.

In the latter, we find that Na ion is positioned so as to interact with the oxygen atoms of phosphate group and head glycerol group. A constrained optimization of the DMPG (A) and DMPG(B) proposed conformations in crystal structures was also done so as to fix the torsion angles to the values proposed in the present chapter. These optimizations resulted in high energy conformations which lie above 35 kcal/mol with respect to the ground state conformation.

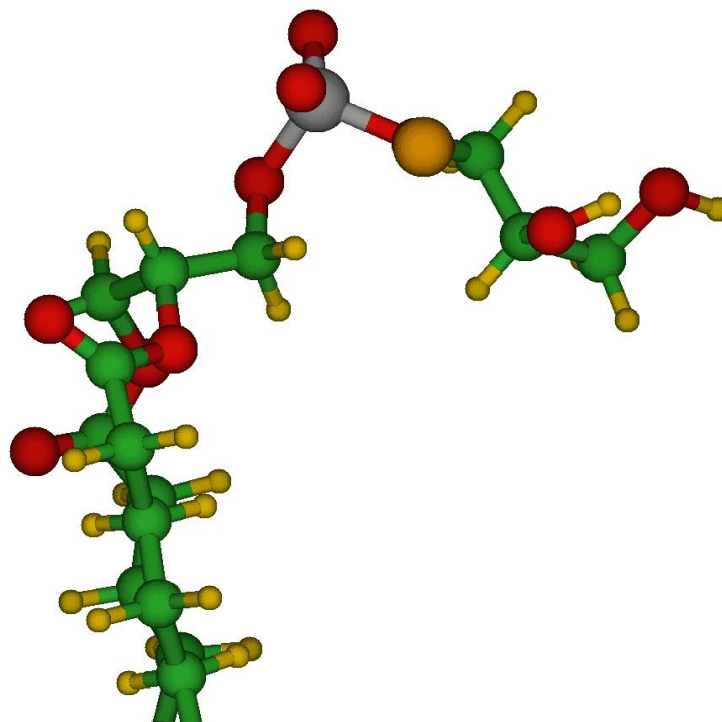


Figure 3.5. Orientation of the phosphate group and the head glycerol group with respect to the tail glycerol group in DMPG(B) conformation after generating it from the fractional atomic coordinates given in reference 35.

Table 3.3. Torsion angles (in degrees) obtained following the optimization of the proposed experimental conformations at DFT method.

Torsion angle	Experimentally proposed Torsion angle value in DMPG(A)	Torsion angle value in DMPG(A) after full relaxation at DFT level	Experimentally proposed Torsion angle value in DMPG(B)	Torsion angle value in DMPG(B) after full relaxation at DFT level
α_1	<u>-146</u>	<u>-171</u>	<u>116</u>	<u>77</u>
α_2	-76	-69	58	51
α_3	<u>-86</u>	<u>-109</u>	<u>78</u>	<u>138</u>
α_4	<u>143</u>	<u>-139</u>	<u>-147</u>	<u>140</u>
α_5	180	175	-173	-179
α_6	-66	-77	67	71
θ_1	151	168	71	73
θ_2	-78	-69	179	169
θ_3	64	54	45	62
θ_4	-63	-64	-58	-57
β_1	159	147	<u>157</u>	<u>85</u>
β_2	178	-170	180	174
β_3	178	-164	<u>-50</u>	<u>5</u>
β_4	-179	-163	-175	-179
γ_1	164	159	122	104
γ_2	-170	-169	179	177
γ_3	110	106	142	146
γ_4	-57	-58	174	169

Thus, the conformations proposed to exist in single crystal structures are high in energy as compared to various low energy conformations in the present DFT study. Significantly, as mentioned earlier, the head glycerol group in the DMPG(A) and DMPG (B) conformations, point away from both the carbonyl oxygen atoms due to the preferential sitting of Na^+ at the phosphate head group. (see Figure 3.5) However, in contrast, various conformations proposed by NMR study [4-5] and recent theoretical studies [6, 48, and 49] indicate that glycerol head group is inclined towards one of the carbonyl oxygen atoms thereby minimizing the intra-molecular electrostatic interaction. The low energy conformations seen in the present study relate closely to the conformations proposed to exist in the above studies.

These observations are in line with earlier results where the DMPC conformations proposed by a single crystal X-ray study [7] were found to be high lying in comparison with the DFT based ground state conformations.[29] The present study, thus consolidates this observation that the low lying conformations obtained from the DFT study on an anionic DMPG- Na^+ lipid agree more with the NMR conformational predictions (where a head group is inclined towards the carbonyl oxygen atoms) as compared to the conformations proposed to exist in single crystals. The fact that the lipid conformations present in the NMR solutions and liquid crystalline phases [2-6] differ from those present in the single crystals[7] has been emphasized also in many other experimental works. The reason for this discrepancy between the various conformations that co-exist in the NMR lipid solutions and those observed in single crystal X-ray studies may be attributed to the fact that in single crystal structures, the packing ratio is quite high and the inter-molecular forces

contribute significantly. However, in lipid solutions, micellar solutions, and bilayer solutions there are no stringent requirements governing the packing of the molecules and in this case, the intra-molecular forces dominate the orientation of the lipid molecules.

3.3.3. Conformational Analysis in the presence of water molecules and hydration energy

DMPG bilayers are seen to adapt to varying water content [50]. However, the most saturated case is seen to be a ratio of 4 water molecules per one lipid molecule [50]. Hence, in this chapter, we have attempted to analyze the orientation of water molecules around the cation in the lowest energy conformation. We have varied the number of water molecules from one to four to evaluate the cases of minimal to maximum hydration state of the molecule. Following the optimization of the Na-DMPG-H₂O complexes, we have analyzed the perturbation in the DMPG structure and the corresponding effect on the Na-O bond distances. Figure 3.6 gives the pictorial representations of Na-DMPG-nH₂O (n=1, 2, 3, and 4) complexes. In Table 3.4, we present the structural and electronic properties of Na-DMPG-nH₂O (n=0-4) complexes. The hydration energy given in the Table is calculated by using following formula:

$$\Delta E_{\text{hydration}} = - [E (\text{DMPG} \cdot (\text{H}_2\text{O})_n) - E (\text{DMPG}) - n E (\text{H}_2\text{O})]$$

where, n = number of water molecules.

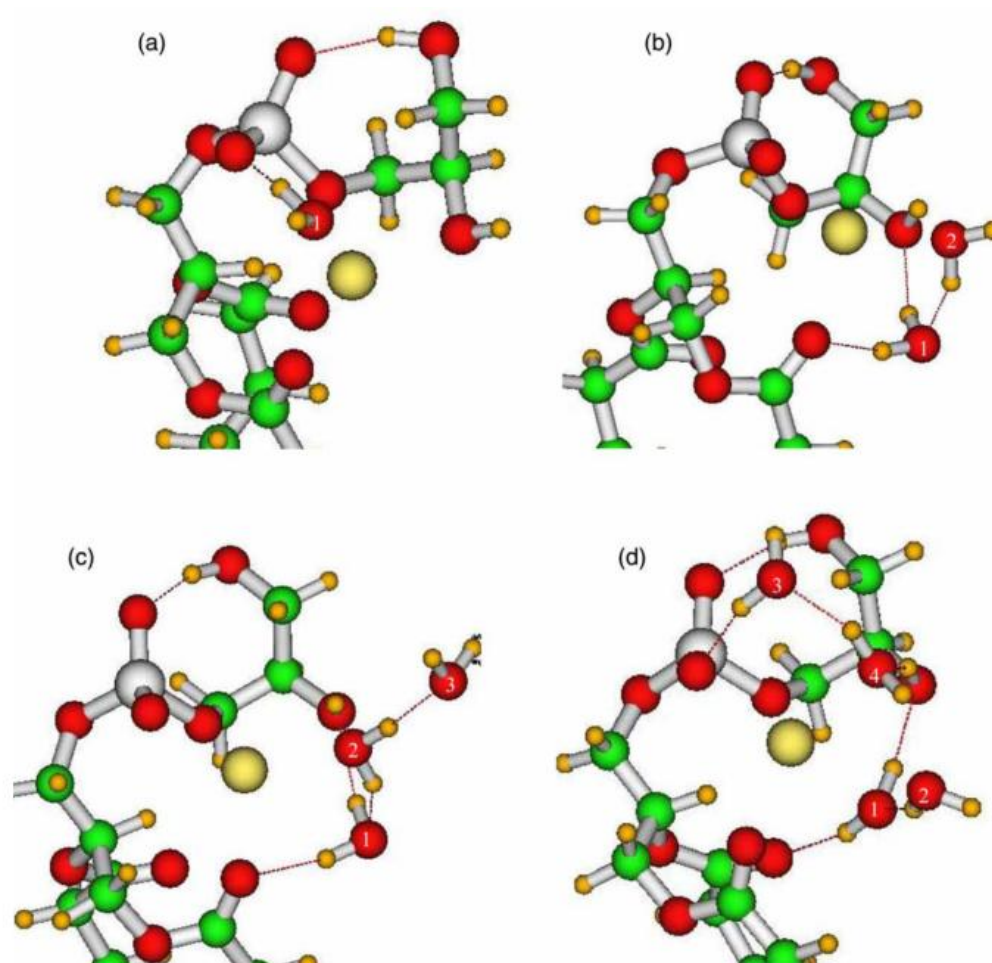


Figure 3.6. Structural orientation of the energetically favorable Na-DMPG-Na-1H₂O (a), Na-DMPG-Na-2H₂O (b), Na-DMPG-Na-3H₂O (c) and Na-DMPG-Na-4H₂O (d) complexes. The oxygen atoms of the water molecules are highlighted by Arabic numbers in each case for the sake of clearer representation of the picture.

As anticipated, the hydration energy increases with the number of water molecules. On scaling it with the number of water molecules, we note that hydration energy is lowest for the case of three water molecules. Analysis of the structural modifications following the hydration with one to three water molecules shows, that the number of Na-O bonds remains to be four. However, one of Na-O bond is between the Na ion and water molecule (Na-O_{water}), which occurs at the cost of a bond between Na ion and one of the oxygen atoms of the phosphate group (Na-O_{lipid}). For the case of Na-DMPG-4H₂O, Na ion makes a bond with two water molecules in addition to the three bonds with oxygen atoms of the lipid molecule. There is/are also additional hydrogen bond/s between phosphate group and the water molecule/s. This results in a smaller P-C distance as compared to that of an un-hydrated DMPG conformation as seen from the Table 3.4. This value is quite low in case of lipid molecule surrounded by two and three water molecules respectively and hence a lower H-E/n energy (hydration energy/number of water molecules) for these two cases. In all, Na-DMPG molecule with one and four water molecules seem to be more stable. Some charge transfer from water molecules to Na ion is seen in cases of lipid-water molecule complexes.

Table 3.4. Hydration energy (H-E), structural parameters and Mulliken charges for Na-DMPG-nH₂O (n=0, 1, 2, 3, and 4) complexes. Hydration energy per number of water molecules given in the third column is obtained by scaling the hydration with the number of water molecules. All distances are given in Å. Energy values are given in kcal/mol and charges given are in a.u.

n	H-E	H-E/n	Charge on Na	Net charge on PO ₄	Net charge on O=C=O group of γ chain (β chain)	Charge on head glycerol group	Average charge on water molecule	No. of Na-O _{lipid} bonds	No. of Na-O _{water} bonds (No. of hydrogen bonds)	Average Na-O _{lipid} bond distance	Average distance between P-C _{ester} atoms	O=C _{lipid} C=O distance
0	0.00	0.00	0.525	-1.051	0.014 (0.010)	0.032	--	4	--	2.322	5.178	3.673
1	21.748	21.748	0.555	-1.131	0.019 (0.002)	0.046	0.034	3	1 (2)	2.327	5.118	3.670
2	35.739	17.869	0.528	-1.088	0.002 (0.002)	0.038	0.061	3	1 (4)	2.327	4.837	3.644
3	45.843	15.281	0.522	-1.091	0.006 (0.004)	0.261	0.087	3	1 (5)	2.336	4.760	3.650
4	77.397	19.349	0.421	-1.103	0.029 (0.006)	0.053	0.153	3	2 (7)	2.380	5.005	3.71

3.4. Conclusions

The present chapter discusses various possible conformations available for a lipid molecule in gas phase. These conformations are seen to agree very well with the ones proposed to exist in lipid monomeric solutions. The energy of a given conformation is also seen to depend upon various factors such as on Na-O bonds, the orientation of the glycerol group with respect to the phosphate group. The conformations in which Na⁺ coordinates with oxygen atoms of head and tail glycerol groups along with those of phosphate groups are energetically more favorable. This position of Na⁺ is in agreement with the experimental observations. The presence of water molecules have moderately affect the electronic and structural properties of a lipid molecule, specially, the phosphate-tail glycerol group interactions.

3.5. References

- [1] Hauser H, Pascher I, Pearson R H, Sundell S, *Biochim Biophys Acta* 650 (1981)21.
- [2] Hauser H, Guyer W, Pascher I, Skrabal P, Sundell S, *Biochemistry* 19 (1980) 366.
- [3] Hauser H, Pascher I, Sundell S, *Biochemistry* 27(1988) 9166.
- [4] Hong M, Schmidt-Rohr K, Zimmermann H, *Biochemistry* 35 (1996) 8335.
- [5] Bruzik K S, Harwood J S, *J Am Chem Soc* 119 (1997) 6629.
- [6] Aussenac F, Laguerre M, Schmitter J-M, Dufourc E J, *Langmuir* 19 (2003) 10468.
- [7] Pearson R H, Pascher I, *Nature* 281(1979) 499.
- [8] Jeffery K, Richard M V, Alfredo J F, Joseph W O C, Douglas J T, Carlos M R, Igor V, MacKerell A D, Richard W P, *J Phys Chem B* 114 (2010) 7830.
- [9] Henin J, Shinoda W, Klein M L, *J Phys Chem B* 113(2009) 6958.
- [10] Lopez Cascales J J, Berendsen H J C, Garcia de la Torre J, *J Phys Chem* 100(1996) 8621.
- [11] Weiner S J, Kollman P A, Nguyen D T, Case D A, *J Comput Chem* 7(1986) 230.
- [12] Duan Y, Wu C, Chowdhury S, Lee M C, Xiong G M, Zhang W, Yang R, Cieplak P, Luo R, Lee T, Caldwell J, Wang J M, Kollman P, *J Comput Chem* 24 (2003) 1999.
- [13] Kaminski G A, Friesner R A, Tirado-Rives J, Jorgensen W L, *J Phys Chem B* 105(2001) 6474.

- [14] Feller S E, MacKerell Jr A.D, J Phys Chem B 104(2000) 7510.
- [15] Akutsu H, Nagamori T, Biochemistry 30(1991) 4510.
- [16] Vanderkooi G, Biochemistry 30(1991) 10760.
- [17] Stauch T R, Mol Simul 10(1993) 335.
- [18] Marrink S J, Mark A E, Biophysical J 87(2004) 3894.
- [19] Florian J, Baumruk V, Strajbl M, Bednarova L, Stepanek J, J Phys Chem 100 (1996) 1559.
- [20] Liang C, Ewig C S, Stouch T R, Hagler A T, J Am Chem Soc 115(1993) 1537.
- [21] Pullman B, Pullman A, Berthod H, Gresh N, Physics Letters, 33(1975) 11.
- [22] Landin J, Pascher I, Cremer D, J Phys Chem A 101(1997) 2996.
- [23] Pohle W, Gauger R R, Bohl M, Mrazkova E, Hobza P, Biopolymers 74 (2004) 27.
- [24] Mrazkova E, Hobza P, Bohl M, Gauger D R, Pohle W, J Phys Chem B 109 (2005) 15126.
- [25] I-Feng K, Douglas J T, J Phys Chem B 105 (2001) 5827,
- [26] Snyder J A, Madura J D, J Phys Chem B 112 (2008) 7095.
- [27] Yin J, Zhao Y P, J colloid and interface science 329 (2009) 410.
- [28] Thirumoorthy K, Nandi N, Vollhardt D, Oliveria Jr O N, Langmuir 22 (2006) 5398.
- [29] Krishnamurty S, Stefanov M, Mineva T, Begu S, Devoisselle J M, Goursot A, Zhu R, Salahub D R, J Phys Chem B 112 (2008) 13433.
- [30] Goursot A, Mineva T, Krishnamurty S, Salahub D. R, Can J Chem 87 (2009)

1261.

- [31] Krishnamurty S, Stefanov M, Mineva T, Begu S, Devoisselle M, Goursot A, Zhu R, Salahub D R, *Chem Phys Chem* 9 (2008) 2321.
- [32] Mineva T, Krishnamurty S, Goursot A, Salahub D R, (communicated)
- [33] Cronan J E, *Annu Rev Microbiol* 57 (2003) 203.
- [34] Buckland A G, Wilton D C, *Biochim Biophys Acta* 1483 (2000) 199.
- [35] Pascher I, Sundell S, Harlos K, Eibl H, *Biochim Biophys Acta* 896 (1987) 77.
- [36] Koster A M, Calaminici P, Casida M E, Moreno F R, Geudtner G, Goursot A, Heine T, Ipatov A, Janetzko F, Campo M J, Patchkovskii S, Reveles J U, Salahub D R, Vela A, The deMon deVelopers, (2006) Cinvestav: Mexico City.
- [37] Zhang Y, Yang W, *Phys Rev Lett* 80 (1998) 890.
- [38] Lee C, Yang W, Parr R G, *Phys Rev B* 37 (1988) 785.
- [39] Goursot A, Mineva T, Kevorkyants R, Talbi D, *J. Chem. Theory Comput* 3 (2007) 755.
- [40] Godbout N, Salahub D R, Andzelm J, Wimmer E, *Can J Chem* 70 (1992) 560.
- [41] Koster A M, Flores-Moreno R, Reveles J U, *J Chem Phys* 121 (2004) 681.
- [42] Dunlap B I, Connolly J W D, Sabin J R, *J Chem Phys* 71 (1979) 4993.
- [43] Reveles J U, Koster A M, *J. Comp Chem* 25 (2004) 1109.
- [44] Zhao W, Rog T., Gurtovenko A A, Vattulainen I, Karttunen M, *Biophys J* 92 (2007) 1114.
- [45] Wood R, Palenik J, *Inorganic Chemistry* 38 (1999) 3926.

- [46] Pandit S A, Berkowitz M L, Biophys J 82 (2002) 1818.
- [47] Mukhopadhyay P, Monticelli L, Tieleman D P, Biophys J 86 (2004) 1601.
- [48] Leekumjorn S, Sum A K, BioPhys J 90 (2006) 3951.
- [49] Pandey P R, Roy S, J Phys Chem B (2011) 3155.
- [50] Kodama M, Nakamura J, Miyata T, Aoki H, J Thermal Analysis 51 (1998)

91.

CHAPTER 4

**Understanding the orientation of
water molecules around the
phosphate and attached
functional groups in a
phospholipid molecule**

Abstract

The adsorption of water molecules around a polar region (in particular around the phosphate moiety) in the phospholipid molecules is studied in the present work. Phospholipid molecules with different functional groups are known to respond in varying fashion to the water molecules. Hence, we attempt to study the adsorption of water molecules around the phosphate group as a consequence of the change in functional group attached to the phosphate group, viz., PE (Phosphatidyl ethanolamine), PC (Phosphatidyl choline) and PG (Phosphatidyl Glycerol). Since the latter is anionic in nature the charge is compensated by Na^+ counterion. Upto seven water molecules are adsorbed around the phosphate groups in model systems mimicking phospholipid molecule. The corresponding changes in the structural and electronic aspects are analyzed. The significant difference between the PE and PC model systems is the formation of clathrate like structure in the latter. It is noticed that as the number of water molecules increases to seven both the hydrogen atoms in the water molecule participate in the hydrogen bonding. However in the PG model system charge compensating counter ion prevents the water molecule to form clathrate like structures. The adsorption sites for water molecules are validated by density functional theory based reactivity descriptors viz., Fukui functions in PE model system.

4.1. Introduction

Phospholipid molecules are the building blocks of any biological membrane. The two principal regions of a phospholipid molecule are the polar group (we refer this to as head) which is hydrophilic in nature and non polar, hydrophobic alkyl chains (which we refer to as tails). The basic conformation of the phospholipid molecule is governed by the torsion angles among the atoms within it. The conformational orientation in turn affects the chemical properties and also inters atomic molecular packing. However, the most critical factors controlling the chemical properties as well as the molecular packing are functional groups attached to the phosphate group. The functional groups also play a role in determining the essential physical properties of a lipid molecule such as, its surface charge density. Importantly, the presence of different functional groups modifies the overall charge of a phospholipid molecule making it as a zwitterionic, anionic or cationic. The overall charge on the molecule modulates its molecular interactions with the components present in aqueous phase resulting in different membrane responses towards the incoming ion, protein, drug molecule etc. Hence, depending on the functional group in the molecule, its application is seen to vary viz. drug delivery, protein-lipid interaction, solvation etc [1]. In other words, the chemical and physical response of any biological membrane is controlled by the chemical structure of the constituting phospholipid molecules.

One of the first factors to be affected by the chemical structure of a lipid molecule is the orientation of water molecules around it. The binding capacity or specifically “hydration force” [2-4] arises due to the association of water molecules to the polar region of the phospholipid. The behaviour of the water molecules at

the polar site of phospholipids depends on the structure and type of the functional group attached to the phosphate moiety. In addition to the functional groups, the counter ion present to compensate the charges on the phospholipids also modifies the hydration behaviour. Presence of different functional groups at the polar region changes entirely the electrostatic interaction involved and hence the hydration behaviour too.

X-ray and other experimental studies show that for individual phospholipid molecule in gas phase, the functional groups tend to orient towards the phosphate group due to electrostatic interactions [5]. However, the molecule adopts an extended form in the presence of water and neighbouring phospholipid molecule [6]. The strong dipole of the head region of phospholipid is responsible for its interaction with water molecules present in the vicinity of interaction. Water molecules are present in spaces between the two phospholipid head region resulting in the formation of intra molecular and intermolecular H-bond bridges.

Various experimental and computational studies have been carried out on phospholipid molecules in recent decades [7-13]. Experimental studies also direct the characteristics of single phospholipid molecular structure in various assemblies. Emphasis has been laid on the structure and dynamics of phospholipid monomer within an assembly in order to understand the bilayer functional role in biological membranes [14-19]. Internal monomer properties are better preserved in single crystal structure, since the intermolecular forces are less dominant than the intra-molecular forces [13-14]. The single crystal atomic positions are therefore used for the fluid phase simulation. However, this may not be true in the case of crystalline state since strong intermolecular electrostatics is involved [13].

It is difficult to study the bilayer structure using quantum mechanics due to its large size. Therefore model system like Methyl phosphate ion and methylphosphocholine model systems have been studied well using Hartree Fock and DFT respectively [20-25]. The effect of continuum solvation model has been studied on PE and PC model system using Hartree Fock [23]. However, the study of hydration of different functional groups attached to the phosphate group with explicit water molecules using more accurate methods is still eluding. Semi empirical PM3 method has been also used to study the interaction of dipyrindamole with DMPC (dimyristoyl phosphatidyl choline) [26]. In addition to the head group the tail region has also been taken into account in the more extended form of model system to study the various conformations and their energetic as a result of intra molecular interactions involved in the phospholipid system [27-28]. However, in such cases more extensively classical molecular dynamics methods have been used to study biological membrane properties. The force fields used in these classical molecular dynamics simulations to reproduce the experimental properties are parameterized using QM calculations on small model molecules [29-33]. The MD study has been devoted to large number of structural properties and has explored, till date dihedral angle values [26-29], head group flexibility [34-35], tail orientation [32], phase changes [36-37], hydration effect [38-40], interaction with ions [33] and molecules [41- 42] and evaluation of local order parameter [43-44]. In addition to this, recently Parthasarathi et al have studied the significant interaction of mannose sugar with two different phospholipids using DFT [45]. Parthasarathi et al have shown the importance of tail influence on phospholipid interaction with other molecules.

To evaluate the role of water in modifying the structural and electronic properties of lipid molecules as a function of functional group, we have chosen three model systems viz., DMPC (dimyristoyl phosphatidyl choline), DMPE (dimyristoyl phosphatidyl ethanolamine) and DMPG (dimyristoyl phosphatidyl glycerol). The background for choosing these molecules is as follows: The main constituents of lipid bilayer in the animal cells are DMPC and DMPE. In case of latter, the choline group in DMPC ($N(CH_3)_3$) is replaced by the amine group NH_3 , leading to differences in the physical properties of both, more importantly, in their hydration behaviour where lamellar phases of PE are less strongly hydrated than the PC in bilayer system [46]. The main structural difference is that the sheer volume of PC is greater than PE and also the non-hydrogen atom of PC are arranged in branched fashion and heavy atoms of PE are arranged in linear manner which together makes a lot of difference in the physicochemical properties. Therefore, we attempt here to study the hydration of both PC and PE model head group system with varying number of water molecules. In addition to these two neutral systems we have one charged model system viz; model system of DMPG (dimyristoyl phosphatidyl glycerol) for studying hydration and the effect of counter ion on hydration.

The more preferable sites of hydration in head groups are phosphate, carbonyl and carboxyl group which determine the hydrophilicity of the head group by directly forming the H-bonds with the water molecules. The hydration of hydrocarbon chains is quite weak due to the non polar nature of it; therefore we are restricting our study here to only the shortened model system of the head group region. Hence, we attempt to study the structure, hydration energy and

electrostatics involved during the interaction of water molecules with three different model systems.

We also attempt to predict the site of hydration of the model system of PE head group using Fukui functions [47]. Finite difference approximation has been used to calculate these reactivity descriptors. From the values of Fukui functions we can predict which site of the molecule is more reactive than the other for hydration. Therefore the concept of local reactivity descriptors can give the information beforehand without forming the complex of lipid head group model system and water molecules.

The chapter is organized as follows: In section 4.2 we give the brief overview of the local reactivity descriptors (LRD). Section 4.3 presents the methodology and computational details. Section 4.4 contains the Results and Discussion on the present study and Section 5 presents the Conclusions.

4.2. Local Reactivity Descriptors

Density based response functions, called local and global reactivity descriptors (LRD and GRD), are derived from density function theory (DFT) [48]. Within the framework of density functional theory, Parr and co-workers have introduced several important chemical tools [49]. DFT has provided the theoretical basis for the concepts like electronic chemical potential, electro negativity, and hardness, collectively known as global chemical reactivity descriptor [50]. Fukui function [46] can be interpreted either as the change of electron density $\rho(r)$ at each point r when the total number of electrons is changed or as the sensitivity of chemical potential of a system to an external perturbation at a particular point r .

Therefore, the expression of Fukui function can be written as:

$$f(r) = (\partial\rho(r)/\partial N)_{v(r)} = (\partial\mu/\partial v(r))_N \quad (4.1)$$

The eq. (4.1) involves the N -discontinuity problem [51-52] leading to the introduction of both right- and left-hand derivatives.

$$f^+(r) = (\partial\rho(r)/\partial N)_{v(r)}^+ \quad (4.2)$$

For a nucleophilic attack and

$$f^-(r) = (\partial\rho(r)/\partial N)_{v(r)}^- \quad (4.3)$$

For an electrophilic attack,

The finite difference method, using the electron densities of N_0 , N_{0+1} , N_{0-1} defines

$$f^+(r) \approx \rho_{N_{0+1}}(r) - \rho_{N_0}(r) \quad (4.4a)$$

$$f^-(r) \approx \rho_{N_0}(r) - \rho_{N_{0-1}}(r) \quad (4.4b)$$

$$f^o(r) \approx \frac{1}{2}(\rho_{N_{0+1}}(r) - \rho_{N_{0-1}}(r)) \quad (4.4c)$$

In order to describe the site reactivity or site selectivity, Yang *et al.* [47] proposed atom condensed Fukui function, based on the idea of electronic population around an atom in a molecule, similar to the procedure followed in population analysis technique. The condensed Fukui function for an atom k undergoing nucleophilic, electrophilic or radical attack can be defined respectively as

$$f_k^+ \approx q_k^{N_o+1} - q_k^{N_o} \quad (4.5a)$$

$$f_k^- \approx q_k^{N_o} - q_k^{N_o-1} \quad (4.5b)$$

$$f_k^o \approx \frac{1}{2}(q_k^{N_o+1} - q_k^{N_o-1}) \quad (4.5c)$$

where q_k is the electronic population of the k^{th} atom of a particular species.

The first and second partial derivatives of $E[\rho]$ with respect to the number of electron N under the constant external potential $v(r)$ are defined as the chemical potential μ and the global hardness η of the system respectively [50].

$$\mu = \left(\frac{\partial E}{\partial N} \right)_{v(r)} \quad \eta = \frac{1}{2} \left(\frac{\partial^2 E}{\partial N^2} \right)_{v(r)} \quad (4.6)$$

The inverse of the hardness is expressed as the global softness,

$$S = 1/2\eta \quad (4.7)$$

The global descriptor of hardness has been an indicator of overall stability of the system. When the two molecules interact, particular site, which is the most reactive site of the molecules are involved for the bond formation. So reaction between two reactants is always local. That's why the site-selectivity of a chemical system cannot be studied using the global descriptors of reactivity. For this, appropriate local descriptors need to be defined. An appropriate definition of local softness $s(r)$ is given by [47],

$$s(r) = \left(\frac{\partial \rho(r)}{\partial \mu} \right)_{v(r)} \quad (4.8)$$

such that

$$\int s(r) dr = S \quad (4.9)$$

Rewriting Eq (8) and the definition of global softness, we can write

$$s(r) = \left(\frac{\partial \rho(r)}{\partial N} \right)_{v(r)} \left(\frac{\partial N}{\partial \mu} \right)_{v(r)} \quad (4.10)$$

$$= f(r) S \quad (4.11)$$

The condensed local softness, s_k^+ and s_k^- are defined accordingly for nucleophilic and electrophilic attack, respectively. This can determine the behaviour of different reactive sites with respect to the hard and soft reagents. Subsequently, Gazquez and Mendez proposed a local version of HSAB principle, which generally states that the interaction between any two chemical species will not necessarily occur through their softest centres, but rather through those whose Fukui functions are nearly equal [53-55].

4.3. Methods and Computational Details

The standard nomenclature of the head group torsion angles has been depicted in Figure 4.1. The model system as depicted in Figure 4.1 is the model system of consideration in the present study with varying functional groups attached to the phosphate moiety. The systematic change in α torsion angle produces many conformers (nearly 50 conformations) which are low lying in energy (ΔE varies from 0 to 7 kcal/mol). We note that the various bond lengths (such as P=O, P-O, C-H etc.) and bond angles (such as O-P-O, O=P=O etc.) were not varied during the process of generating various conformations. The bond lengths and bond angles have limited flexibility within the tetrahedral symmetry and it is the variation in the torsion angles that leads to a wide range of

conformations. All the model systems having different conformations were optimized using deMon2k program [56]. The calculations were performed using a Generalized Gradient Approximation (GGA) of PBE exchange functional [57] and LYP correlation functional [58].

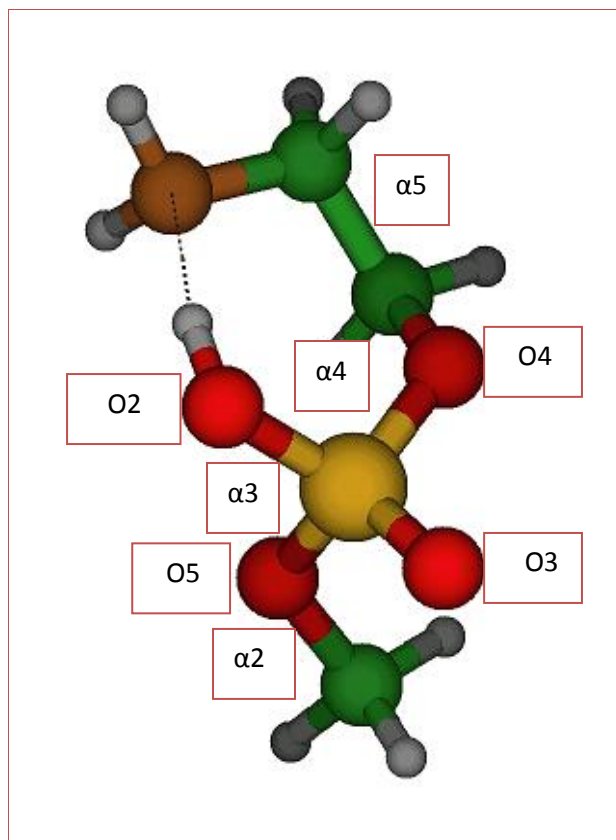


Figure 4.1. The gas phase optimised PE head group model system showing the nomenclature of torsional angles and atoms.

All the atoms were described using double zeta plus valence polarization (DZVP) basis sets [59]. A2 auxillary function was used for fitting the density. The exchange correlation functional was numerically integrated on an adaptive grid with an accuracy of 10^{-5} [60]. The Coulomb energy was calculated by the

variational fitting procedure proposed by Dunlap, Connolly and Sabin [61- 62]. A quasi-Newton method in internal redundant coordinates with analytical energy gradients was used for optimizing the systems [63]. The structure was considered to be optimized once the Cartesian gradient and displacement vectors reached a threshold of 10^{-4} and 10^{-3} respectively.

We have then taken one of the low lying (in terms of energy) conformer to see the hydration effect on PC model system. Similarly we obtained the various conformations for PE and PG model systems. The lowest energy conformer for all the model systems is then used to study the hydration. The models, which we have studied in this chapter, are head groups of DMPE, DMPC and DMPG. Two of them are neutral models (viz., DMPC and DMPE) and the other one is charged (viz., DMPG model system). Therefore we have taken into account both the neutral and charged head groups to study the hydration. The systematic addition of 1 to 7 water molecules to each of the model system is used for calculating the hydration energy and also the electrostatics involved during hydration. The lowest energy conformer with varying number of water molecules is then optimized using Gaussian09 software [64]. The optimization was performed using 6-311G**++ basis set and B3LYP exchange and correlation functional [65] for all the model systems.

Hirshfeld population has been calculated for the prediction of hydration site using Fukui functions. The reason for using the Hirshfeld population is that it leads non-negative FF and thus avoids the difficulty of obtaining the rank ordering of reactivity in a molecule. Roy et al, analyzed the procedure of giving non negative Fukui indices using Hirshfeld electronic population [66]. Hirshfeld population

analysis is defined relative to the “deformation density” using stockholders’ partitioning technique [67].

4.4. Results and Discussion

In our previous study we have obtained various low lying conformations which are lower in energy than the experimentally found conformers [28]. Therefore, there can be many other conformations possible which are lower in energy than what we know presently from the experimental results. To obtain many such conformations we have systematically varied α torsional angle (see Figure 4.1 for details) for the PC, PE and PG head group model system. Experimentally, it is proposed that the conformations of the molecule depend mainly on intra molecular interactions and to stabilise these conformations intermolecular interactions are required [68]. Therefore to study intra molecular electrostatic interactions which are involved dominantly in the polar region of phospholipids, we attempt to study model systems with different functional groups in gas phase and in the presence of varying number of water molecules. The model systems of DMPE, DMPC and DMPG have been tailored up to the glycerol C1 atom as shown in Figure 4.1 of PE model system.

Using deMon2k we have optimised several conformations and studied in detail the lowest 47 conformers of PC head group model system. The optimised conformers are analysed to understand their electronic and structural in each of the conformer. The energetic profile and structural parameters of these 47 conformers have been depicted in Table 4.1. The energetic profile of these conformers varies from 0-7 kcal/mol. We have found many conformers which are degenerate in

energy. The degenerate conformers are mirror image of each other. In a previous work of Krishnamurthy *et al.* [27], it was observed that despite the differences in combinations of torsion angles, all the conformers share a common geometric profile, which includes a balance of attractive, repulsive, and steric forces between and within specific groups of atoms of the DMPC molecule. Similarly, we note a balance of attractive and repulsive forces in the 12 nearly degenerate conformers with the ΔE value within the range of 1 kcal/mol. The attraction between the phosphate group and the choline group is decreasing in higher energy conformers. This is due to the increase in inter atomic distance between P and N atoms. The inter atomic distance (P-N) increases from 3.85 Å to 4.23 Å. The effect of different functional group on the phosphate group reflects the role of intra molecular interactions involved in different conformers of the head group model system and also in full phospholipid molecule. We have also obtained the lowest energy conformer for PE and PG head group model systems using the similar approach of systematically varying torsional angles. The head group model systems in the present study have been categorised into two different groups of neutral and charged category.

Table 4.1. The structural parameters of the generated conformers of PC headgroup models.

Conformers	α_2	α_3	α_4	α_5	P—N (Å)	H18—O 3(PO ₄) (Å)	H19—O 2(PO ₄) (Å)	O—P—O free	O—P—O bound	ΔE (kcal/m ol)
1	74	112	110	-65	3.85	1.98	2.07	123	100	
2	-74.3	-112	-110	65	3.85	1.98	2.07	123	100	
3	-74.3	-112	-110	65	3.85	1.98	2.08	123	101	0
4	74.3	112	110	-65	3.85	1.98	2.07	123	100	
5	-74.3	-112	-110	65	3.85	1.98	2.08	123	100	
6	76	-163	-49	-66	3.82	4.15	2.05	122	97	
7	-76	163	49	66	3.82	4.15	2.05	122	97	0.18
8	77	-169	-119	65	3.99	2.04	3.52	123	96	
9	-78	169	119	-65	3.99	2.04	3.54	123	96	0.75
10	-78	170	120	-65	4	2.04	3.56	123	96	
11	77	-165	-118	65	3.98	3.41	2.03	123	96	
12	74	92	71	47	3.89	2.37	4.46	124	100	
13	-74	-92	-71	-47	3.89	2.36	4.49	124	100	1.06
14	164	118	108	-67	3.83	2	2.03	120	96	1.19
15	74	154	47	66	3.8	2.04	3.95	122	98	
16	-74	-154	-47	-66	3.81	2.03	3.97	122	98	1.38
17	-177	-72	-117	71	3.99	2	3.12	122	96	2.008
18	-80	-138	120	-67	4.03	2.79	4.4	126	95	
19	-80	-138	120	-67	4.03	2.79	4.4	126	95	2.07
20	80	138	-120	67	4.03	2.78	4.4	126	95	
21	-150	-141	120	-68	4.02	2.68	4.4	123	92	
22	150	141	-120	68	4.02	2.72	4.4	123	92	2.32
23	-175	-100	-69	-47	3.85	3.83	3	122	96	2.69
24	75	-170	-70	122	3.9	3.53	3	121	97	
25	-75	170	70	-122	3.9	3.17	4.25	121	97	
26	75	-170	-70	122	3.91	3.01	2.27	121	97	3.32
27	-75	170	70	-122	3.9	3.17	4.24	121	97	
28	150	141	-120	69	4.02	4.41	2.66	123	92	
29	74	167	70	-122	3.91	3.15	4.23	121	98	
30	-74	-167	-70	122	3.91	3.01	3.56	121	98	3.76
31	75	-170	-70	122	3.9	3	3.55	121	97	
32	-75	170	70	-122	3.9	3.16	4.23	121	97	4.14
33	-77	-57	-67	125	4.05	1.99	5.63	125	99	
34	77	57	67	-125	4.06	1.99	5.64	125	99	4.32
35	77	57	67	-125	4.06	1.99	5.64	125	99	
36	77	57	68	-126	4.06	1.99	5.64	125	99	
37	-77	-57	-68	126	4.06	1.99	5.64	125	99	5.14
38	77	57	68	-126	4.06	1.99	5.64	125	99	
39	-77	-57	-68	126	4.06	1.99	5.64	125	99	
40	166	167	71	-123	3.9	3	3.58	119	94	
41	-162	-167	-71	123	3.9	3.03	3.64	121	96	5.33
42	-162	-96	60	70	4.06	4.07	3.97	123	96	6.02
43	163	96	-60	-70	4.08	4.28	3.95	121	99	6.08
44	164	89	-83	123	4.12	5.83	3.32	122	99	6.9
45	-159	-59	-66	123	4.04	1.99	5.6	121	96	
46	159	59	66	-123	4.04	1.99	5.6	121	97	7.34
47	76	89	-67	143	4.23	3.99	4.1	121	99	7.71

4.4.1. Hydration behaviour of neutral head groups

In order to understand the structural and conformational behaviour of the PE and PC model systems the torsion angles have been measured in the presence and absence of explicit water molecules. As shown in Table 4.2(a), the torsion angle α_3 undergoes a noticeable change with the addition of a water molecule. It changes from 42° to 91° with the addition of one water molecule; however this change gets stabilised with respect to the successive addition of water molecules. The cause of change of α_3 torsion angle is due to the phosphate group which interacts with the neighbouring water molecules. Thus, a critical number of water molecules are required for the stabilizing the torsion angles near to the phosphate group. We also noticed a proton transfer from NH_3^+ to the PO_4^- functional group in the gas phase and with one water molecule in the PE head group model system. Interestingly, the proton transfer does not depend on the distance between the two groups e.g distance is same in the case of gas phase (i.e no water molecule around the phosphate group) and model with seven water molecule. Therefore, it is worth noticing that the proton transfer depends on the number of water molecules in the first hydration shell of the PE head group. However, the change in α_3 torsion angle makes the PO_4 group to move parallel to the bilayer plane away from the NH_3 group, but the distance between these groups does not change much due to the electrostatic interaction between the two charged groups of the head region of PE.

Table 4.2(a). Structural parameters of PE head group in gas phase and with varying number of water molecules.

Model Systems	Torsional angles				Bond distances				
	α_2	α_3	α_4	α_5	P=O2	P-O3	P-O4	P-O5	P-NH ₂
Gas Phase	95	42	92	-72	1.48	1.58	1.62	1.63	3.47
1 water	82	91	89	-60	1.50	1.59	1.62	1.65	3.28
3 water	80	74	92	-71	1.49	1.52	1.62	1.66	3.41
5 water	77	82	89	-74	1.50	1.51	1.62	1.66	3.43
7 water	80	66	100	-58	1.49	1.51	1.62	1.69	3.42

The partial CHelpG charges of the various functional groups of PE model system have been calculated to support the electrostatic interactions. The partitioning scheme of CHelpG point charges are very well explained in the literature and describe electrostatics quite accurately [69]. The CHelpG charges are considerably less dependent upon molecular orientation. Although Clark et al showed that VESPA charges are less sensitive to molecular orientation [70-71], However, CHelpG charges work well while predicting the electrostatics for our

model systems of phospholipid molecule. CHEPLG charges and other electrostatic properties are shown in Table 4.2(b). The charge on NH_3 is quite low in gas phase and with one water molecule as compared with more number of water molecules. The partial charge on NH_3 increases to 0.622 from 0.284 as going from one water molecule to three water molecule system. The reason for this is the proton transfer from NH_3 to PO_4 group. The atomic distance between P-N atoms also decreased from 3.47 to 3.28 Å from gas phase to one water solvated state. The change in the atomic distance is due to the H-bond formation of water molecule which involves both the functional groups. This decrease in atomic distance reflects back when we calculate the dipole moment of the system. Dipole moment of a system quantitatively can explain the charge separation. The PE head group dipole moment in the gas phase is 7.70 debye, which changes to 3.14 Debye in the 1-water solvated state as depicted in Table 4.2(b). It has also been observed that the charge on the N atom of NH_3^+ functional group is increasing which implies that the electro-positivity of N increases with the addition of water molecules since the hydrogen atoms in NH_3^+ are involved in the hydrogen bond formation.

Table 4.2(b). Partial charges of atoms/group and hydration energy calculation of the model system of PE head group.

Partial charges on Atom/molecule	Gas Phase	Hydration States						
		1 water	2 water	3 water	4 water	5 water	6 water	7 water
		PO ₄	-1.027	-0.923	-1.03	-1.187	-1.199	-1.17
NH ₃	0.333	0.284	0.386	0.622	0.631	0.621	0.635	0.617
CH ₃	0.243	0.239	0.227	0.216	0.215	0.219	0.21	0.214
(CH ₂) ₂	0.45	0.479	0.436	0.331	0.381	0.345	0.308	0.302
Dipole moment (debye)	7.7	3.14	4.16	6.3	5.02	7.62	7.51	6.43
Hydration Energy (ΔH) (kcal/mol) at 0K	---	-12.11	-12.29	-11.76	-12.17	-11.24	-11.13	-11.05
Hydration Energy (Δ) (kcal/mol) at 298K	---	-10.4	-10.72	-10.13	-10.21	-9.44	-9.34	-9.17
ΔG (kcal/mol) at 298K	---	-0.27	-0.84	-0.2	-0.35	-0.17	-0.22	-0.21
Counterpoise Corrected (kcal/mol) at 0K	---	-10.92	-11.51	-11.15	-11.4	-10.76	-10.72	-10.62

From the earlier studies, it is very well understood that the phosphate moiety of the phospholipids is the active region of hydration [22]. It is also observed that there are many possibilities of water molecules in the first, intermediate and second hydration shell. Up to six water molecules may be accommodated in the first hydration shell. Intermediate hydration shell has two to five water molecules. It has been reported that the average energy of water attachment is approximately -23 kcal/mole for $n = 2$ and 3 and decreases when n increases further, down to **-17.3** for $n = 6$ [54]. Therefore, we started with the phosphate group and kept on adding water molecules systematically up to 7. The hydration energy calculation showed that the PE model system solvated with 2 explicit water molecules has the highest counterpoise corrected hydration energy per water molecule. The hydration energy for 2 water molecular system is -11.51 kcal/mol. One of the water molecules is hydrogen bonded with O of phosphate group and the other water molecule has bridged structure involving both its hydrogen atoms in the hydrogen bonding with free oxygen atoms of phosphate group. The model system with 7 water molecule has hydration energy ~ 1 kcal/mol less than that of 2 water molecule system. The hydrogen atoms of NH_3 group are all involved in H-bond formation i.e two with water molecules and one with PO_4 group in 7 water molecule model system (Figure shown in Table 4.2(a)). There is a formation of clathrate like structure of water molecules around the polar groups of head group model system.

Similar to the DMPE shortened model system, DMPC has also been shortened to study the structural and electronic properties in the presence and absence of varying number of water molecules. We notice the increase in P—N distance with the addition of water molecules in PC head group model system

which shows the straightening of the head group. We also noticed a significant change in α_3 torsion angle in PC head group model as in case of PE. The bond distance oxygen with the phosphorus in PO_4^- shows a minor change from gas phase to hydrated phase as depicted in Table 4.3(a). Unlike in the case of PE, there is no proton transfer due to the presence of bulkier choline group $\text{N}(\text{CH}_3)_3$ in the PC. In an earlier study it was shown experimentally, that DMPC is more favourable for hydration than DMPE [46]. Also, in the previous experimental studies it has been shown that although the CH_3 groups would not be expected to bind strongly to water, it would appear that entropic considerations may be of major significance in the binding process. In agreement to the experimental studies, we also observed a significant contribution of entropy in both PC and PE hydrated model systems as depicted in Table 4.2 (b) and Table 4.3 (b). We also notice that trend of ΔG is different from ΔH in both PE and PC. However, the change of trend is remarkably different in case of PE hydrated systems. Therefore, the entropy has a significant role while calculating the hydration energy for both the model systems. The change of trend of ΔG is more clearly shown in Figures 4.2 and 4.3 for PE and PC water complexes respectively. It has also been concluded that the hydration of lipids with phosphatidylcholine head groups is more favourable than phosphatidylethanolamine as can be seen by comparing ΔG values of PC and PE hydrated model systems. This shows that the contribution of entropy is significant in PC model system.

Table 4.3(a). Structural parameters of PC head group in gas phase and with varying number of water molecules.

Model Systems	Torsional angles				Bond distances				
	α_2	α_3	α_4	α_5	P=O2	P-O3	P-O4	P-O5	P- N(CH ₃)
Gas Phase	74	112	110	-65	1.51	1.52	1.65	1.74	3.85
1 water	74	84	114	-72	1.52	1.52	1.65	1.72	3.97
3 water	71	74	118	-72	1.52	1.51	1.65	1.70	4.03
5 water	70	80	116	-76	1.52	1.51	1.64	1.72	4.07
7 water	67	81	123	-71	1.54	1.52	1.64	1.67	4.09

Table 4.3(b): Partial charges of atom/group and hydration energy calculation of the model system of DMPC.

Partial charges on Atom/molecule	Gas Phase	Hydration States						
		1 water	2 water	3 water	4 water	5 water	6 water	7 water
PO ₄	-1.234	-1.244	-1.187	-1.177	-1.185	-1.050	-1.171	-1.154
N(CH ₃) ₃	0.676	0.782	0.741	0.825	0.851	0.775	0.911	0.909
CH ₃	0.213	0.210	0.214	0.209	0.218	0.202	0.212	0.235
(CH ₂) ₂	0.344	0.341	0.296	0.240	0.216	0.257	0.202	0.269
Dipole moment (debye)	12.54	11.21	10.26	9.04	7.71	7.05	5.40	4.78
Hydration Energy (kcal/mol)	---	-13.85	-13.32	-13.27	-13.42	-12.65	-12.67	-12.94
Hydration Energy at 298 K	---	-12.14	-11.51	-11.52	-11.62	-10.80	-10.89	-11.06
ΔG (kcal/mol) at 298K	---	-3.58	-2.56	-2.15	-2.13	-1.16	-1.71	-1.30
Counterpoise corrected (kcal/mol) at 0K	---	-12.73	-12.15	-12.61	-12.67	-12.10	-12.21	-12.38

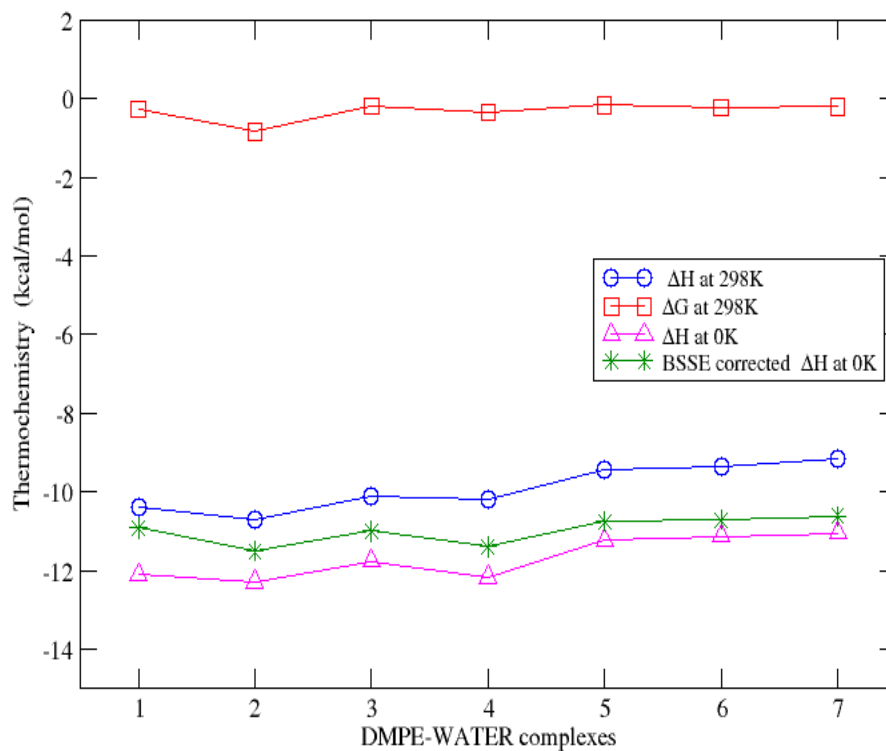


Figure 4.2. Thermo chemistry explained of DMPE model system with increasing number of water molecules.

*Each point on X-axis denotes the PE- $n\text{H}_2\text{O}$ where $n=1$ to 7

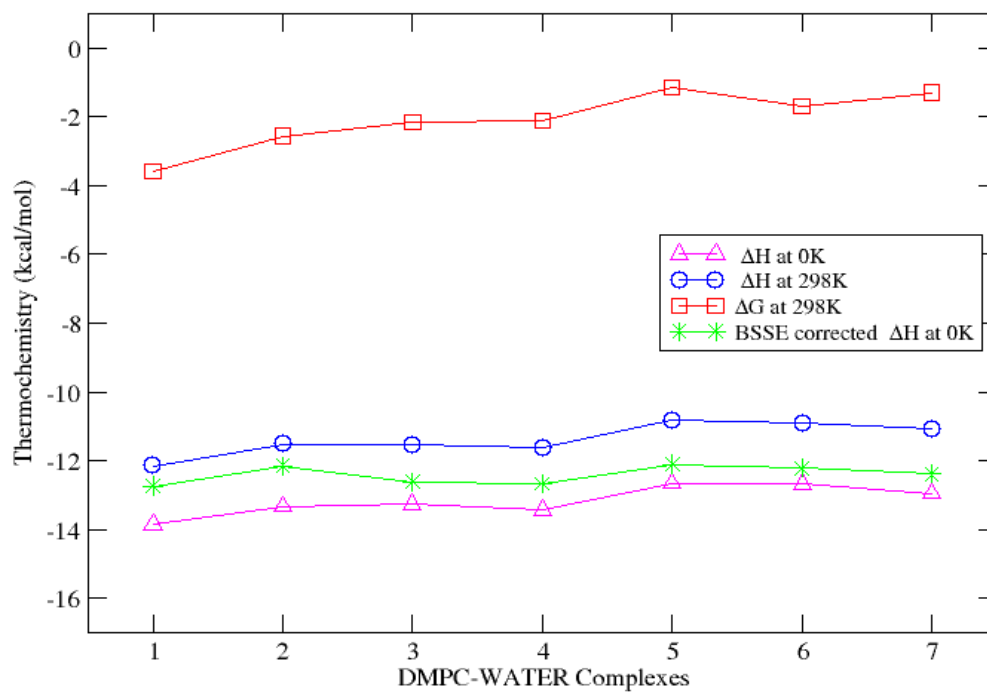


Figure 4.3: Thermochemistry explained of DMPC model system with varying number of water molecules.

*Each point on X-axis denotes the PC- $n\text{H}_2\text{O}$ where $n=1$ to 7

The change of partial charge on N is not significant unlike in the case of PE model system. We attribute this to the presence of bulkier CH₃ groups attached to it. Therefore, the effect of water on N atom is almost negligible in terms of partial charge. With the addition of water molecules, there is a gradual change in the electro positivity of choline group and electro-negativity of phosphate group which changes from 0.676 to 0.909 and -1.234 to -1.154 respectively. The prominent positive and negative groups in the PC model system are well separated which is responsible for its higher dipole moment as depicted in Table 4.3(b). However, the dipole moment gradually decreases with the addition of water molecule. The reason for the same can be explained by the orientation of the water molecules in the model systems which reduce the overall charge separation.

4.4.2. Hydration behaviour of charged head groups

The PG head group model system has one negative charge which is compensated by putting Na⁺ as the counter ion. As observed in the case of neutral head group model system, charged phospholipid model system also undergoes a change in only α_3 torsion angle and the straightening of the head group model system observed while hydration. The atomic distance between phosphate group P and C of CH₂OH depicts this straightening upon addition of water molecules. It has changed from 3.84 (gas phase) to 5.29 (7 water molecules) as shown in Table 4.4(a). As concluded in our previous study [28], the DMPG molecular structure stabilises as a function of number of Na-O bonds. Therefore, we also measured the number of Na-O bonds both ionic (<2.34 Å) and coordinate (>2.34 Å). In this case, Na⁺ is surrounded by both the phosphate group oxygen atoms as well as the

oxygen atoms in the water molecules (typically called as hydration of the counter ion). The number of Na-O bonds increase upon hydration in the model system. The partial charge on Na atom changes upon hydration and oscillates with respect to the number of oxygen atoms of water. Therefore the charge on the Na⁺ is getting distributed to the oxygen atoms of water in addition to the oxygen atoms of head group. The hydration energy in the case of PG is higher with respect to the PE and PC model systems. This is due to the presence of counter ion which is hydrated in addition to the other polar groups in the model system. The trend of ΔH with and without counterpoise (BSSE) corrections follow the same path, however the difference is noticed quantitatively in the values as it is well known that without counterpoise correction the hydration energy value is little higher than that depicted in Fig 4. We also note that the formation of clathrate like structure of the water molecules is not seen around the counter ion.

Therefore, for hydrating counter ion, clathrate like structure of water molecules is not favourable. The negative charge on the dipoles of the hydroxyl group of PG head group might have been expected to significantly perturb the dipole moment, but the counter ion present to compensate the charge makes the glycerol group bends towards the phosphate group. Therefore, both the groups bend towards the counter ion thereby making that region more polar. As a result, we noticed lower dipole moment in the PG than in case of PE and PC head group model system. However, like in the PC and PE head group the dipole moment in PG head group also decreases with the addition of more number of water molecules as shown in Table 4.4(b).

Table 4.4(a). Structural parameters of DMPG in gas phase and with varying number of water molecules

Model Systems	Torsional angles				Bond distances					
	α_2	α_3	α_4	α_5	P=O	P-O3	P-O4	P-O5	Na-O	P-CH ₂ OH
Gas Phase	-72	-133	-69	-55	1.51	1.50	1.67	1.60	3 (ionic)	3.84
1 water	-67	-132	-71	-56	1.52	1.50	1.66	1.61	3 (ionic) 1 (coordinate)	3.87
3 water	-65	-115	-83	-67	1.52	1.50	1.66	1.61	3 (ionic) 1 (coordinate)	4.20
5 water	-72	-111	-85	-69	1.51	1.51	1.64	1.61	3 (ionic) 2 (coordinate)	4.43

7 water	-70	-86	-92	-59	1.51	1.52	1.64	1.61	2(ionic) 3 (coordina te)	5.29
---------	-----	-----	-----	-----	------	------	------	------	-----------------------------------	------

Table 4.4(b): Partial charges of atom/group and hydration energy calculation of the model system of PG head group

Partial charges on Atom/molecule	Gas Phase	Hydration States						
		1 water	2 water	3 water	4 water	5 water	6 water	7 water
PO ₄	-1.183	-1.108	-1.175	-1.220	-1.159	-0.713	-1.268	-1.293
Na	0.850	0.824	0.795	0.866	0.842	0.840	0.933	0.951
Glycerol	0.014	0.026	0.041	0.037	0.019	0.018	0.006	0.006
CH ₃	0.222	0.212	0.208	0.228	0.240	0.244	0.233	0.242
Dipole (debye)	7.149	5.372	5.427	5.291	6.332	4.339	2.008	2.637
Hydration Energy (kcal/mol) at 0K	---	-17.16	-15.58	-14.82	-14.66	-13.77	-14.42	-13.29
Counterpoise Corrected (kcal/mol) at 0K	---	-16.23	-14.41	-14.19	-13.21	-12.95	-13.51	-14.34

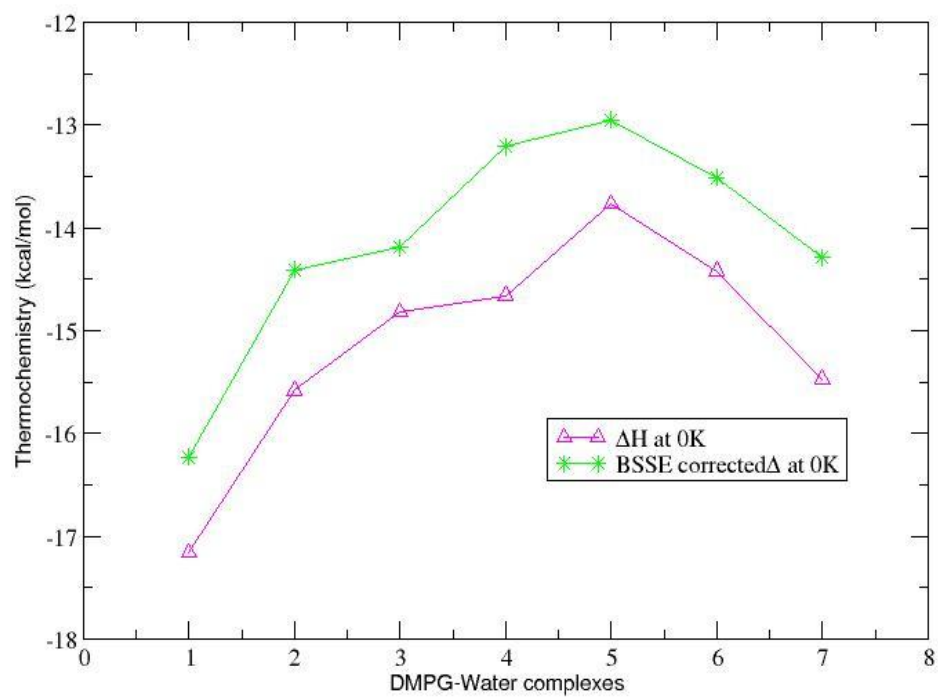


Figure 4.4. Thermochemistry explained of DMPG model system with varying number of water molecules.

*Each point on X-axis denotes the PG- $n\text{H}_2\text{O}$ where $n=1$ to 7

The surface charge and the molecular structures of the above systems are very different and therefore one should expect the orientation of water molecules to be different in all these cases. Our present study is in agreement with the previous experimental studies of surface sum frequency generation spectroscopy which proves that the interfacial water near the different head groups of phospholipid (either charged or neutral) behaves similarly in terms of orientation of the OH bond of water molecules towards the bulk water [72]. We have also observed the same orientation of water in each of the different head group model systems (PE, PC and PG) i.e., O-H group pointing towards the bulk water. The strength of H-bond increases in the order of PE<PC<PG.

4.4.3. Prediction of Hydration sites using Local Reactivity Descriptors

Local reactivity descriptors predict the site of interaction of nucleophile and electrophile attack. These descriptors have been used widely to predict the organic reactions and substituent effects [73]. We have calculated the Fukui functions for the PE head group in the gas phase, one and two water molecule model system to predict the site of water molecule interaction. As depicted in Table 4.5(a) for the gas phase and Table 4.5(b) for the one water molecule system, the Fukui function values have been validated and also studied geometrically for validation. As shown in Table 4.5(a), the Fukui function value for H7 atom (Hydrogen attached to the N) is having the highest value and it is the best H-bond donor atom having N attached to it. In addition to the H7, O2 is the atom which is having next higher Fukui function value. Therefore, both H7 and O2 make the H-bond with water molecule where H7 act as an H-bond donor atom having N

Table 4.5(a). Local reactivity descriptors for PE head group gas phase.

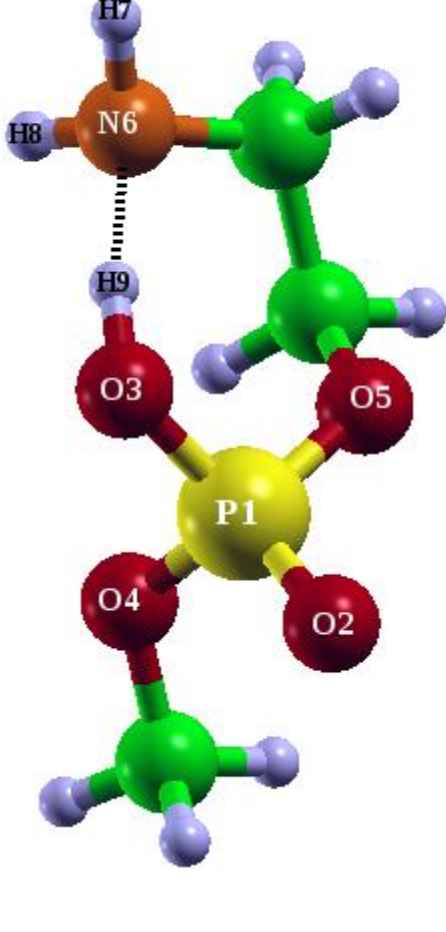
<u>PE gas phase model system</u>	Atoms	Fukui Functions
	P1	0.0853
	O2	0.1979
	O3	0.0761
	O4	0.0369
	O5	0.0811
	N6	0.1018
	H7	0.2153
	H8	0.1883
	H9	0.0167

Table 4.5(b). Local reactivity descriptors for PE head group with 1 water molecule.

<u>PE 1 water model system</u>	Atoms	Fukui Function
	P1	0.0466
	O2	0.0888
	O3	0.0571
	O4	0.0813
	O5	0.0796
	N6	0.1073
	H7	0.0298
	H8	0.2010
	H9	0.0160
	O10	0.0470
	H11	0.0840
	H12	0.0154

Table 4.5(c): Local reactivity descriptors for PE head group with 2 water molecules.

PE 2 water model system		Atoms	Fukui Functions
		P1	0.0445
		O2	0.0782
		O3	0.0670
		O4	0.0657
		O5	0.0660
		N6	0.0985
		H7	0.0242
		H8	0.1529
		H9	0.0110
		O10	0.0698
		H11	0.0500
		H12	0.0101
		O13	0.0327
		H14	0.1047
		H15	0.0183

attached to it while O2 is an H-bond acceptor. We also note that the higher value of f_k^+ of H7 predicts that it will react with a nucleophile. In the complex of one water molecule the H7 was making H-bond with the water oxygen. We also looked upon the Hirshfeld population of the added water molecule. The population shows that water molecule has 10.036 electrons and hence gains electrons from the system. The H7 and O2 has higher f_k^+ and f_k^- value respectively, where at one site O2 will donate electrons and H7 will accept electrons from the oxygen atom of the added water molecule. The electron density of the H7 of PE head group model system in gas phase is 0.8739 which later on increased to 0.9027 while interacting with a water molecule. Therefore, H has higher f_k^+ value and O2 of the phosphate group on the other hand has higher f_k^- value where its electron density decreases from 8.4095 to 8.3898 during complex formation.

Therefore the site of hydration can be predicted before hand by calculating the local reactivity descriptors. Likewise we can predict the site of hydration for the second water molecule when the model system is already interacting with one water molecule. According to the values of Fukui function as shown in Table 4.5(b) the next site of hydration is H8 of NH_3 showing the highest f_k^+ value. Therefore we validate in these calculations the ability of Fukui functions to predict the site of interaction in biological molecules.

In addition to the gas phase and 1 water PE head group model system, we continued to calculate the Fukui function values of 2 water PE head group model system to predict the site of interaction of third water molecule. It is well known

that the water molecules very close to the head group form a cage like structure and form the innermost hydration shell around it. Therefore, the third water molecule surely makes H-bond with the water molecules and forms the cage like structure. Table 4.5(c) shows the considerably high value of H8 which predicts the site of next water molecule. Recently analytical Fukui function was implemented in deMon2k programme [74]; however using the approximate Fukui function also we have got the satisfactory results for predicting the hydration sites.

4.5. Conclusions

In the present chapter, the hydration behaviours of different head group system viz; PE, PC and PG have been explored. Our study reveals substantial changes in the hydration properties of different head groups. A clathrate like structure was seen to form in PE model system during hydration. This structure is missing when the hydrogen atoms are replaced by methyl groups (PC model system) in the functional group. In PE hydrated model system all three hydrogen atoms of $-\text{NH}_3^+$ are involved in H-bond with water molecules. However, similar behaviour is not observed in PC model system due to the presence of bulkier choline group. In agreement to the experimental studies we also observed the significant contribution of entropy in both PC and PE hydrated model systems. However hydration phosphatidylcholine head group model system is more favourable than phosphatidyl ethanolamine as can be seen by comparing ΔG values of PC and PE hydrated model systems. Thus, the contribution of entropy is significant in hydrated PC model systems. The presence of counter ion in PG head group model system makes water to behave differently and prevent the

water molecules to form clathrate like clusters. The hydration of PG model system is even favourable than PC model system due to the presence of counter ion which also needs to be hydrated apart from the functional groups present in the PG head group. The functional group attached to the phosphate group is involved mainly in both intra molecular and intermolecular interactions and hence makes the phospholipid behave differently in the presence of water, ligand or any other molecules.

In addition to this, the condensed Fukui function value of each atom is used to predict the active site of hydration. Therefore to prevent the large complex geometry optimization we can have the information on the site of hydration of the next water molecule before without doing quantum chemical optimization. The results of Fukui function also shows that the phosphate moiety is the preferable site of hydration as proved by many experimental studies also.

4.6. References

- [1] Kinnunen P K J, *Chem and Phys of Lipids* 57 (1991) 375.
- [2] Fitter J, Lechner R E, *J Phys Chem B* 103 (1999) 8036.
- [3] Leikin S, Parsegian V A, Rau *Annu Rev Phys Chem* 44 (1993) 369.
- [4] J Katsaras J, Jeffrey K K, *Europhys Lett* 38 (1997) 43.
- [5] Pascher I, Lundmark M, Nyholm PG, Sundell S, *Biochim Biophys Acta* 113 (1992) 339.
- [6] Pullman B, Berthod H, Gresh N, *FEBS Letters* 53 (1975) 199.
- [7] Berger O, Edholm O, Jahnig F, *Biophys J* 72 (1997) 2002.
- [8] Landin J, Pascher I, Cremer D, *J Phys Chem* 99 (1995) 4471.
- [9] Leonenko Z V, Finot E, Ma H, Dahms T E S, Cramb D T, *Biophys J* 86 (2004) 3783.
- [10] Li W, Lagowski J B, *Chem Phys Lipids* 103 (1999) 137.
- [11] Marrink S J, Berger O, Tieleman P, Jahnig F, *Biophys J* 74 (1998) 931.
- [12] Meyer H W, Semmler K, Rettig W, Pohle W A, Ulrich S, Grage S, Selle C, Quinn P J, *Chem. Phys. Lipids* 105 (2000) 149.
- [13] Bhide S Y, Berkowitz M L, *J Chem Phys* 125 (2006) 94713.
- [14] Hauser H, Pascher I, Pearson R H, Sundell S, *Biochim Biophys Acta* 650 (1981) 21.
- [15] Hauser H, Guyer W, Pascher I, Skrabal P, Sundell S, *Biochemistry* 19 (1980) 366.
- [16] Hauser H, Pascher I, Sundell S, *Biochemistry* 27 (1988) 9166.

- [17] Hong M, Schmidt-Rohr Z H, Zimmermann H, *Biochemistry* 35 (1996) 8335.
- [18] Bruzik K S, Harwood S, *J Am Chem Soc* 119 (1997) 6629.
- [19] Aussenac F, Laguerre M, Schmitter J M, Dufourc E J, *Langmuir* 19 (2003) 10468.
- [20] Florian J, Baumruk V, Strajbl M, Bednarova L, Stepanek J, *J Phys Chem* 100 (1996) 1559.
- [21] Liang C, Ewig C S, Stouch T R, Hagler A T, *J Am Chem Soc* 115 (1993) 1537.
- [22] Pullman B, Pullman A, Berthod H, Gresh N, *Theor Chem Acc* 40 (1975) 93.
- [23] Landin J, Pascher I, Cremer D, *J Phys Chem A* 101 (1997) 2996.
- [24] Pohle W, Gauger D R, Bohl M, *Biopolymers* 74 (2004) 27.
- [25] Mrazkova E, Hobza P, Bohl M, Gauger D R, Pohle W, *J Phys Chem B* 109 (2005) 15126.
- [26] Thirumoorthy K, Nandi N, Vollhardt D, Oliveira O N, *Langmuir* 22 (2006) 5398.
- [27] Krishnamurthy S, Stefanov M, Mineva T, Begu S, Devoisselle J M, Goursot A, Zhu R, Salahub D R, *Phys Chem B* 112 (2008) 13433.
- [28] Mishra D, Pal S, Krishnamurthy S, *Mol Simulation* 37 (2011) 953.
- [29] Weiner S J, Kollman P A, Nguyen D T, Case D A, *J Comput Chem* 7 (1986) 230.
- [30] Duan Y, Wu C, Chowdhury S, Lee M C, Xiong G M, Zhang W, Yang R, Cieplak P, Luo R, Lee T, Caldwell J, Wang J M, Kollman P, *J Comput Chem* 24 (2003) 1999.

- [31] Kaminski G A, Friesner R A, Tirado-Rives J, Jorgensen W L, *J Phys Chem B* 105 (2001) 6474.
- [32] Feller S, MacKerell A D Jr, *J Phys Chem B* 104 (2000) 7510.
- [33] Akutsu H, Nagamori T, *Biochemistry* 30 (1991) 4510.
- [34] Vanderkooi G, *Biochemistry* 90 (1991) 10760.
- [35] Stauch T R, *Mol Simulation* 10 (1993) 335.
- [36] Egberts E, Marrink S J, Berendsen H J C, *Eur Biophys J* 22 (1994) 423.
- [37] Marrink S J, Mark A E, *Biophys J* 87 (2004) 3894.
- [38] Murzyn K, Zhao W, Karttunen M, Kurziel M, Rog T, *Biointerphases* 1 (2006) 98.
- [39] Rog T, Murzyn K, Pasenkiewicz-Gierula M, *Chem Phys Lett* 352 (2002) 323.
- [40] Pandey P R, Roy S, *J Phys Chem B* 115 (2011) 3155.
- [41] Vanderkoi G, *Biophys J* 66 (1994) 1457.
- [42] Chanda J, Bandyopadhyay S, *Langmuir* 22 (2006) 3775.
- [43] Högberg C J, Lyubartsev A, *J Phys Chem B* 110 (2006) 14326.
- [44] Thaning J, Högberg C J, Stevansson B, Lyubartsev A, Maliniak A, *J Phys Chem B* 111 (2007) 13638.
- [45] Pathasarathi R, Jianhui T, Redondo A, Gnankaran S, *J Phys Chem A* 115 (2011) 12826.
- [46] Lis L J, McAlister M, Fuller N, Rand R P, Parsegian V A, *Biophys J* 37 (1982) 667.
- [47] (a) Yang Y, Parr R G, *Proc Natl Acad Sci U.S.A.*, Hardness, softness, and the Fukui function in the electronic theory of metals and catalysis.

- 82 9(1985) 6723. (b) Yang W, Mortier W J, The use of global and local molecular parameters for the analysis of the gas-phase basicity of amines. *J Am Chem Soc* 108 (1986) 5708.
- [48] Parr R G, Yang W, *Density-functional theory of atoms and molecules*: Oxford University Press, New York (1989).
- [49] Parr R G, Yang W, *J Am Chem Soc* 106 (1984) 4049.
- [50] (a) Pearson R G, *J Am Chem Soc* 85 (1963) 3533 (b) Sen K D, *Chemical Hardness Struct. Bonding* (Ed); Springer-Verlag: Berlin 80 (1993) (c) Parr R G, Pearson R G, Absolute hardness: companion parameter to absolute electronegativity. *J Am Chem Soc* 105 (1983) 7512 (d) Parr R G, Donnelley R A, Levy M, Palke W E, *Electronegativity: The density functional viewpoint*. *J Chem Phys* 68 (1978) 3801 (e) Pearson R, Absolute electronegativity and absolute hardness of Lewis acids and bases. *J Am Chem Soc* 107 (1985) 6801.
- [51] Perdew J P, Parr R G, Levy M, Balduz J L, *Phys Rev Lett* 49 (1982) 1691.
- [52] Zhang Y, Yang W, *Theor Chem Acc* 103 (2000) 346.
- [53] Gazquez J L, Mendez F, *J Phys Chem* 98 (1994) 4591.
- [54] Mendez F, Gazquez J L, *J Am Chem Soc* 116 (1994) 9298.
- [55] Gazquez J L, Martinez A, Mendez F, *J Phys Chem* 97 (1993) 4059.
- [56] Köster A M, Calaminici P, Casida M E, Flores M R, Geudtner G, Goursot A, Heine T, Ipatov A, Janetzko F, Martin delCampo J, Patchkovskii S, Reveles J U, Salahub D R, Vela A, (2006) *The deMon deVelopers*; Cinvestav: Mexico City.
- [57] Zhang Y, Yang W, *Phys Rev Lett* 80 (1998) 890.

- [58] Lee C, Yang W, Parr R G, Phys Rev B: Condens. Matter Phys 37 (1988) 785.
- [59] Godbout N, Salahub D R, Andzelm J, Wimmer E, Can J Chem 70 (1992) 560.
- [60] Kořster A M, Flores-Moreno R, Reveles J U, J Chem Phys 121 (2004) 681.
- [61] Dunlap B I, Connolly J W D, Sabin J R, J Chem Phys 71 (1979) 4993
- [62] Mintmire W, Dunlap B I, Phys ReV A 25 (1982) 88.
- [63] Reveles J U, Kořster A M, J Comput Chem 25 (2004) 1109.
- [64] Frisch M J, Trucks G W, Schlegel H B, Scuseria G E, Robb M A, Cheeseman J R, Scalmani G, Barone V, Mennucci B, Petersson G A, Nakatsuji H, Caricato M, Li X, Hratchian H P, Izmaylov A F, Bloino J, Zheng G, Sonnenberg J L, Hada M, Ehara M, Toyota K, Fukuda R, Hasegawa J, Ishida M, Nakajima T, Honda Y, Kitao O, Nakai H, Vreven T, Montgomery Jr J A, Peralta J E, Ogliaro F, Bearpark M, Heyd J J, Brothers E, Kudin K N, Staroverov V N, Kobayashi R, Normand J, Raghavachari K, Rendell A, Burant J C, Iyengar S S, Tomasi J, Cossi M, Rega N, Millam N J, Klene M, Knox J E, Cross J B, Bakken V, Adamo C, Jaramillo J, Gomperts R, Stratmann R E, Yazyev O, Austin A J, Cammi R, Pomelli C, Ochterski J W, Martin R L, Morokuma K, Zakrzewski V G, Voth G A, Salvador P, Dannenberg J J, Dapprich S, Daniels A D, Farkas Ö, Foresman J B, Ortiz J V, Cioslowski J, Fox D J Gaussian 09 Revision A.1 Inc, Wallingford CT, (2009).
- [65] Becke A D, J Chem Phys. 98 (1993) 5648.

- [66] Roy R K, Pal S, Hirao K, J Chem Phys 110 (1999) 8236.
- [67] Hirshfeld F L, Theor Chim Acta 44 (1977) 129.
- [68] Frischleder H, Lochmann R, Int. J of Quant Chem 16 (1979) 203.
- [69] (a) Breneman M. C, Wiberg K. B, J Comput Chem 11 (1990) 361. (b)
Thanikaivelan P, Padmanabhan J, Subramanian V, Ramasami T,
Theor Chem Acta 107 (2004) 326.
- [70] Beck B and Clark T. Robert C. Glen, J Mol Mod 1 (1995) 176.
- [71] Beck B, Clark T, and Glen RC, VESPA: J Comput Chem 18 (1997)
744.
- [72] Sovago M, Vartiainen E, Bonn M, J Chem Phys 131 (2009) 161107.
- [73] Vleeschouwer F D, Jaque P, Geerlings P, Toro-Labbé A, De Proft F, J
Org Chem 75 (2010) 4964.
- [74] Moreno R F, J Chem Theor Com 6 (2010) 48.

CHAPTER 5

Ionization Potential and Structure

Relaxation of Adenine, Thymine,

Guanine and Cytosine Bases and

Their Base Pairs: A quantification

of reactive

sites

Abstract

We present in this chapter Density Functional Theory (DFT) calculations using B3LYP/6-31++G** method to show relaxation in geometry of base pairs on cation radical formation. The changes in hydrogen bond length and angles show that in the cationic radical form the structure of the base pairs relaxes due to the distribution of charge. Eventually according to a recent study it has been found that, upon excitation hole transfer from base to sugar occurs which results in sugar radical formation and leads to strand breakage [45]. One hydrogen bond increases, while the other decreases in Adenine-Thymine (AT) base pair and in case of Guanine-Cytosine (GC) base pair, one increase and other two decrease. Same is the case with bond angles for both the base pairs. Analysis of the electron density map of Singly Occupied Molecular Orbital (SOMO) reveals that electron is transferred mainly from adenine and guanine bases in the cationic radical formation of AT and GC base pair respectively.

The reactive sites of bases have been analyzed using condensed Fukui functions in a relaxed and frozen core approximation. The effects of relaxation on the reactivity indices are also analyzed.

5.1. Introduction

The process of charge transfer in biomolecules is currently a topic of interest for most important problems of molecular biophysics and biochemistry. Generally, DNA (deoxyribose nucleic acids) molecule in equilibrium state does not have any free charge carriers. Damage to DNA is due to the high energy radiations as a result of which it forms the transient charged radicals. Excess charge on individual bases and base pair leads to DNA damage [1-4]. Photo-excitation within DNA, upon exposure to UV radiation and chemical reactions of DNA involve transfer of holes and electrons. An accurate description of the electron affinities would explain the distribution of the excess electron in DNA [5-11]. Specific interest to study electron transfer in DNA elucidates the motion of radicals along the molecule to cause destruction resulting in mutagenesis and carcinogenesis.

The bases (purines and pyrimidine) present in DNA form hydrogen bonds between them with their respective complementary base, which plays a vital role in biological systems. Pairing is also the mechanism by which codons on messenger RNA molecules are recognized by anticodons on transfer RNA during protein translation. Some DNA or RNA-binding enzymes can recognize specific base pairing patterns that identify particular regulatory regions of genes. These hydrogen bonds help in maintaining the structure and specificity of systems. In particular, the hydrogen bond determines the magnitude and the nature of the interactions of the biomolecules and is consequently responsible for the important unique properties of nucleic acids [12]. The stability of DNA and RNA structure is not only due to the H-bond base pairing, but also the base stacking, which is actually an interaction

between pi orbital of the aromatic rings of the bases and London dispersion forces [13]. Due to the small size and existence of experimental data, these base pairs have been chosen as prototype of DNA structure in theoretical investigations. The interesting information about their electronic structure and the weakly held molecular complexes can be obtained by quantum chemical treatment [14-18].

A spontaneous DNA mutation induced by proton transfer in the Guanine, Cytosine base pairs with an energetic perspective [19] is a motivation to study electron transfer in DNA bases. *Ab Initio* calculations were applied to study nucleic acid bases and their hydrogen bonded and stacked complexes, H-bonding of bases[20] were first investigated by the *ab initio* methods in 1986-1988. A real breakthrough in the quality of *ab initio* studies of bases and base pairs occurred around 1994-1995, when the first high level *ab initio* calculation with consistent treatment of electron correlation effects became feasible[2]. Lesions in DNA are caused by electrons with high and low energy resulting in cancer cell formation. So, the mechanisms of primary and secondary damage to purine and pyrimidine base pairs have been under intense investigations in recent years [21-35]. It has also been demonstrated recently that even very low energy electrons can induce strand breaks in DNA [22, 25, 36, 37, 38]. The structures and energetics of the closed shell [34, 39, 40], H-abstracted [33], and deprotonated [28] A-T and G-C base pairs and bases have been explored. This tells the change in the conformation of the native structure when it exposed to the outside environment with UV or some chemical agents involving electron transfer. Electron correlation is necessary to obtain accurate charge distribution and dipole moments [41]. Effect of base stacking on the acid-base

properties of adenine cation radical as well as studies of deprotonation states of guanine cation radical using both ESR and DFT both have also been reported [42,43]. Advanced *ab initio* calculations for calculating stacking energy in the gaseous environment provide a benchmark for the experimental studies to give reference data for the magnitude and conformation of bases and base pairs [44]. It has been found that upon excitation, of base cation radicals in DNA and in model systems, hole transfer from base to sugar occurs resulting in sugar radical formation and strand break formation [45]. Effect of base sequence on deprotonation of guanine cation radical has found that the positive charge in guanine radical in oligonucleotide is delocalized over the extended pi orbitals of DNA bases [46].

Quantification of reactive sites for individual bases has already been done in the presence of water as medium and it shows the changes in reactivity descriptors of the bases in the presence of water [47]. Fukui Functions represent the descriptors of reactivity and will be used for the present study [48]. From a practical point of view, quantitative knowledge of the energies and geometry of these molecular interactions is particularly important for the development and validation of the studies for the design of artificial receptor molecules. Thus our main focus is to study the structure relaxation of cation radical of DNA base pairs. The reactive atoms of base pairs from Fukui functions give the location for electrophilic and nucleophilic attack to know the reactive centers in DNA. In addition to this, analysis of molecular orbitals for the cations radical of bases and base pairs shows from where the electron transfer in the cationic radical systems of the base pairs.

5.2. Theoretical Background

Density based response functions, called local and global reactivity descriptors (LRD and GRD), are derived from density function theory (DFT) [49]. Within the framework of density functional theory, Parr and coworkers have introduced several important chemical tools [50]. DFT has provided the theoretical basis for the concepts like electronic chemical potential, electro negativity, and hardness, collectively known as global chemical reactivity descriptor [51].

Fukui function [52] can be interpreted either as the change of electron density $\rho(r)$ at each point r when the total number of electrons is changed or as the sensitivity of chemical potential of a system to an external perturbation at a particular point r .

$$f(r) = (\partial\rho(r)/\partial N)_{v(r)} = (\partial\mu/\partial v(r))_N \quad (5.1)$$

The latter point of view, by far the most prominent in the literature, faces the N -discontinuity problem of atoms and molecules [53, 54] leading to the introduction of both right- and left-hand-side derivatives, to be considered at a given number of electrons, $N = N_0$:

$$f^+(r) = (\partial\rho(r)/\partial N)_{v(r)}^+ \quad (5.2)$$

for a nucleophilic attack provoking an electron increase in the system, and

$$f^-(r) = (\partial\rho(r)/\partial N)_{v(r)}^- \quad (5.3)$$

for an electrophilic attack provoking an electron decrease in in the system.

The finite difference method, using the electron densities of N_0 , $N_0 + 1$, $N_0 - 1$, defines

$$f^+(r) \approx \rho_{N_o+1}(r) - \rho_{N_o}(r)$$

and

(5.4)

$$f^-(r) \approx \rho_{N_o}(r) - \rho_{N_o-1}(r)$$

In frozen core approximation $f^+(r)$ can be written as $\rho_{\text{LUMO}}(r)$ and $f^-(r)$ is $\rho_{\text{HOMO}}(r)$. In order to describe the site reactivity or site selectivity, Yang *et al.* [52] proposed atom condensed Fukui function, based on the idea of electronic population around an atom in a molecule, similar to the procedure followed in population analysis technique [55]. The condensed Fukui function for an atom k undergoing nucleophilic, electrophilic or radical attack can be defined respectively as

$$f_k^+ \approx q_k^{N_o+1} - q_k^{N_o}$$

$$f_k^- \approx q_k^{N_o} - q_k^{N_o-1}$$

$$f_k^o \approx \frac{1}{2} (q_k^{N_o+1} - q_k^{N_o-1}) \quad (5.5)$$

where q_k 's are electronic population of the k th atom of a particular species.

The condensed local softness, s_k^+ and s_k^- are defined accordingly for nucleophilic and electrophilic attack, respectively.

The valence adiabatic ionization potential (AIP) presented in this chapter has been calculated by the difference between the energies of the appropriate cation radical and neutral species at their respective optimized geometries.

$$\text{AIP} = E_{\text{cation}} - E_{\text{neutral}} \quad (5.6)$$

5.3. Computational Details

Becke devised three-parameter hybrid density functional (B3) [56] which has been used with the correlation function of Lee, Yang and Parr(LYP) [57]. In addition we have performed single point energy calculation to calculate reactivity of base pairs and bases alone by using Fukui functions.

The molecular geometries of the purines and pyrimidines bases (Gua, Cyt, Ade and Thymine) and base pairs(AT and GC) and their cationic radical forms were completely optimized using B3LYP/6-31++G** method. The bond length study in charged base pairs is studied and the perturbation in bond length is shown in Table 1. Condensed Fukui Functions were calculated for bases and base pairs from equation (5.5) using both Lowdin population analysis (LPA) [58] and Mulliken population analysis (MPA). But, the condensed Fukui functions of the reactive atoms in the frozen core approximation have been calculated only by MPA.

The DFT calculations were performed using GAMESS [59] system of programs. Using B3LYP/6-31++G** optimized geometries, the structures,

shown in Figures 5.1 and 5.2, were generated by MOLDEN molecular modeling software [60]. The atomic numbering scheme for A, T, G and C bases are similar as those shown for AT and GC base pairs in Figures 5.1 and 5.2, respectively. All molecular orbital plots has been constructed using MOLDEN software package using the optimized structure of B3LYP/6-31++G**.

5.4. Results and Discussion

5.4.1. Geometry The optimized geometry of AT and GC base pairs are shown in Figure 5.1 and Figure 5.2. Here in this chapter we study the relaxation in structures by removal of an electron from the optimized neutral system. In the earlier studies, these changes in structure, specifically hydrogen bond length and energy with transfer of electron and proton have already been done by targeting some specific atoms of base pairs [61-62]. Table 5.1 shows the bond length of intermolecular H-bond as well as the bond angles of the respective system calculated using B3LYP/6-31++G** method. The AT base pair have two H-bonds. It is observed that one of them increases, while the other decreases in its cationic radical form as compared to neutral H-bond length. In the case of GC base pair there are three H-bonds. It is observed that one of them increases in charged system, while the other two decreases compared with the neutral system. These changes occur due to the relaxation caused by the loss of an electron. Bond length and bond angles of the base-pairs and their cation radical are presented in Table 5.1.

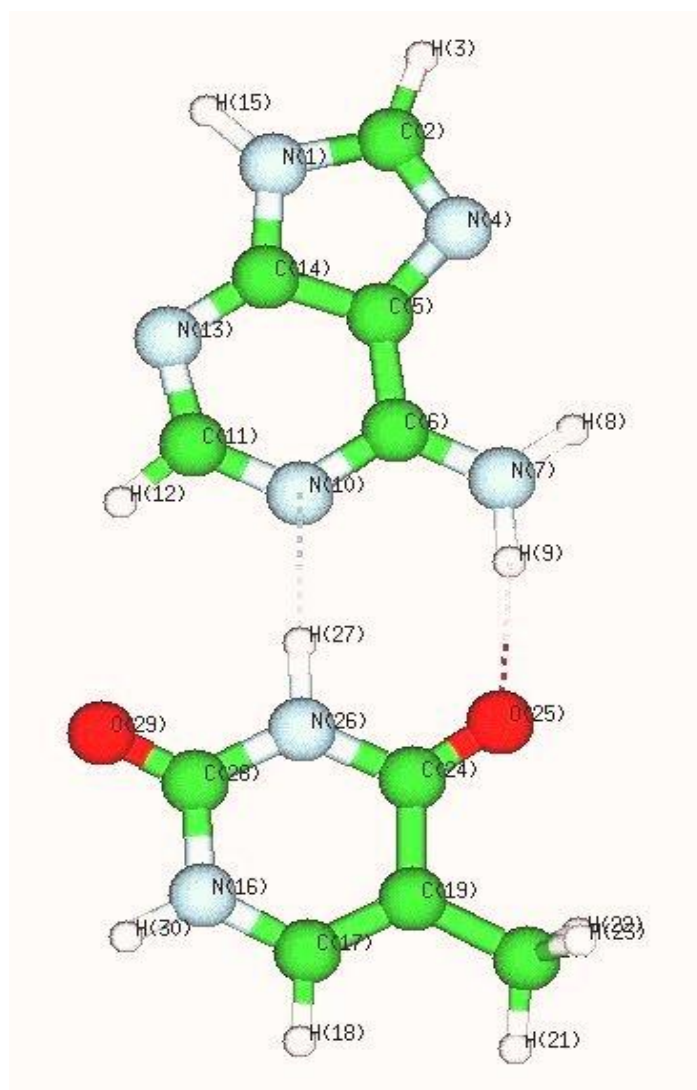


Figure 5.1 Optimized structures of Adenine-Thymine base pair.

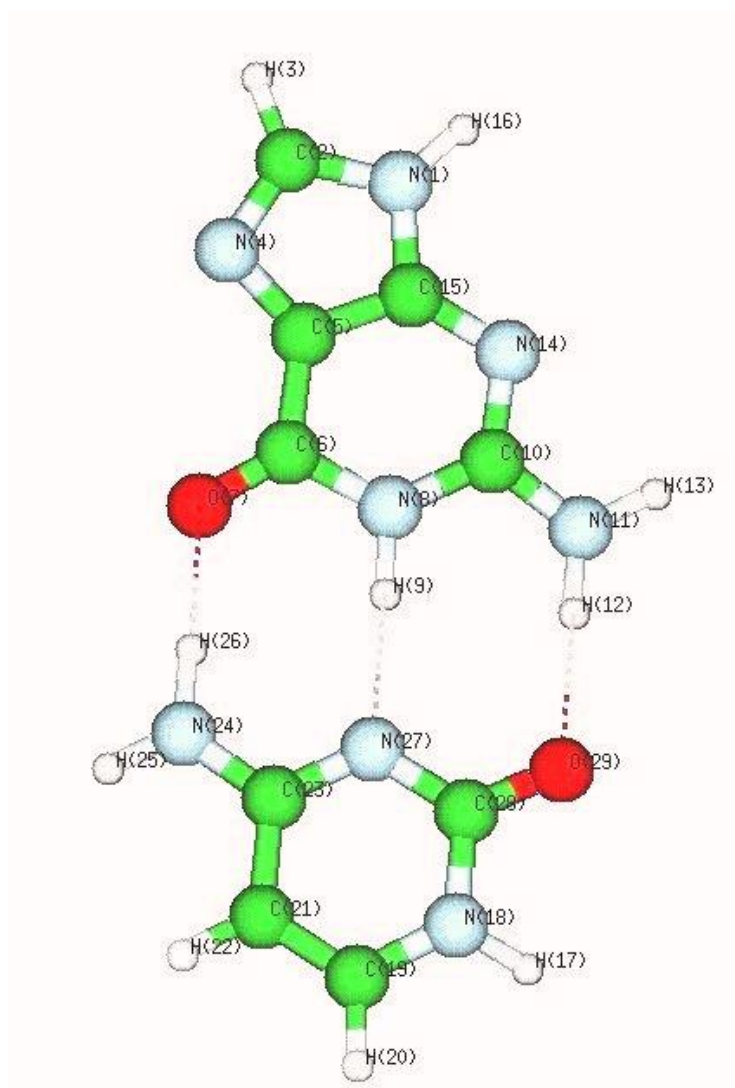


Figure 5.2: Optimized structure of Guanine-Cytosine base pair.

Table 5.1 Change in bond lengths and bond angles in neutral and cation radical of AT and GC base pairs.

Property		Atoms	Neutral	Cation radical
AT base pair	Bond	H9-O25	1.953	1.491
	Length	N10-H27	1.818	2.051
	Bond Angle	N7-H9-O25 N10-H27-N26	171.841 177.890	175.822 169.780
GC base pair	Bond	H12-O29	1.932	1.646
	lengths	H9-N27 O7-H26	1.912 1.750	1.771 1.926
	Bond angles	N11-H12-O29 N8-H9-N27 O7-H26-N24	176.850 174.940 175.618	177.700 178.754 173.581

As shown in Table 5.1, for AT base pair, the bond length between H9-O25 gets shorter in the cationic radical form, by 0.462 Å. The other H-bond between N10-H27 increases by 0.233 Å in cationic radical form. In the case of GC, the three H-bonds are there and these are in between H12-O29, H9-N27 and O7-H26 among them the bond length of O7-H26 has increased in cationic radical form while the H12-O29 and H9-N27 decreases. Bond angles changes are also depicted in Table 5.1. We have also calculated the adiabatic Ionization Potential of the individual bases and base pairs and the values are presented in Table 5.2. It shows that the ionization potential of the bases and base pairs varies from 0.2 – 0.3 eV.

The optimized structure of AT and GC base pairs with B3LYP functional showed that AT has planar structure while GC is non-planar. The reason for non-planarity is the amino group which is taking part in H-bonding and showing the pyramidalization effect [63]. It was also found that water molecules present in the DNA aqueous solution also promotes the non-planarity in the GC base pair [64].

5.4.2. Reactivity study of nucleobases and base pairs

The nature of the sites of ultimate localization of positive and negative charge and unpaired spin is obviously of great importance in understanding the mechanism of radiation-induced damage to DNA [65-66]. In the present chapter, we study the reactive centers for nucleophilic and electrophilic attack by calculating Fukui functions from Lowdin population analysis (LPA) and Mulliken population analysis (MPA) of the nucleobases and base pairs. These values are tabulated for Adenine,

Thymine, AT, Guanine, Cytosine and GC in Table 5.3, Table 5.4, Table 5.5, Table 5.6, Table 5.7 and Table 5.8 respectively.

Table 5.2 Adiabatic Ionization Potential (IP) for bases and base pairs.

Base pairs	Adiabatic IP (eV)	Expt[a]	Expt[b]	B1LYP 6311 +G(d,p) [c]
Adenine	8.008	8.26	7.80	7.95
Thymine	8.729	8.87	8.80	8.66
Guanine	7.597	7.77	7.85	7.52
Cytosine	8.563	8.45	8.68	8.47
A-T base pair	7.621	---	---	---
G-C base pair	6.848	---	---	---

[a] Photo ionization mass spectrometry in gas phase [68].

[b] Photoelectron spectra. Band onset [69].

[c] Radical cations of DNA bases [70].

Table 5.3 Reactive centers for nucleophilic and electrophilic attack for Adenine

Adenine Atoms	Values of f_k^+	Adenine atoms	Values of f_k^-
H(15)	0.351991	N(7)	0.192508
H(3)	0.212198	N(10)	0.123908
H(9)	0.144831	C(2)	0.112724
C(2)	0.095755	C(5)	0.087335
H(8)	0.044323	C(11)	0.075155

Table 5.4 Reactive centers for nucleophilic and electrophilic attack for Thymine

Thymine Atoms	Values of f_k^+	Thymine atoms	Values of f_k^-
H(18)	0.231939	C(19)	0.177859
H(30)	0.206574	O(29)	0.151251
C(17)	0.125191	N(16)	0.150988
O(25)	0.071289	O(25)	0.130424
H(21)	0.064533	C(17)	0.094151

Table 5.5 Reactive centers for nucleophilic and electrophilic attack for the Adenine-Thymine base pair

Adenine- Thymine base pair Atoms	Values of f_k^+ with LPA and MPA		Adenine- Thymine base pair Atoms	Values of f_k^- with LPA and MPA	
	LPA	MPA		LPA	MPA
H(15)	0.16347	0.19881	N(7)	0.132131	0.11801
H(3)	0.12657	0.77526	N(13)	0.086316	0.11703
C(17)	0.10507	0.12416	C(2)	0.082391	0.04338
H(18)	0.10256	0.68561	C(5)	0.062462	0.05903
H(30)	0.07709	0.26669	C(19)	0.060497	0.04374

Table 5.6 Reactive centers for nucleophilic and electrophilic attack for the Guanine

Guanine Atoms	Values of f_k^+	Guanine atoms	Values of f_k^-
H(12)	0.288783	O(7)	0.144931
H(16)	0.172966	C(2)	0.131902
H(13)	0.149004	C(5)	0.115616
H(9)	0.083857	N(14)	0.110022
H(3)	0.083672	N(11)	0.107941

Table 5.7 Reactive centers for nucleophilic and electrophilic attack for the Cytosine

Cytosine Atoms	Values of f_k^+	Cytosine atoms	Values of f_k^-
H(25)	0.233519	O(29)	0.255331
H(20)	0.215712	C(21)	0.180521
H(22)	0.159526	N(27)	0.132532
H(17)	0.103446	N(18)	0.109954
H(26)	0.068447	N(24)	0.080535

Table 5.8 Reactive centers for nucleophile and electrophile attack for the Guanine-Cytosine base pair

Guanine- Cytosine base pair Atoms	Values of f_k^+ with LPA and MPA.		Guanine- Cytosine base pair Atoms	Values of f_k^- with LPA and MPA.	
	LPA	MPA		LPA	MPA
H(20)	0.18185	1.01622	N(11)	0.129034	0.12120
C(19)	0.120605	0.08111	C(2)	0.119282	0.07750
H(16)	0.118459	0.39978	N(14)	0.118361	0.14249
H(17)	0.096895	0.34505	O(7)	0.114567	0.12602
H(22)	0.061881	0.32519	C(5)	0.113164	0.06416

We observed that nucleophilic and electrophilic attack centers are different in individual bases and in base pairs. But surprisingly when adenine pairs with thymine the Fukui function of its reactive atoms are same and thus the electrophiles and nucleophiles are expected to attack on Adenine in AT base pair [35]. Thus, after pairing thymine lost its reactivity towards nucleophile and electrophile attack. For both AT and GC base pairs the atom which are having highest f_k^- value that is the center for electrophile attack are the H-bonded atoms or H-bond atoms. This is due to the presence of electron cloud near H-bond so when an electrophile attacks it will preferably looks for an electron rich region. Results of frozen core Fukui functions for reactive atoms and orbitals are presented using MPA in Table 5.9 and Table 5.10 for AT and GC base pair respectively. Thus, we observed that the five most reactive atoms for AT base pair are H(15), H(3), C(17), H(18) and H(30) for nucleophilic

attack and N(7), N(13), C(2), C(5) and C(19) for electrophilic attack. For GC base pair these atoms are H(20), C(19), H(16), H(17), H(22) and N(11), C(2), N(14), O(7), C(5) for nucleophile and electrophile centers respectively. The orbital analysis of the Fukui function shows that the $2p_z$ orbital is the most reactive in the case of atoms like C, N and O and for the Hydrogen atom the $1s$ orbital is the most reactive. Theoretical study of molecular recognition of base pairs interacting via multiple sites, using various density response functions have been studied by *Pal et al.* [67].

Table 5.9 Reactive centers of AT base pair by frozen core approximation.

Atoms	ρ_{LUMO}^p	Atoms	ρ_{HOMO}^p
H(15)	1.7720	N(7)	0.1679
N(13)	0.5715	N(13)	0.0870
C(17)	0.2143	C(2)	0.0787
H(18)	0.0385	C(5)	0.0565
H(30)	0.0010	C(19)	0.0479

Table 5.10 Reactive centers of GC base pair by frozen core approximation

Atoms	ρ_{LUMO}	Atoms	ρ_{HOMO}
H(20)	0.6657	N(11)	0.4260
C(19)	0.3256	C(2)	0.1397
H(16)	0.1349	N(14)	0.0962
H(17)	0.0823	O(7)	0.0899
H(22)	0.0419	C(5)	0.0813

5.4.3. Electron density of the base and base pair cations radical

We looked upon the Molecular Orbitals of individual bases and base pairs and by looking into the electron densities of atoms of cations radical SOMO, we have observed for GC base pair in the cation radical form that the electron loss is from the guanine base. Fig 3 shows that the molecular orbital SOMO for guanine cation radical shows the same electron density in GC cation radical SOMO. Therefore, excess positive charge lies on guanine which is 0.9831. In the case of AT base pair electron is lost from adenine by looking into the electron density maps shows in Figure 5.4 which is in good agreement with the experimental ESR results [39]. The atoms present there for hydrogen bond formation in guanine shows the effective change in charges for neutral and cationic radical system which accounts for the change in the bond lengths of GC base pair.

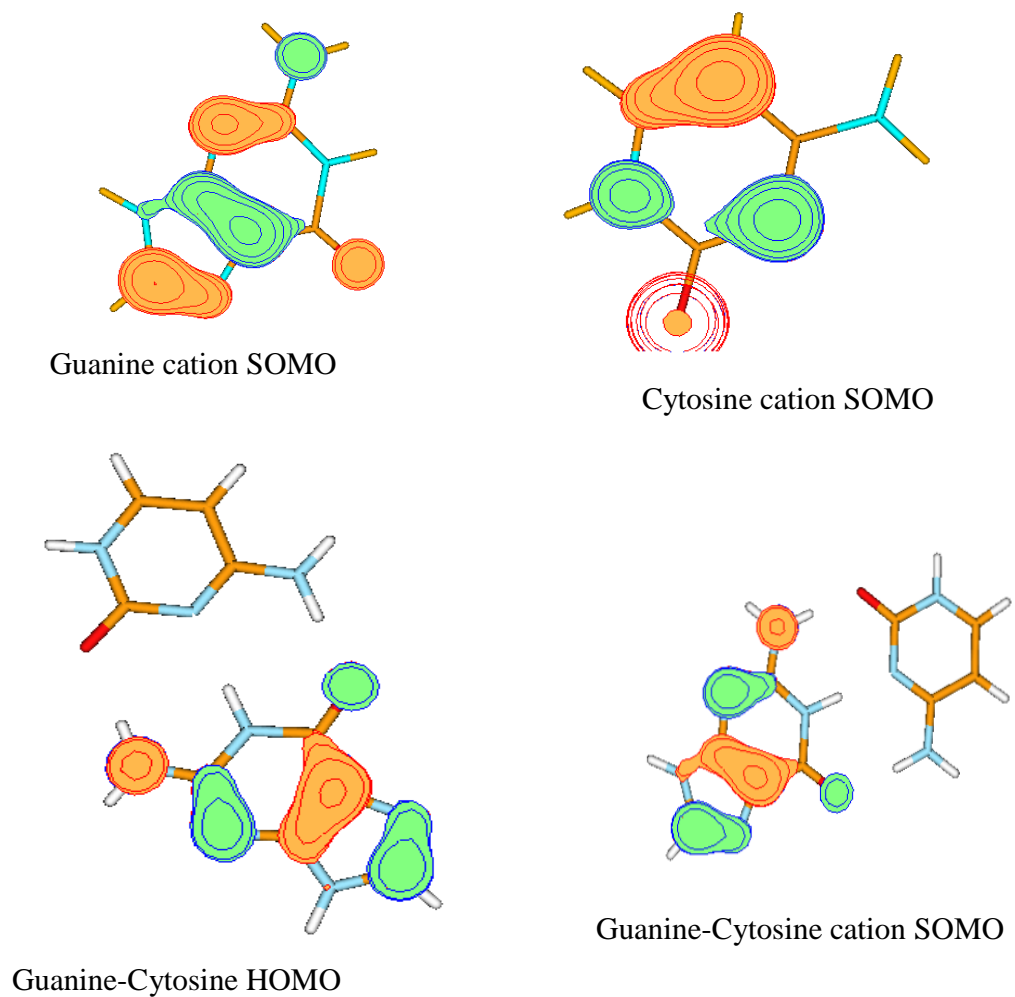


Figure 5.3 Quantitative comparison of molecular orbitals of GC cation. GC cation HOMO is quite similar to the individual Guanine cation HOMO and signifies that the electron lost from the Guanine.

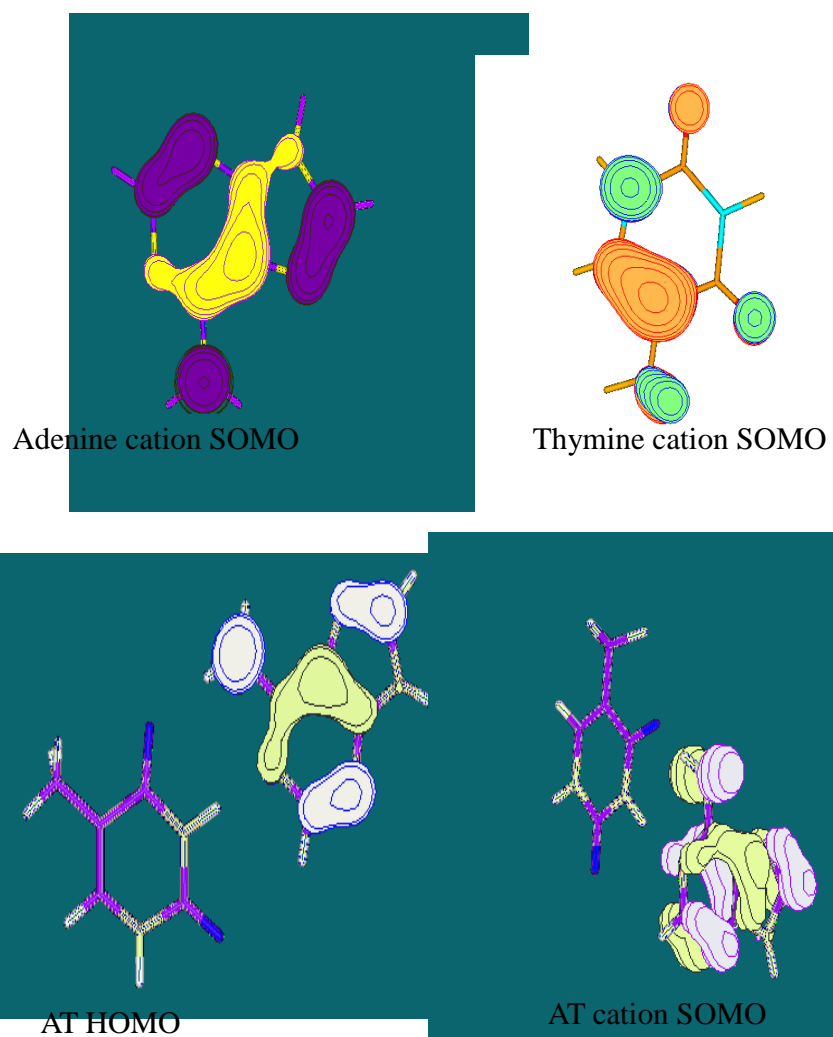


Figure 5.4 Quantitative comparison of molecular orbitals of AT cation. AT cation HOMO is quite similar to the individual Adenine cation HOMO and signifies that the electron lost from the Adenine.

5.5. Conclusion

We have shown change in H-bond length and bond angles of the subunits of DNA i.e base pair AT and GC in the cationic radical system. With the loss of an electron, intermolecular H-bond distance changes. Reactive centers of the bases and base pair obtained from calculation with either relaxed or frozen-core approach are mostly near the hydrogen bonds for electrophile attack and the reactivity sites change in individual bases as it pairs with its complementary base. In the case of thymine, its reactivity decreases as it pairs with the adenine. Thus, we can conclude on the sites of electrophilic and nucleophilic attack in the base pairs and allowing one to predict the sites of reactivity.

5.6. References

- [1] Steenken S, Telo J P, Novais H M, Candeias L P, J Am Chem Soc 114 (1992) 4701.
- [2] Colson A O, Sevilla M D, Int J Radiat Biol 67 (1995) 627.
- [3] Desfranc C, Abdoul-Carime H, Schermann J P, J Chem Phys 104 (1996) 7792.
- [4] Huels M A, Hahndorf I, Illenberger E, Sanche L, J Chem Phys 108 (1998) 1309.
- [5] Cai Z, Sevilla M D, J Phys Chem B 104 (2000) 6942.
- [6] Messer A, Carpenter K, Forzley K, Buchanan J, Yang S, Razskazovskii Y, Cai Z, Sevilla M D, J Phys Chem B 104 (2000) 1128.
- [7] Cai Z, Gu Z, Sevilla M D, J Phys Chem B, 104 (2000) 10406.
- [8] Giese B, Spichty M, Chem Phys Chem 1 (2000) 195.
- [9] Giese B, Spichty M, Wessely S, Pure and Appl Chem 73 (2001) 449.
- [10] Berlin Y A, Burin A L, Ratner M A, J Am Chem Soc 123 (2001) 260.
- [11] Bixon M and Jortner J, J Phys Chem A 105 (2001) 10322.
- [12] Watson J D, Crick F H C, Nature 171 (1953) 737.
- [13] Hanlon S, Biochem Biophys Res Commun 23(1966) 861.
- [14] Hobza P and Sponer J, Chem Rev 99 (1999) 3247 ; Sponer J, Leszczynski J, Hobza P, J Biomol Struct Dynam 14 (1996) 117.
- [15] Sponer J, Leszczynski J, Hobza P, J Phys Chem 100 (1996) 1965
- [16] (a) Guerra C F, Bickelhaupt F M, Angew Chem, Int Ed. Engl. 1999, 38, 2942; (b) Gould I R, Kollman P A, J Am Chem Soc 116 (1994) 2493 ; (c) Hutter M, Clark T, J Am Chem Soc 118 (1996) 7574 ; (d) Brameld K, Dasgupta S; (e) Goddard W A III, J Phys Chem B 101(1997) 4851.

- [17] Kawahara S, Wada T, Kawauchi S, Uchimarui T, Sekino M, *J Phys Chem A* 103 (1999) 8516
- [18] Yanson I K, Teplitsky A B, Sukhodub L R, *Biopolymers* 18 (1979) 1149.
- [19] Hanna M W, Lippert J L (Ed.), *Molecular complexes*, Foester R, London:Eleck Vol.1; Scheiner S, (Ed.), *Molecular Interactions*, 1997.
- [20] Hobza P, Sandorfy C, *J Am Chem Soc* 109 (1987) 1302.
- [21] Bera P P, Schaefer H F, *Proc Natl Acad Sci USA*. 102(2005) 6698.
- [22] Berdys J, Anusiewicz I, Skurski P, Simons J, *J Am Chem Soc* 126(2004) 6441.
- [23] Abdoul-Carime H, Gohlke S, Illenberger E, *Phys Rev Lett* 92 (2004) 168103.
- [24] Ptasinska S, Denifl S, Scheier P, Illenberger E, Mark T D, *Angew Chem Int Ed* 44 (2005) 6941
- [25] Boudaiffa B, Cloutier P, Hunting D, Huels M A, Sanche L, *Med Sci* 16 (2000) 1281.
- [26] Collins G P, *Sci Am*, 289 (2003) 26.
- [27] Evangelista F A, Paul A, Schaefer H F, *J Phys Chem A*, 108 (2004) 3565.
- [28] Kumar A, Knapp-Mohammady M, Mishra PC and Suhai S, *J Comput Chem* 25 (2004) 1047.
- [29] Li X F, Sevilla M D, Sanche L, *J Phys Chem B* 108 (2004) 19013.
- [30] Liu B, Hvelplund P, Nielsen S B, Tomita S, *J Chem Phys*, 121 (2004) 4175.
- [31] Luo Q, Li J, Li Q S, Kim S, Wheeler S E, Xie Y M, Schaefer H F, *Phys Chem Chem Phys* 7 (2005) 861.
- [32] Luo Q, Li Q S, Xie Y M, Schaefer H F, *Collect Czech Chem Commun* 70 (2005) 826.

- [33] Profeta L T M, Larkin J D, Schaefer H F, Mol Phys 101 (2003) 3277.
- [34] Richardson N A, Wesolowski S S, Schaefer H F, J Phys Chem B 107 (2003) 848.
- [35] Steenken S, Chem Rev 89 (1989) 503.
- [36] Sanche L, Phys Scripta 68 (2003) C108.
- [37] Boudaiffa B, Cloutier P, Hunting D, Huels M A, Sanche L, Science 287 (2000) 1658.
- [38] Li X F, Sevilla M D, Sanche L, J Am Chem Soc 125 (2003) 13668–13669.
- [39] Richardson N A, Wesolowski S S, Schaefer H F, J Am Chem Soc 124 (2002) 10163.
- [40] Li X F, Cai Z L, Sevilla M D, J Phys Chem A 106 (2002) 9345.
- [41] Nowak M J, Lapinski L, Kwiatkowski J S, Leszczynski J, (ed.) in Computational Chemistry: Reviews of Current Trends Leszczynski J, (1997) World Scientific press, Singapore vol. 2, pp. 140–216.
- [42] Adhikary A, Kumar Anil, Khanduri D, Sevilla M D, JACS 130 (2008) 10282.
- [43] Adhikary A, Kumar Anil, Becker D, Sevilla M D, J Phys Chem B 110 (2006) 24171.
- [44] Hobza P, Sponer J, J Am Chem Soc 124 (2002) 11802.
- [45] Kumar A, Sevilla M D, J Phys Chem B 110 (2006) 24181.
- [46] Kobayashi K, Yamagami R, Tagawa S, J Phys Chem B 112 (2008) 10752.
- [47] Sivanesan D, Subramanian V, Unni Nair B, J Mol Str (Theochem) 544 (2001) 123.
- [48] Fukui K, Science 218 (1982) 747.

- [49] Parr R G, Yang W, J Am Chem Soc 106 (1984) 4049.
- [50] Parr R G, Yang W, Density-functional theory of atoms and molecules; Oxford University Press, New York, 1989.
- [51] (a) Pearson R G, J Am Chem Soc 85 (1963) 3533; (b) Sen K D, in Chemical Hardness Struct Bonding (Ed) Springer-Verlag, Berlin, 1993; Vol. 80; (c) Parr R G, Pearson R G, J Am Chem Soc 105 (1983) 7512; (d) Parr R G, Donnelly R A, Levy M, Palke W E, J Chem Phys 68 (1978) 3801; (e) Pearson R, J Am Chem Soc 107 (1985) 6801.
- [52] (a) Parr R G, Yang W, J Am Chem Soc 106 (1984) 4049; (b) Yang Y, Parr R G, Proc Natl Acad Sci U.S.A. 821 (1985) 6723; (c) Yang W, Mortier W J, J Am Chem Soc 108 (1986) 5708.
- [53] Perdew J P, Parr R G, Levy M, Balduz J L, Phys Rev Lett 49 (1982) 1691
- [54] Zhang Y, Yang W, Theor Chem Acc 103 (2000) 346.
- [55] Bachrach S M, Lipkowitz K B, Boyd(Ed) D B, Reviews in computational chemistry, VCH, New York, 1995, vol 5,171.
- [56] Becke A D, J Chem Phys 98 (1993) 5648.
- [57] Lee C T, Yang W T, Parr R G, Phys Rev B At Mol Opt Phys 37 (1988) 785.
- [58] Lowdin P O, J Chem Phys 21 (1953) 374; Lowdin P O, J Chem Phys 18 (1950) 365; Mulliken R S, J Chem Phys 23 (1955) 1833.
- [59] Schmidt M W et al., J Comput Chem 14 (1993) 1347.
- [60] Schaftenaar G, Noordik J H J, Comput-Aided Mol Des 14 (2000) 123.
- [61] Lind M C, Bera P P, Richardson N A, Wheeler S E, Schaefer III H F, PNAS 103 (2006) 7554.

- [62] Sunghwan K, Lind M C, Schaefer III H F, J Phys Chem B 112 (2007) 3545.
- [63] Noriyuki, Danillov V I, Chemical Physics Letters 404 (2005) 164.
- [64] Kumar Anil, Sevilla M D, Suhai S, J Phys Chem B 112 (2008) 5189.
- [65] (a) Lemaire D G E, Bothe E, Schulte-Frohlinde D Znt, J Radiat Biol 45 (1984) 351. (b) Deeble D J, von Sonntag, C Ibid 46 1984, 247.
- [66](a) Boon P J, Cullis P M, Symons M C R, Wren B W, J Chem SOC, Perkin Trans. 2 (1984) 1393. (b) Cullis P M, Sym-ons M C R, Radiat Phys Chem 27 (1986) 93.
- [67] Pal S, Chandrakumar K R S, J Phys Chem B 105 (2001) 4541.
- [68] Orlov V M, Smirnov A N, Varshavsky Y M, Tetrahedron Lett 48 (1976) 4377.
- [69] Lias S G, Bartmess J E, Liebman J F, Holmes J L, Levin R D, Mallard W G, J Phys Chem Ref Data 17 (1988) 1.
- [70] Improta R, Scalmani G, Barone V, Int J of Mass Spec 201 (2000) 321–336.

CHAPTER 6

Role of Substituents on the Reactivity and Electron Density Profile of Diimine Ligands

Abstract

In this chapter, we study the reactivity of diimines like 2, 2'-bipyridine, 1, 10-phenanthroline and 1, 2, 4-triazines using density based reactivity descriptors. We discuss the enhancement or diminution in the reactivity of these ligands as a function of two substituent groups, namely methyl (-CH₃) group and phenyl (-C₆H₅) group. The global reactivity descriptors explain the global affinity and philicity of these ligands whereas the local softness depicts the particular site selectivity. The intermolecular reactivity trends for the same systems are analyzed through the philicity and group philicity indices. The σ -donor character of these ligands is quantified with the help of electron density profile. In addition, the possible strength of interaction of these ligands with metal ion is supported with actual reaction energies of Ru-L complexes.

6.1. Introduction

Aromatic nitrogen heterocycles represent an important class of ligands in coordination chemistry [1]. Among them monodenate ligands, such as pyridine, chelating ligands, such as 2,2'-bipyridine and its analogues, 1,10-phenanthroline readily form stable complexes with most of the transition metal ions and have been extensively used in both analytical and preparative coordination chemistry [2-6]. The particular reasons for this property include (i) the versatile coordination behavior due to the good σ -donor and π -acceptor characteristics and the flexibility of the α -diimine molecule, and (ii) the apparently facile activation of the metal coordinated α -diimine for a whole range of both stoichiometric and catalytic reactions [7-14]. Such compounds are also used to model important bio-inorganic systems such as some metalloproteins and are finding applications as photosensitizers which are used in dye-sensitized solar cells. The charge-transfer properties of photosensitizers can be tuned by substituting the different functional groups. The ability of α -diimines to form ionic and neutral guest compounds makes them useful precursors in supramolecular chemistry [15-19]. Six-membered aromatic nitrogen heterocycles have relatively low energy π^* orbitals which act as good acceptors of metal d-orbital electron density in metal-ligand back bonding. Thus metal-ligand interactions are governed by the specific metal and ligand involved [20-21]. Such complexes can exhibit interactions, such as electron transfer, magnetic coupling and inter-valence transfer [21]. The interaction between the metal center and ligand takes place via the π system.

These kinds of metal-ligand interactions can be tuned by conjugation between the coordination sites. The measure of some important electronic properties such as ionization energy, electron affinity etc., through the introduction of electron donating (ED) or electron withdrawing (EW) substitutions follows a long established method in bio-chemical and molecular electronics engineering [22-26]. ED or EW substituent can increase or decrease the energies of highest occupied molecular orbital (HOMO) and lowest unoccupied molecular orbital (LUMO) relative to that of bare molecule, allowing a significant modification of the molecular electronic properties. Therefore, fine tuning of the ligand using different functional groups can help in designing various metal-ligand reactions which can be used in various chemical and biochemical process as mentioned earlier.

Theoretical descriptors using conceptual density functional theory have been used extensively in recent years to calculate chemical properties [27]. Recent studies describe the utility of these concepts in both qualitative and quantitative terms in the field of molecular structure, chemical bonding, reactivity and selectivity of molecules [28-35]. Among these, density based descriptors such as, global reactivity descriptors, local reactivity descriptors and local hard soft acid base principle, principle of maximum hardness are extensively used to understand the chemical systems and its reactivity [36-40]. The global reactivity descriptors chemical potential (μ), electronegativity (χ), hardness (η) and philicity (w) [41-42] have systematized the study of overall stability of the chemical species in this area.

Concerning the local descriptors specifically the Fukui function (FF), $f(r)$, the local softness $s(r)$ and the local philicity $w(r)$ have attracted recent attention. The

atom condensed versions of these descriptors are frequently used to study site selectivity and intra molecular reactivity of various systems probing accurate electrophilic and nucleophilic attacks [43a]. There are many other local reactivity descriptors used for site reactivity and selectivity namely multiphilic descriptors, local ionization energy, reactivity-selectivity descriptor etc. [43]. Although these indices were successful in generating the experimentally observed intra molecular reactivity trends in several cases, Roy *et al.* [44] showed that relative electrophilicity and relative nucleophilicity, based on the ratio of electrophilic and nucleophilic FFs (or local softness) and its inverse, are more reliable descriptors to generate improved intra molecular reactivity trends compared to those obtained from condensed FF indices. Further, the description of the inter-molecular reactivity has been analyzed by Krishnamurty and Pal using the concept of group softness where the group consists of the reacting atoms and the atoms that are directly connected to the reacting atoms [45]. In addition, a specific quantity, philicity $w(r)$, defined by Parr *et al.* [46a] and its condensed version are rigorously used in explaining reactivity. Recently, Tanwar *et al* [48] proposed two reactivity descriptors viz. Normalized Fukui Function (NFF) and Bond Deformation Kernel (BDK) for comparative studies on the systems with varying number of atoms. A local version of the hard-soft-acid-base (HSAB) principle, proposed by Gazquez and Mendez [49], and pursued by Pal and co-workers [50], as well as, Geerlings and co-workers [51] to a variety of chemical situations, is suited to semi-quantitative description of interaction energy.

In this chapter, we study the role of substituent towards the enhancement and/or diminution of the reactivity of 2, 2' bipyridine and its analogues with

Ruthenium metal using these descriptors. For this purpose, we consider various substituted diimines. The effect of methyl and phenyl groups on the reactivity of these diimines will be studied within the framework of Frozen Core Approximation (FCA). The reliability of FCA has been already discussed by Kulkarni *et al.* in analyzing the ligand characteristics [27d].

The present chapter has been organized as follows. In section 6.2, we describe theoretical background leading to definitions of various global and local reactivity descriptors. Section 6.3 provides the computational details and the methodology used for the calculations. In section 6.4 we focus on the results and discussion of the various calculations for the systems under consideration.

6.2. Theoretical Background

Density based descriptors of reactivity

The chemical potential (μ), global hardness η and philicity (w) are global descriptors which indicate overall stability of the system [21-24]. The global descriptor of a molecule is just the square of the electronegativity divided by its chemical hardness

$$\frac{\mu^2}{2\eta} \quad (6.2.1)$$

$$\mu = \left(\frac{\partial E}{\partial N} \right)_{v(r)} \quad (6.2.2)$$

where $v(r)$ is defined as the external potential

$$\eta = \frac{1}{2} \left(\frac{\partial^2 E}{\partial N^2} \right)_{v(r)} \quad \text{or} \quad \eta = \frac{1}{2} \left(\frac{\partial \mu}{\partial N} \right)_{v(r)} \quad (6.2.3)$$

Under the FCA and finite difference approximation, the working equation of chemical potential and hardness turns out as follows,

$$\mu = \frac{E_{HOMO} + E_{LUMO}}{2} \quad (6.2.4)$$

$$\eta = \frac{E_{LUMO} - E_{HOMO}}{2} \quad (6.2.5)$$

Higher the chemical hardness of an ensemble of the system with constant chemical potential, more stable is the system.

The global softness (S) is the half inverse of the hardness and is related to the overall reactivity of the system. A more powerful global reactive index defined as philicity as follows [46].

$$W = \frac{\mu^2}{2\eta} \quad (6.2.6)$$

The response of the electron density at each point in space to the variation in the number of electrons is defined as Fukui Function (FF) by Parr and Yang [17]. Fukui functions have been used widely to measure the reactivity parameters [45].

$$\left(\frac{\partial^2 E}{\partial N \partial v(r)} \right) = \left(\frac{\partial \rho(r)}{\partial N} \right)_{v(r)} = f(r) \quad (6.2.7)$$

A related local property, called local softness is defined as

$$s(r) = \left(\frac{\partial \rho(r)}{\partial \mu} \right)_{v(r)} \quad (6.2.8)$$

so that we obtain

$$\int s(r)dr = S \quad (6.2.9)$$

from equation (6.2.8) and (6.2.9), it is seen that

$$s(r) = f(r)S \quad (6.2.10)$$

Using left and right derivatives with respect to number of particles, electrophilic and nucleophilic Fukui functions and corresponding local softness and local philicity index is written as,

$$f^+(r) = \rho_{N+1}(r) - \rho_N(r), s^+(r) = f^+(r)S, w^+(r) = f^+(r)w \quad (6.2.11)$$

$$f^-(r) = \rho_N(r) - \rho_{N-1}(r), s^-(r) = f^-(r)S, w^-(r) = f^-(r)w \quad (6.2.12)$$

ρ_N in the above expression represents the electron density on atom k for N -electron system. Similarly, ρ_{N+1} and ρ_{N-1} are the electron densities of the $(N+1)$ and $(N-1)$ electronic systems calculated at the geometry of the N -electron system, respectively. To describe the reactivity of atom k in a molecule, Yang and Mortier [46] defined the condensed quantities as follows,

The condensed electrophilic FF and local softness:

$$f_k^+ = q_k(N+1) - q_k(N), s_k^+ = f_k^+S \quad (6.2.13)$$

and the condensed nucleophilic FF and local softness;

$$f_k^- = q_k(N) - q_k(N-1), s_k^- = f_k^-S \quad (6.2.14)$$

where, $q_k(N)$, $q_k(N-1)$ and $q_k(N+1)$ are the electronic population of the k^{th} atom in the N , $(N-1)$ and $(N+1)$ electronic systems, respectively. Under FCA the atom-condensed Fukui functions will be nothing but the respective atomic population of

HOMO or LUMO orbitals. These condensed FFs and local softness has been used as a reliable descriptor of reactivity and site selectivity to predict the intra molecular reactivity.

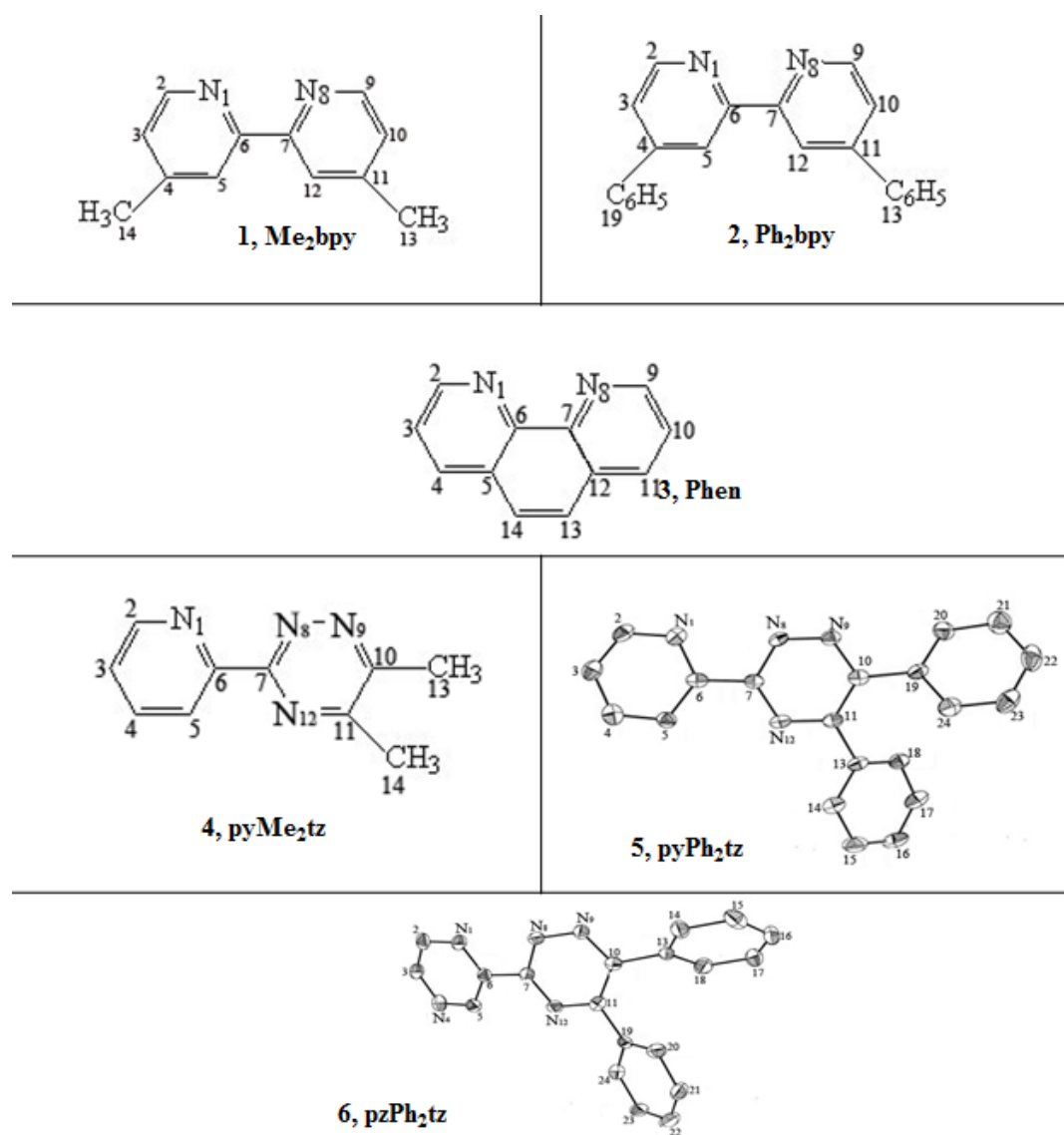


Figure 6.1: Structural representations of various substituted analogues of diimines considered as ligands in the present work.

Note: Depending upon the number of nitrogen atoms present in the systems, it is further categorized as substitution at i) 2,2'-bipyridine (**1**, **2**), ii) 3-(2-pyridinyl)-1,2,4-triazine (**4**, **5**) and iii) 3-(2-pyrazinyl)-1,2,4-triazine (**6**). Along with these systems an extremely important and widely used α -diimine 1,10-phenanthroline (**3**) is also studied.

Earlier Krishnamurty *et al.* [39a] proposed “group softness” to describe intermolecular reactivity trends in carbonyl compounds and organic acids. They defined group softness as,

$$s_g = \sum_{k=1}^n s_k \quad (6.2.15)$$

where n is the number of atoms bonded to the reactive atom, s_k is the atom-condensed softness of the atom k , and s_g is the group softness. Roy *et al.* [44] defined the relative electrophilicity and relative nucleophilicity as (f^+/f^-) and (f^-/f^+) , respectively and further it is used to predict the intra molecular reactivity trend.

Similarly the local atom-condensed philicity, w_A^a in the definition is given by [46c],

$$w_A^a = Wf_A^a, \forall a = +, -, 0 \quad (6.2.16)$$

The corresponding intermolecular electrophilicity and nucleophilicity condensed to the atom can be calculated using equation (6.2.16). This quantity is found to be useful in predicting the extent of partial electron transfer that contributes to the lowering of the total binding energy by maximum flow of electrons [46-47].

6.3. Computational Details

In our previous study which explains the donor-acceptor character of the 2, 2'-bipyridine and its important analogues viz; 3-(2-pyridinyl)-1,2,4-triazine and 3-

(2-pyrazinyl)-1,2,4-triazine where $-\text{CH}$ group were substituted by N atoms in basic bipyridine ring [27d]. In the present chapter, we further substitute here with methyl and phenyl groups in the concerned ligands. The Figure 6.1 presents all these systems. Along with these systems, an extremely important and widely used α -diimine 1, 10-phenanthroline (3) is also studied. Substituents considered here are mainly the methyl group ($-\text{CH}_3$) and the phenyl group ($-\text{C}_6\text{H}_5$). Thus the systems studied are: i) 1,Me₂bpy, ii) 2,Ph₂bpy, iii) 3,Phen, iv) 4,pyMe₂tz, v) 5,pyPh₂tz, vi) 6,pzPh₂tz. The nature of the substituent i.e. methyl and phenyl groups are analyzed and have been used to predict the trends in global and local reactivity. The optimization of all these systems is carried out with DFT using the restricted Hartree-Fock (RHF) procedure as employed in GAMESS [52a]. The functional used is hybrid functional B3LYP. The basis set used for the geometry optimization and property analysis is 6-31G (d, p). For the computation of the corresponding cations and anions of these systems, restricted open shell Hartree-Fock (ROHF) procedure is used under the FCA. The electronic population on the atoms for these neutral, anionic and cationic systems is obtained from Löwdin population analysis [53]. The ionization energy, electron affinity and all other related properties reported here are calculated under FCA. These properties along with condensed version of local softness and the local philicity are computed and are used to explain the substituent effect describing the reactivity of the diimines.

The Ru-ligand interaction energy and all other thermo chemical analysis have been computed using the GAUSSIAN [52b]. Considering the heavy nature of metal atom effective core potential (ECP) LANL2 [54] have been used for calculating

interaction energy. Further, we ensure the complete optimization of all individual ligands and their complexes with non-negative frequency analysis. The pictorial representation of one of the Ru-ligand complex studied in the present chapter has been shown in Figure 6.2.

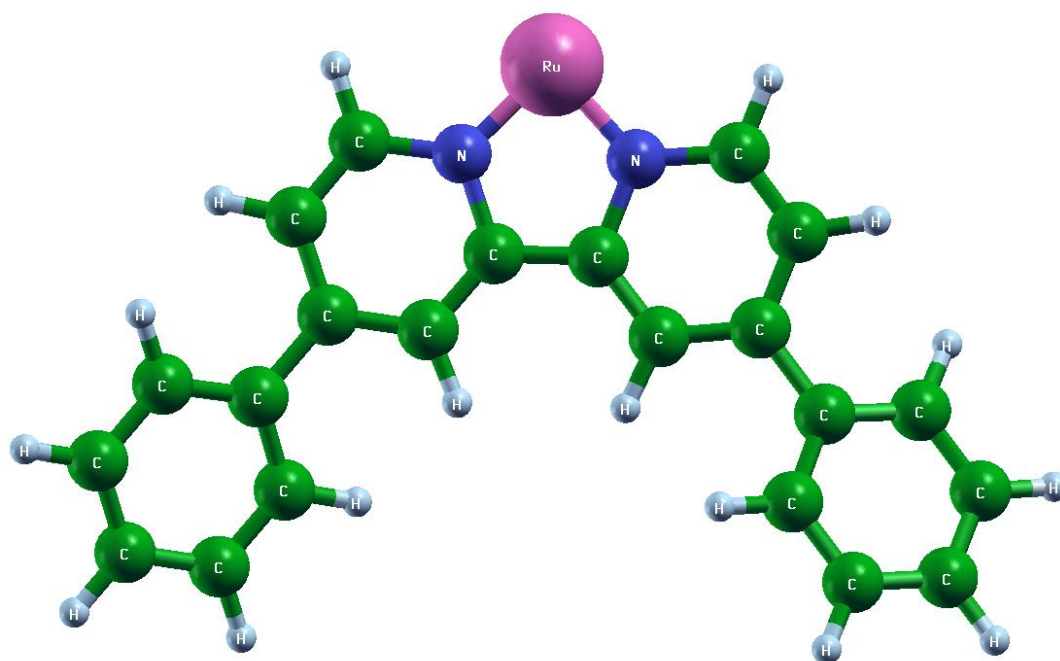


Figure 6.2: The Ru-ligand complex where ligand is 2,2'-bipyridine substituted with the phenyl group.

6.4. Discussion

The substituent $-\text{CH}_3$ exerts electron donating (+I) and hyperconjugative effect whereas $-\text{C}_6\text{H}_5$ exerts electron withdrawing (-I) effect and depending on the system to which it is attached and the manner in which it is attached determine the structural parameters and the change in the atomic charge redistribution and properties like ionization energies and electron affinities etc. It may be noted however, that we have observed that the substituents of diimine do not change the structural parameters, but only affect the other properties and the consequent reactivities

6.4.1. Global reactivity

The calculated ionization energy and the electron affinity values of these diimines along with global reactivity descriptors are summarized in Table 6.1. The ionization energy and electron affinity are among the primary energy considerations used in quantifying chemical systems. In general, the electron affinity increases as more number of $-\text{CH}$ groups are substituted by nitrogen atoms in the diimine ring as shown in our previous study [27d]. These additional N atoms holds partial negative charge more effectively compared to C atoms at the same position, ultimately increasing its overall affinity. Therefore, one may expect the phenyl ring to affect the affinity of 5,pyPh₂tz and 6,pzPh₂tz. However, the bulky phenyl substitution at adjacent carbon atoms causes steric hindrance and loses the planarity with the triazine ring of the system. The lower affinity values of 2,2'-bipyridine substituents viz; structure 1, 2 and 3 highlights the step up π -acceptance of the diimines containing more number of N atoms in structure 4, 5 and 6. In addition, the affinity comparison

between the 1, Me₂bpy and 2,Ph₂bpy systems clearly highlights the significance of hyperconjugative effect of methyl group in stabilizing the 1, Me₂bpy like systems.

The ionization energy physically signifies a measure of the reluctance of a molecule to surrender an electron. The overall trend observed for ionization energies among the 6 diimines is: 4, pyMe₂tz < 5, pyPh₂tz < 6, pzPh₂tz < 1, Me₂bpy < 3, Phen < 2, Ph₂bpy. Following the trend one can conclude that the ionization energy decreases with the increase of N atoms. Further, the methyl substituent show lower ionization energy than the phenyl substituent, when compared between the molecules containing the same number of N atoms. This suggests that the systems with methyl substituent contribute more towards electron donating character. The above results demonstrate the strongest influence of the type and position of the substitution on the electronic properties of the diimines.

Table 6.1: Global Properties of the systems: Chemical Potential, Hardness, Softness and Philicity (Values in Atomic Units)

System	Electron Affinity	Ionization Energy	Hardness	Chemical Potential	Softness	Philicity
1, Me ₂ bpy	0.0419	0.2261	0.0921	-0.1340	5.4288	0.0974
3, Phen	0.0491	0.2265	0.0887	-0.1378	5.6369	0.1070
2, Ph ₂ bpy	0.0556	0.2285	0.0864	-0.1420	5.7836	0.1166
4,pyMe ₂ tz	0.0628	0.2160	0.0766	-0.1394	6.5274	0.1268
5, pyPh ₂ tz	0.0676	0.2185	0.0754	-0.1430	6.6269	0.1355
6, pzPh ₂ tz	0.0770	0.2240	0.0737	-0.1507	6.7842	0.1540

Similar conclusion can be drawn from the chemical potential and hardness parameters reported in Table 6.1. Based on the principle of maximum hardness (MHP), the molecular stability has been extensively studied employing chemical potential and chemical hardness. According to this principle, the minimum energy system has maximum chemical hardness value. Hence, MHP is a qualitative tool to study the stability of the system. In the present investigation, the chemical hardness values decreases straightly from 0.0921 to 0.0737 for 1, Me₂bpy and 6, pzPh₂tz respectively. The substituent with -R effect and -I effect (phenyl group) destabilizes the diimines than that containing the substituent with +I (methyl group) effect. However, the global softness increases with the N substitution and the phenyl substitution, predicting higher polarizability, hence reactivity of the systems. To analyze the change in electrophilic power of the diimines system upon ED and EW

substitution, the molecular electrophilic power has been calculated. In general, the substituted N atoms enhance the electrophilic power of the diimines irrespective of the nature and position of the methyl and the phenyl substitution. In addition, the EW phenyl group contributes more to the increment of overall electrophilic power as shown in Table 6.1.

Thus, the overall global reactivity of diimines is increasing as the number of N atoms in the ring increases as depicted by the softness values of Table 6.1. In comparing reactivity of systems containing same number of N atoms in the ring, the ED methyl group stabilizes and hence makes it less reactive system where as phenyl group increases its reactivity. The phenyl groups when substituted on the adjacent C atoms of the ring (5 and 6) suffer from steric hindrance and lose its planarity with diimine rings. Therefore, tuning of the substitution either with ED or EW functional groups allows these systems to be more reactive and can be shown to be more interactive with metals.

6.4.2. Intra and inter molecular reactivity trend

Although the global reactivity descriptors explain the reactivity of these systems, it is very important to understand the individual atom activity to design new materials. Hence, in this section we analyze the electrophilic and nucleophilic nature of functional ring atoms with the help of atom condensed local softness descriptors, namely, electrophilic, s_k^+ and nucleophilic, s_k^- . Similarly, philicity descriptors are used to discuss the inter-molecular reactivity trend among these molecules. The electrophilic and nucleophilic local softness descriptors calculated under FCA are

presented in Table 6.2 and Table 6.3 for that of 2,2'-bipyridine substituents and -1,2,4-triazine substituents, respectively.

In our previous study, we have shown that the 2, 2'-bipyridine exerts σ -donor character through the N atoms and π -acceptor character through C atoms [27d]. As we consider various substituents to this ligand, the individual atom of the ring shows diverse reactivity. In case of methyl substituent, 1,Me₂bpy, the nucleophilicity of both N atoms and electrophilicity of C₃-C₁₀, C₆-C₇ enhances.

Table 6.2: Atom condensed local softness descriptors of the systems.

Atom	1,Me ₂ bpy		2,Ph ₂ bpy		3,Phen	
number	s_k^+	s_k^-	s_k^+	s_k^-	s_k^+	s_k^-
1	0.5180	1.9314	0.6037	0.3823	0.2595	0.2352
2	0.0638	0.1811	0.0642	0.1774	0.6513	0.5127
3	0.7659	0.1527	0.5339	0.9824	0.0375	0.0143
4	0.2761	0.0113	0.4483	0.1287	0.5748	0.3955
5	0.2739	0.0994	0.0236	0.1443	0.2272	0.1976
6	0.7330	0.1789	0.3383	0.3919	0.1708	0.3999
7	0.7330	0.1789	0.3382	0.3919	0.1708	0.3999
8	0.5180	1.9314	0.6036	0.3823	0.2595	0.2352
9	0.0638	0.1811	0.0642	0.1774	0.6513	0.5127
10	0.7659	0.1527	0.5339	0.9824	0.0375	0.0143
11	0.2761	0.0113	0.4483	0.1287	0.5748	0.3955
12	0.2739	0.0994	0.0236	0.1443	0.2272	0.1976
13	0.0141	0.0124	0.1801	0.1726	0.8584	1.0428
14	0.0141	0.0124	0.2001	0.1382	0.8584	1.0428

Note: Figures in bold indicates descriptor values of N atom where as other indicate C atom's descriptor values

Table 6.3: Atom condensed local softness descriptors of the systems.

Atom	4,pyMe ₂ tz		5,pyPh ₂ tz		6,pzPh ₂ tz	
number	s_k^+	s_k^-	s_k^+	s_k^-	s_k^+	s_k^-
1	0.1301	0.4105	0.3209	0.4212	0.6794	0.4440
2	0.0572	0.0437	0.0232	0.0496	0.0492	0.0758
3	0.2851	0.0330	0.3716	0.0415	0.7188	0.0723
4	0.0243	0.0051	0.1590	0.0053	0.3090	0.2321
5	0.2352	0.0581	0.1435	0.0650	0.1377	0.0935
6	0.2220	0.0446	0.2572	0.0466	0.5095	0.0739
7	0.5652	0.4289	0.6917	0.4368	0.8672	0.431
8	0.2619	2.0863	1.0409	2.0756	0.6804	1.9093
9	1.5048	1.7866	0.1420	1.7567	0.1125	1.7015
10	0.7579	0.4169	0.6602	0.4102	0.8681	0.3920
11	0.5788	0.2000	0.9719	0.2134	0.4712	0.2114
12	1.6349	0.8020	0.1152	0.7377	0.1571	0.7274
13	0.0246	0.1129	0.1769	0.1006	0.0704	0.0982
14	0.0292	0.0258	0.2074	0.0222	0.0918	0.0230

Note: Figures in bold indicates descriptor values of N atom where as other indicate C atom's descriptor values

reactivity enhancement can be attributed to the +I effect and hyperconjugative effect of -CH₃ group. On the contrary, in phenyl group substitution, 2,Ph₂bpy, these N atoms are no longer nucleophile, instead, their s_k^+ values predict them to be competent electrophile. The EW nature i.e. -R effect of phenyl group increases electron density at C₃-C₁₀, thus transferring nitrogen atom's nucleophilic nature to them. In general, the other atoms present in the 2,Ph₂bpy shows higher s_k^+ values over their respective s_k^- values, making this system strong π -acceptor rather than σ -donor. In continuation to this, nitrogen atoms of 1, 10 phenanthroline (3,Phen) are found to be weak nucleophile. Also their electrophilic descriptors, s_k^+ , are as good as their respective nucleophilic descriptors, s_k^- . Hence, here, N atoms are not even strong electrophile. Similarly, the ring C atoms, C₂-C₉, C₄-C₁₁ and C₁₃-C₁₄ exert equally prominent s_k^+ values as their respective s_k^- values, which make this system average σ -donor and π -acceptor. On the other hand, the substituted 1, 2, 4-triazine ligands (structure 4, 5, 6) (see Table 6.3) showing the major donation at N₈ and N₉ whereas N₁₂ partially contributes. No significant donation is observed through N₁ and/or N₄ of pyridine ring. However, in case of 4,pyMe₂tz when we look at the s_k^+ value (1.6349) of N₁₂, it is almost double that of its s_k^- value (0.8020) thereby proving it to be potential nucleophile attacking site in addition to C₇, C₁₀ and C₁₁ as nucleophile attacking sites. Similarly, in case of 5,pyPh₂tz and 6, pzPh₂tz, C₃, C₇, C₁₀ and C₁₁ of triazine ring affirm electrophilicity. In addition, the N₁ and/or N₄ of the pyridine ring confirm nucleophile attack from their adequate s_k^+ values. Therefore,

the -R effect of phenyl group affects the reactivity if and only if the phenyl ring is planar with diimine ring; else it has no role in strengthening the reactivity of ligand.

Table 6.4 and Table 6.5 focuses on the atom-condensed philicity and group philicity of bipyridine substituents and -1,2,4-triazine substituents, respectively. The philicity index is used to compare the inter-molecular reactivity trends among these substituted ligands. In case of bipyridine substituents, both the pyridine rings show similar probability of electrophilic or nucleophilic attack. The 1,Me₂bpy molecule shows equal extent of nucleophilicity and electrophilicity, hence results in σ -donor and π -acceptor type of ligand. However, 2,Ph₂bpy shows higher nucleophilicity than the electrophilicity, hence it is better π -acceptor ligand. The 3, phen ligand, on the contrary shows stronger electrophilicity compared to its nucleophilicity, hence concluded to be better σ -donor ligand. This is consistent with the local softness descriptor analysis. In case of -1,2,4-triazine substituents, the group philicity index of triazine ring is more than the adjacent pyridinyl or pyrazinyl rings of 4, pyMe₂tz to 6,pzPh₂tz. This predicts that the overall reactivity of triazine ring is higher than the adjacent ring as well as than that of the bipyridine substituents. The -CH₃ group substituted ligand (4,pyMe₂tz) do not show large difference in the w_k^+ and w_k^- values. Nonetheless, this difference is noteworthy when -C₆H₅ group is substituted to these ligands. In general, the nucleophilicity of triazine ring is higher than the respective electrophilicity value, indicating their enhanced π -acceptance.

Table 6.4: Atom condensed philicity and group philicity of the systems.

Atom number	1,Me ₂ bpy		2,Ph ₂ bpy		3,Phen	
	w_k^+	w_k^-	w_k^+	w_k^-	w_k^+	w_k^-
1	0.0093	0.0346	0.0121	0.0077	0.0044	0.0040
2	0.0011	0.0032	0.0012	0.0035	0.0112	0.0088
3	0.0137	0.0027	0.0107	0.0198	0.0006	0.0002
4	0.0049	0.0002	0.0090	0.0025	0.0099	0.0068
5	0.0049	0.0017	0.0004	0.0029	0.0039	0.0034
6	0.0131	0.0032	0.0068	0.0079	0.0029	0.0069
Σ	<i>0.047</i>	<i>0.0456</i>	<i>0.0402</i>	<i>0.0443</i>	<i>0.0329</i>	<i>0.0301</i>
7	0.0131	0.0032	0.0068	0.0079	0.0029	0.0069
8	0.0093	0.0346	0.0121	0.0077	0.0044	0.0040
9	0.0011	0.0032	0.0012	0.0035	0.0112	0.0088
10	0.0137	0.0027	0.0107	0.0198	0.0006	0.0002
11	0.0049	0.0002	0.0090	0.0025	0.0099	0.0068
12	0.0049	0.0017	0.0004	0.0029	0.0039	0.0034
Σ	<i>0.0474</i>	<i>0.046</i>	<i>0.0402</i>	<i>0.0443</i>	<i>0.0329</i>	<i>0.0301</i>

Note: Figures in bold indicates descriptor values of N atom where as other indicate C atom's descriptor values

Table 6.5: Atom condensed philicity and group philicity of the systems.

Atom	4,pyMe ₂ tz		5,pyPh ₂ tz		6,pzPh ₂ tz	
number	w_k^+	w_k^-	w_k^+	w_k^-	w_k^+	w_k^-
1	0.0025	0.0079	0.0065	0.0086	0.0154	0.0100
2	0.0011	0.0008	0.0004	0.0010	0.0011	0.0017
3	0.0055	0.0006	0.0076	0.0008	0.0163	0.0016
4	0.0004	9.9E-05	0.0032	0.0001	0.0070	0.0052
5	0.0045	0.0011	0.0029	0.0013	0.0031	0.0021
6	0.0043	0.0008	0.0052	0.0009	0.0115	0.0016
Σ	<i>0.0183</i>	<i>0.0112</i>	<i>0.0258</i>	<i>0.0127</i>	<i>0.0544</i>	<i>0.0222</i>
7	0.0109	0.0083	0.0141	0.0089	0.0196	0.0097
8	0.0050	0.0405	0.0212	0.0424	0.0154	0.0433
9	0.0292	0.0347	0.0029	0.0359	0.0025	0.0386
10	0.0147	0.0080	0.0135	0.0083	0.0197	0.0088
11	0.0112	0.0038	0.0198	0.0043	0.0106	0.0048
12	0.0317	0.0155	0.0023	0.0150	0.0035	0.0165
Σ	<i>0.1027</i>	<i>0.1108</i>	<i>0.0738</i>	<i>0.1148</i>	<i>0.0713</i>	<i>0.1217</i>

Note: Figures in bold indicates descriptor values of N atom where as other indicate C atom's descriptor values

6.4.3. Electron density analysis

Table 6.6 presents the electron density values calculated at different distances (experimentally observed for metal approach) for the bipyridine substituents and triazine substituents. It may, however, be noted that experiments have been carried out in solution phase whereas our calculations are done on the gas phase molecules. As our main interest here is to count the σ -donation character of these molecules, we focus on the $\rho(r)$ numbers. The electron density value for 3,Phen ligand is maximum among the 6 ligands. This outcome is in agreement with the previous reactivity analysis where 3,Phen was found to be good σ -donor ligand. The reason of such strong interaction can be attributed to the specific geometrical features of 3,Phen. 3,Phen having two N donor atoms, separated by two carbon atoms, form a five member ring, a chelate ring. The diimine part of the 3,Phen delocalizes the electrons in the chelate ring as well as in three aromatic rings, eventually increasing the electron density of ligand. Such chelation is no longer effective for phenyl substituted ligands (2, 5) as their $-R$ effect fails to delocalize electron density cloud through resonance thus reducing it at diimine nitrogen. Conversely, electron density value for phenyl substituted pyridinyl triazine ligand (6) is significantly higher. In case of 5, pyPh₂tz only one phenyl ring is out of diimine ring plane whereas second phenyl ring, which is planar with diimine ring, pertains $-R$ effect, finally reducing electron density at the chelating N atoms. However, in case of 6,pzPh₂tz both phenyl rings are non planar to diimine ring, which assists to resonate charge in the chelating ring. Surprisingly, electron density of methyl substituted ligand is less. This suggests that

enhancement of σ -donation cannot be increased sufficiently by substitution of merely -CH₃ group, instead, a group with stronger +I effect is needed to improve the σ -donor character of these ligands.

Table 6.6: Comparative density values of 2,2'-bipyridine substituents and triazine substituents

Distance		Density*10 ⁻⁴ (a. u.)					
from N							
atoms							
N(1)	N(8)	1,Me ₂ b py	2,Ph ₂ bpy	3,Phen	4,pyMe ₂ t z	5,pyPh ₂ tz	6,pzPh ₂ t z
2.25	2.13	3.83	0	165.65	3.93	4.1	68.91
2.26	2.10	4.18	0	184.98	4.43	4.66	68.94
2.29	2.12	3.74	0	165.65	3.85	4.06	63.12

6.4.4. Reaction energies for Ru-ligand interaction

Relevance of calculations presented in the previous section can be verified by actually evaluating the reaction energies for Ru-ligand interaction. Hence, we have calculated the interaction energy, enthalpy and free energy of complex formation for the considered ligands when complexes with Ru metal atom. These quantities are tabulated in Table 6.7 and Table 6.8 for basic ligands and substituted ligands, respectively. The actual interaction energies have been calculated using the following conventional formula.

$$E_{ABint} = [E_{ABcomplex} - (E_A + E_B)]$$

Table 6.7: Comparative reaction energies for Ru complexes of 2,2'-bipyridine and triazine .

Properties	Relative		
	Reaction Energies (kcal/mol)		
	(2,2'-bipyridine)- Ru	(3-(2-pyridinyl)- 1,2,4-triazine)-Ru	(3-(2-pyrazinyl)- 1,2,4-triazine)-Ru
Interaction Energy(ΔE)	0.0	13.8	17.0
Enthalpy(ΔH)	0.0	13.9	17.2
Free Energy(ΔG)	0.0	12.7	15.6

We have already discussed the reactivity of 2,2'-bipyridine and its important analogues 3-(2-pyridinyl)-1,2,4-triazine and 3-(2-pyrazinyl)-1,2,4-triazine, which are generated by substitution of -CH group by N-atoms in the bipyridine ring in our previous publication^{27(d)}. In the present study, we briefly recall this, which is necessary for understanding the possible influence of substituents on the strength of their interaction with metal ions. The previous study concluded that 2,2'-bipyridine is a better σ -donor and its analogues are better π -acceptors. In line with this, our reaction energy values (as shown in Table 6.7) show complex formation of Ru metal atom more favorable for both triazines compared to bipyridine. Although, reaction with the Ru metal is exothermic for all these three basic ligands, these values are increasing with the number of N atoms. While making the complex formation with Ru metal the pyridinyl triazine interaction energy is 14 kcal/mol and pyrazinyl triazine is 17 kcal/mol relative to the bipyridine ligand. This stability is also reflected while measuring the metal ligand bonding distances. In case of bipyridine complex, Ru metal is optimized at 1.76 Å from both nitrogen donor atoms. However, in triazine complexes the Ru metal gets closer to triazine ring nitrogen atom N (8) and is stable at 1.72 Å bond distance. We explain this extra stability of latter complexes from the charges built on the Ru metal atom in the respective complexes. The Natural Population Analysis (NPA) depicts that the positive charge on Ru is higher in triazine complexes (0.515 and 0.549 a.u. in pyridinyl and pyrazinyl, respectively) than that in bipyridine complex (0.447 a.u.). In addition, we also calculate the gross orbital population. It has been shown in the earlier studies that the Ruthenium metal undergoes sd hybridization of 5s and 4d orbitals while making the complex with the

ligands [55-58]. In our analysis, the corresponding sd-population in bipyridine complex is 7.36 a.u and triazine complex is 7.22 a.u. This indicates that Ru metal loses its electrons mostly from hybridized sd-orbitals. Thus, the reason for this extra stability can be attributed to the better π -acceptor character of the triazine rings which eventually help back bonding between metal sd-orbitals and ligand π^* -orbitals.

Further, the +I effect of methyl substituted bipyridine (1) shows ~ 3 kcal/mol increase in reaction energies, whereas the -R effect of phenyl ring (2) increases these quantities by ~ 7 kcal/mol (see Table 6.8). Consequently, the methyl substitution at pyridinyl triazine (4) ligand and the phenyl substitutions (which are non planar with reactive rings) at triazine (5, 6) ligands do not impart any effect and the corresponding reaction energies are same as those for the corresponding parent ligand (refer Table 6.7). Briefly, we can conclude that the methyl substituents by their +I effect reduce the π -acceptor character of ligand and on the other hand, phenyl substituents which are planar with active ring by their -R effect enhance the π -acceptor character of ligand. Moreover, all the reaction energies for 3, Ph en ligand are less than bipyridine. In actual complex formation, LUMO (π^* -orbital is much higher in energy (0.0213 a .u.) than the metal bonding d-orbitals (-0.0430 a. u.) of this ligand fails to accept the electron density from HOMO of metal. This fact can be verified by the NPA charges, where the positive charge on Ru (i.e 0.316 a.u) is less in this complex compared to any other complex. Thereby, 3,Ph en can be considered as prominent σ -donor but poor π -acceptor than 2,2'-bipyridine.

Table 6.8: Comparative reaction energies for 2,2'-bipyridine substituents and triazine substituents complexes with Ru.

Properties	Relative Reaction Energies (kcal/mol)					
	(1,Me ₂ bpy)- Ru	(2,Ph ₂ bp y)-Ru	(3,Phen) -Ru	(4,pyMe ₂ tz)-Ru	(5,pyPh ₂ t z)-Ru	(6,pzPh ₂ tz)-Ru
Interaction Energy(ΔE)	3.1	7.1	0.0	15.7	17.3	19.8
Enthalpy(ΔH)	3.1	7.0	0.0	15.8	17.0	19.9
Free Energy(ΔG)	1.4	6.4	0.0	14.3	15.9	18.7

6.5. Conclusion

The effect of substituents on the reactivity and electron density profile of diimines like 2, 2'-bipyridine, 1, 10-phenanthroline and 1, 2, 4-triazines has been illustrated with the help of global and local reactivity descriptors. The global reactivity descriptors such as electron affinity, chemical potential, softness etc. predict that the values of parameters increase with the ligands having more number of N atoms as depicted in our previous study^{27d}. Further, substituting phenyl group in our present study shows higher polarizability and hence higher reactivity of the ligands as concluded from our results of calculation of ionization energy, hardness and other parameters depicted in Table 6.1. Consequently, the ionization potential and hardness parameters suggest that the methyl substitution increases the stability of ligands and hence make it less reactive towards the Ruthenium metal as shown from our present study.

The intra molecular reactivity of these systems is studied with the local softness. The methyl substitution enhances nucleophilic and electrophilic nature of the ring N and C atoms, respectively. The phenyl substitution enhances overall electrophilic nature of the ring atoms. Conversely, local softness descriptor could not express clearly local reactivity of ring atoms in 3, Phen. The inter-molecular reactivity descriptors, philicity and group philicity, suggest that the group electrophilicity of -1,2,4-triazine ligands and phenyl substituted ligands is higher than that of bipyridine ligand and methyl substituted ligands. Hence, these systems can be used for complexation where back bonding with metal is involved. This outcome is

also supported with actual reaction energies of Ru-L complexes as shown in Table 6.8. The Ru-L complexes are formed by s-d hybridization.

The electron density profile of these ligands quantifies the σ -donor character of these ligands. The +I effect of $-\text{CH}_3$ group does not show exceptional density at diimine nitrogen as it does not help chelation. Similarly, the $-\text{C}_6\text{H}_5$ group which is planar (in case of ligand 2 and 5) to diimine ring does not help to increase density due to its -R effect. However, when these groups lose their planarity with diimine ring (as in case of ligand 6) due to steric hindrance, it helps to enhance the density to a substantial value due to +R effect. Among all these ligands, 3,Phen shows extraordinary electron density at the diimine N atoms, which is ascribed to its specific geometrical features.

6.6. References

- [1] Reedijk J, Wilkinson G, Gillard RD, Vol. 2, ed. McCleverty JA Pergamon, Oxford, 73 (1987).
- [2] Blau F *Chem Ber* **21** (1888) 1077.
- [3] a) Taube R, Herzog, S *Z Chem* **2** (1962) 225. b) Herzog S. *Neuere Entwicklungen der anorg.Chemie*, VEB Deutscher Verlag der Wissenschaften, Berlin (1974).
- [4] Lindoy LF, Livingstone SE, *Coord Chem Rev* **2** (1967) 173.
- [5] Konig E, *Coord Chem Rev* **3** (1968) 471.
- [6] McWhinnie WR, Miller JD, *Advan Inorg Chem. Radiochem* **12** (1969) 135.
- [7] Adams RD, *J Am Chem Soc* **102** (1980) 7476
- [8] (a) van Koten G, Vrieze K, *Adv Organomet Chem* **21** (1982) 151. (b) van Koten G, Vrieze K, *Reel Trav Chim Pays Bas*, ZOO **129**(1981).
- [9] Plank V, Klaus J, von Deuten K, Feigel M, Bruder H, tom Dieck H, *Transition Met Chem* **6** (1981) 185.
- [10] (a) Tom Dieck H, Kollvitz W, *Transition Met Chem* **7**, (1982) 154. (b) Diercks R, tom Dieck H, *Z Naturforsch, Teil B* **39** (1984) 180. (c) tom Dieck H, Dietrich J, *Chem Ber* **117** (1984) 694.
- [11] Balk RW, Snoeck T, Stufkens DJ, Oskam A, *Inorg Chem* **19** (1980) 3015.
- [12] Crociani B, Boschi T, Uguagliati P, *Inorg Chim Acta* **48** (1981) 9.
- [13] Reinhold J, Benedix R, Birner P, Hennig H, *Inorg Chim Acta* **33** (1979) 209.
- [14] Walter D, Teutsch M, *Z Chem* **16** (1976) 118.

- [15] Vögtle F *Supramolecular Chemistry An Introduction*, John Wiley & Sons, ed. Chichester, (1991) 9-26 .
- [16] Ziessel R, Lehn JM, *Helv Chim Acta* **73** (1990) 1149.
- [17] Rodriguez-Ubis JC, Alpha B, Plancherel D, Lehn JM, *Helv Chim Acta* **67** (1984) 2264.
- [18] Bilyk A, Harding MM, *J Chem Soc Dalton Trans* **77** (1994).
- [19] Piguet C, Bernardinelli G, Hopfgartner, G, *Chem Rev* **97** (1997) 2005.
- [20] Constable EC, Steel PJ, *Coord Chem Rev* **93**(1989) 205.
- [21] Petersen JD, Murphy WR, Sahai R, Brewer KJ, Ruminski RR, *Coord Chem Rev* **64** (1985) 261.
- [22] Chen J, Reed MA, Rawlett AM, Tour JM, *Science* **286** (1999) 1550.
- [23] Majumder C, Mizuseki H, Kawazoe Y, *J Mol Struct (Theochem)* **681** (2004) 65.
- [24] Yang J S, Liao KL, Wang CM, Hwang CY, *J Am Chem Soc* **126** (2004) 12325.
- [25] Facchetti A, Yoon MH, Stem CL, Hutchison GR, Ratner MA, Marks TJ, *J Am Chem Soc* **126** (2004) 13480.
- [26] Roth JP, Wincek R, Nodet G, Edmondson DE, McIntire WS, Klinman JP, *J Am Chem Soc* **126** (2004) 15120.
- [27] (a) Parr RG, Yang W, (1989) *Density-functional theory of atoms and molecules*; Oxford University Press: New York. (b) Geerlings P, De Proft F, Langenaeker W, *Adv Quantum Chem* **33** (1999) 303. (c) Koch W, Holthausen MC, *A Chemist's Guide to Density Functional Theory*; Wiley-VCH:

- Weinheim (2000). (d) Kulkarni BS, Tanwar A, Pal S, *J Chem Sci* **119** (2007) 489.
- [28] (a) Mayer I, *Chem Phys Lett* **97** (1983) 270. (b) Mayer I, *Chem Phys Lett* **148** (1988) 95. (c) Maity DK, Majumdar DK, Bhattacharya SP, *J Mol Struct (Theochem)* **332** (1995) 1. (d) Gopinath S and Jug K, *Theor Chem Acta* **63** (1983) 497. (e) Bader RFW, *Atoms in molecule: A quantum theory*, Oxford: Oxford University Press (1990).
- [29] Fukui K, 1975, *Theory of Orientation and Stereo Selection*, Springer-Verlag, Berlin.
- [30] (a) Woodward RB, Hoffmann R, *J Am Chem Soc* **87** (1965) 395. (b) *Ibid.* *Acc Chem Res* **1** (1968) 17 (c) *Ibid.* *The Conservation of Orbital Symmetry*, New York, Academic Press (1989).
- [31] (a) Mulliken RS, *J Am Chem Soc* **74** (1952) 811. (b) Orgel LE, Mulliken RS, *J Am Chem Soc* **79** (1957) 4839. (c) Tsubomura H, Mulliken RS, *J Am Chem Soc* **82** (1960) 5966.
- [32] (a) Pearson RG, *Hard and Soft Acids and Bases*, Dowden, Hutchinson, and Ross, Stroudsburg, PA, 1973. (b) Pearson RG, *Chemical Hardness: Applications from Molecules to Solids*, Wiley-VCH Verlag GMBH: Weinheim, 1997.
- [33] Bader RFW, *Atoms in Molecules: A Quantum Theory*, Clarendon Press, Oxford, 1990.
- [34] (a) Politzer P, Truhlar DG, (Eds.) *Chemical Applications of Atomic and Molecular Potentials*, Plenum, New York, 1981. (b) Murray JN, Sen KD,

- (Ed.) *Molecular Electrostatic Potential: Concepts and Applications*, Elsevier, Amsterdam, 1996. (c) Gadre SR, Shirsat RN, *Electrostatics of atoms and Molecules*, Universities Press, Hyderabad, India, 2000.
- [35] Maksic ZB (Ed.) *Theoretical Models of Chemical Bonding: The Concept of the Chemical Bond*, Springer-Verlag, Berlin, 1990.
- [36] Gazquez J L, *J Phys Chem* **101** (1997) 8967.
- [37] Nguyen LT, Le TN, De Proft F, Chandra AK, Langenaeker W, Nguyen MT, Geerlings P, *J Am Chem Soc* **121** (1999) 5992
- [38] (a) Chandra AK, Nguyen MT, *J Phys Chem A* **102** (1998) 6181. (b) Chandra AK, Michalak, Nguyen MT, Nalewajski RF, *J Phys Chem A* **102** (1998) 10182.
- [39] (a) De Proft F, Amira S, Choho K, Geerlings, P *J Phys Chem* **98** (1994) 5227. (b) Langenaekar W, De Decker M, Geerlings P, Raeymaekers P *J Mol Struct (THEOCHEM)* **207** (1994) 115.
- [40] (a) Parr RG, Chattaraj PK *J Am Chem Soc* **113** (1991) 1854. (b) Pearson RG, *J Chem Educ* **64** (1987) 561.
- [41] (a) Pearson RG, *J Am Chem Soc* **85** (1963) 3533. (b) Sen KD, *Chemical Hardness (Structure and Bonding)*, Vol. 80, Springer-Verlag, Berlin, 1993.
- [42] (a) Parr RG, Pearson RG, *J Am Chem Soc* 105 (1983) 7512. (b) Parr RG, Donnelly RA, Levy M, Palke WE, *J Chem Phys* 68 (1978) 3801. (c) Pearson RG, *J Am Chem Soc* 107 (1985) 6801.
- [43] (a) Parr RG, Yang W, *J Am Chem Soc* 106 (1984) 4049. (b) Yang Y, Parr RG, *Proc Natl Acad Sci U. S. A.* 821 (1985) 6723. (c) Yang W, Mortier W, J

- Am Chem Soc 108 (1986) 5708.(d) Politzer P, Murray JS, In *Theoretical Aspects of Chemical Reactivity*, Ed. Toro-Labbe, Elsevier: Amsterdam, 119, (2007). (e) Morell C, Grand A, Guitierrez S, Toro-Labbe A, Using Reactivity-selectivity descriptor in organic molecules (In *Theoretical Aspects of Chemical Reactivity*), ed. Toro-Labbe, Elsevier: Amsterdam, 101 (2007).
- [44] (a) Roy RK, Krishnamuthy S, Geerlings P, Pal S, *J Phys Chem A* 102 (1998) 3746. (b) Roy RK, Pal S, Hirao K, *J Chem Phys* 110 (1999) 8236.
- [45] Krishnamurthy S, Pal S, *J Phys Chem A* 104 (2000) 7639.
- [46] (a) Parr RG, Szentpaly LV, Liu S, *J Am Chem Soc* **121** (1999) 1922. (b) Chattaraj PK, Maiti B, Sarkar U, *J Phys Chem* **107** (2003) 4973. (c) Parthasarathi R, Padmanabhan J, Elango M, Subramanian V, Chattaraj PK, *Chem Phys Lett* **394** (2004) 225. (d) Padmanabhan J, Parthasarathi R, Subramanian V, Chattaraj PK *J Mol Struct.: THEOCHEM* **774** (2006) 49.
- [47] (a) Perez P, Toro-Labbe A, Aizman A, Contreras R, *J Org Chem* **67** (2002) 4747. (b) Domingo LR, Aurell MJ, Perez P, Contreras R, *J Phys Chem A* **106** (2002) 6871. (c) Perez P, Toro-Labbe A, Contreras R, *J Am Chem Soc* **123** (2001) 5527. (d) Perez P, Aizman A, Contreras R, *J Phys Chem A* **106** (2002) 3964.
- [48] Tanwar A, Bagchi B, Pal S, *J Chem Phys* **125** (2006) 214304.
- [49] Gazquez JL, Mendez F, *J Phys Chem* **98** (1994) 4591.
- [50] (a) Pal S, Chandrakumar KRS, *J Am Chem Soc* **122** (2000) 4145 (b) Chandrakumar, KRS, Pal S, *J Phys Chem A* **106** (2002) 5737 (c) Chandrakumar KRS, Pal S, *J Phys Chem A* **105** (2001) 4541.

- [51] (a) De Proft F, Geerlings P, *Chem Rev* **101** (2001) 1451. (b) Geerlings P, De Proft F, Langenaeker W, *Chem Rev* **103** (2003) 1793. (c) Mendez F, Tamariz J, Geerlings P J, *Phys Chem A* **97** (1993) 4059.
- [52] (a) Schmidt MW, Baldrige KK, Boatz JA, Elbert ST, Gordon MS, Jensen JH, Koseki S, Matsunaga N, Nguyen KA, Su SJ, Windus TL, Dupuis M, Montgomery JA, *J. compt. Chem* **14** (1993) 1347. (b) Trucks GW, Schlegel H B, Scuseria G E, Robb MA, Cheeseman JR, et al. Gaussian 09, Revision A.1, Frisch MJ Gaussian Inc., 2009 Wallingford CT.
- [53] Lowdin PO, *J Chem. Phys.* **21** (1955) 374.
- [54] Hay, P.J and Wadt, WR, *J. Chem. Phys* **22** (1985) 270.
- [55] Landis CR, Firman TK, Root DM, Cleveland T, *J Am Chem Soc* **120** (1998) 1842.
- [56] Landis C R, Cleveland T, Firman TK, *J Am Chem Soc* **120** (1998) 2641
- [57] Firman TK, Landis CR, *J Am Chem Soc* **120** (1998) 12650.
- [58] Khan G and Tiwari RP, *Archives of Applied Science Research* **3** (2011) 483.

CHAPTER 7

Conformational Specific Phospholipid Tail Dynamics of anionic DMPC (dimyristoyl Phosphatidyl Glycerol) Molecule: Conclusions and Future Scope

Abstract

The present and last chapter of the thesis discuss the role of intra molecular interaction in the process of melting of bilayer. The main phase transition would be driven by intrinsic structural changes within the lipid molecules, whereas the changes of free volumes and inter molecular interactions could be considered as perturbations. Born–Oppenheimer molecular dynamics (BO–MD) computations are performed for the dimyristoyl phosphatidylglycerol (DMPG) molecule using density functional theory augmented with a damped empirical dispersion correction (DFT–D). Two different conformers of DMPG are studied in the present chapter and both the conformers are showing different distortion behaviour of alkyl chains at near and around the phase transition temperature found experimentally.

The peculiar behaviour of two different conformers of DMPG in distortion opens up the way to understand the intra molecular interaction involved in biomolecules. Therefore, in addition to classical dynamics, quantum based molecular dynamics also answers many hidden questions in biomolecules.

7.1. Introduction

Phospholipid molecules are the primary building blocks of a cell membrane. The phospholipid molecule consists of (a) polar region (commonly referred to as head) with characteristic functional groups and (b) two alkyl chains which compose of a non-polar region. The functional groups associated with the phospholipid molecule, the charge on the lipid molecule, type of ion compensating the charge of each individual molecule, the alkyl chain length etc., plays a predominant role in determining the overall conformation of the molecule within a bilayer. Depending on the conformations which dominate a bilayer, the response properties in a bilayer such as cell-cell recognition, drug delivery system, signal transduction etc. [1-3] vary. The phospholipid molecules when assembled together have fundamental permeability barrier to the passage of polar molecules, ions, drug molecules, peptides, retention of water molecules etc. into or out of a cell. Thus, the structural modifications in each individual phospholipid molecule and their manner of assembling can block or allow the permeation of the same.

At very low temperatures (say at 0 K), all the C-C bonds in both the alkyl chains have ± 180 degree orientation. This is a very ordered state (ordered phase of molecule) of alkyl chains. As a consequence of temperature increase, a disorder begins to set within either of one or both alkyl chains. The disorder essentially is a rotation of C-C bond which modifies a trans dihedral angle to a gauche conformation. The alkyl chains show the kinks due to the gauche conformations within the C-C bond. These rotations occur predominantly at end of the alkyl chain or in the middle of the chain. The rotations occur around a specific temperature commonly referred as T_m . Around or beyond T_m , a molecule has more than one or two C-C rotations in each of its chain (disordered phase of molecule).

These rotations occur at a rate nearly 100 times quicker than the rotation of bonds within the polar (head) group [4].

An occurrence of gauche will considerably change the transport properties of a bilayer [8]. This results in a modification of molecular volume. The chain lengths decrease and inter atomic bond distances between the two alkyl chains increase. This consequently results in a loosening of the molecular packing which decreases the bilayer thickness and increase the average cross-sectional area of the phospholipids within the bilayer [5]. Thus, a phase change in the conformations from all trans to a gauche in any of the alkyl chain is accompanied by an enthalpy and volume change.

The above phase transition is not only driven by the overall geometry of the lipid bilayer formed by the aggregation of lipid molecules, but also by the intrinsic geometrical parameters of the compositional lipid molecules. Interestingly, the volume expansion due to phase transition and isobaric heat capacity have a proportional relationship for a variety of lipid bilayers e.g DMPC (dimyristoyl phosphatidyl choline) ($T_m = 295 - 298 \text{ K}$) [6], DMPG (dimyristoyl phosphatidylglycerol) ($T_m = 296 \text{ K}$ ref), DPPC (dipalmitoyl phosphatidyl choline) ($T_m = 320 \text{ K}$) [7], DLPC ($T_m = 272 \text{ K}$ and 290 K) [8-12]. Hence, a heat capacity curve shows a sharp peak at the T_m .

One of the interesting points concerning the ordered to disordered phase transition is seen for negatively charged DMPG. DMPG is a molecule with a phosphatidylglycerol headgroup and two alkyl chains having 14 carbon atoms each. The negative charge in this lipid is compensated by a positively charged ion interacting with the phosphate group in the head. It has been considered a suitable lipid for membrane modelling because under physiological conditions it shows a

trans to gauche conformational changes at the convenient temperature of 23°C. The specificity of this temperature in case of DMPG arises with varying lipid molecule:cation (commonly Na⁺) ratio. It has been experimentally shown that for solutions higher than 100 mM NaCl, DMPG shows a heat capacity curve similar to that of neutral DMPC. Both have a sharp peak at 23° C ($T_m = 23$). On the other hand, at an ionic strength below 100 mM NaCl, [14] DMPG has a complex heat capacity curve with several peaks between 18 to 35°C [15-19].

It may be attributed, that in case of solutions higher than 100 mM NaCl, the Na⁺: lipid molecule ratio is 1:1 and in this case, the cation-lipid molecule complex mimics the neutral DMPC molecular conformation at the polar region. However, with a modification in Na⁺:lipid ratio, the DMPG undergoes structural modifications. These modifications must necessarily be around the polar head region (as the cation effectively interacts with the polar region) [28-31]. Hence, a modification in the structural parameters of the polar head group reflects in the temperature at which the trans to gauche occurs within the alkyl chains. This is validated further from the fact that various other factors such as type of ion compensating the charge, amount of water molecules around the polar head group also modify the T_m [20-25].

The precise effect of the orientation of the head group, structural changes in the polar region of a lipid molecule and its exact contribution to the stability of all trans conformations in the alkyl chains is relatively unknown and not explored. Hence, in the present work, we explore the various orientations of the polar region of a DMPG molecule and its contribution to the stability of an all trans alkyl chain conformations. Our conformational space is also enriched with one experimentally known conformation of DMPG. Therefore, in the present study we attempt to clear

significant issues like the molecular distortion behaviour of phospholipid, its conformational dependency, the effect of ion on charged phospholipid and consequently how the same is affecting the distortion behaviour of alkyl chains. We also address here the above mentioned issues by simulating the behaviour of various conformations at different temperatures using a BOMD (Born Oppenheimer Molecular Dynamics) methodology. We have chosen two different conformations of DMPG in which one of them is the ground state conformation from our earlier study and the other one is the experimentally known DMPGA conformation [31]. Our results bring out a significant and complex dependency of the C-C bond rotation energy on the cation position and geometrical parameters of the polar region (dihedral angles within the phosphate group, carbonyl groups, glycerol groups and the orientation of all the three with respect to each other).

7.2 Methodology and Computational Details

All the calculations were performed within the framework of DFT using a linear-combination-of-Gaussian-orbitals approach, as implemented in the deMon2k program [32]. The calculations are carried out with the revised Perdew, Burke and Ernzerhof (PBE) exchange [33] and the Lee, Yang and Parr (LYP) [34] correlation functional, augmented by a damped empirical correction for dispersion-like interactions [35,36].

To study the effect of various temperatures on two different conformers of DMPG - Na⁺, among them one is experimentally found DMPGA conformer and the other is the lowest energy conformer found from our previous study [28] first principle molecular dynamics have been performed. All momenta are conserved during the dynamics. The total equilibrated simulation time is 53 ps with a

maximum of 15 ps for 290K for the lowest energy conformer. The simulations are carried out at 240 K, 260 K, 280 K, 290 K, 296 K, and 320 K. The total equilibrated time for the experimental conformer (DMPG A) is 40 ps for the temperature 260 K, 280 K, 290 K, 296 K and 320 K. The temperature of both the system is maintained using the Berendsen thermostat ($\tau=0.5$ ps) in the NVT ensemble, where N is the number of particles, V is the volume and T is the temperature. The nuclear positions were updated with the velocity Verlet algorithm with a time step of 1 fs. DFT-optimized double zeta plus valence polarization (DZVP) basis sets [37] were used for all atoms, associated with automatically generated functions up to $l=2$ for fitting the density [38]. The exchange-correlation potential was numerically integrated on an adaptive grid [39]. The grid accuracy was set to 10^{-5} in all calculations. The accuracy of the presently used DFT-D method has been validated for the energetics and geometries of all-trans n-alkane dimers [35].

To quantify the structural deformations occurring along the molecular dynamics simulations, we used the distance fluctuation criterion initially introduced by Berry et al. [40]. The Berry parameter Δ_B is expressed for a system of N atoms and r_{ij} is the inter atomic distances between atoms i and j as

$$\Delta_B = \frac{2}{N(N-1)} \sum_{i < j} \frac{\sqrt{\langle \Delta r_{ij} \rangle - \langle r_{ij} \rangle^2}}{\langle r_{ij} \rangle}$$

The critical value of Δ_B for the solid to liquid transition of finite system has been suggested to be close to 0.1 [40-43].

7.3. Results and Discussion

Structural changes have been noted in DMPG lowest energy conformer while incubating it at various temperatures viz; 240K, 260K, 280K, 290K, 296K and 320K. The structural changes are dominantly seen in the tail region of the molecule. The dihedral angles of the initial structure used for the molecular dynamics run are depicted in Table 7.1. The lowest temperature (240K) trajectory run of DMPG is to observe the change in conformational behaviour. We note that the conformation of the initial structure retained at the lower temperature run and therefore the same conformation is then used for the higher temperature runs.

7.3.1 Overall structural changes

Structural fluctuations during the molecular dynamics runs are measured with the various inter atomic distances and change in dihedral angles. As shown in Figure 7.1, it is worth noting the change in average C...C bond distance between the β and γ chains as the temperature is increasing. However the average C...C bond distance is not significantly affected up to 296 K. The average C...C bond distance changes from 4.9 Å to 6.3Å. This reveals the fact that chains are getting separated with the increase of temperature and the change is significantly noted around the experimental phase transition temperature. The average change in $\langle \text{Na...O} \rangle$ inter atomic distance shows the sharp peak at 290 K which is due to the movement of the Na^+ ion towards the C=O group. However this change gets saturated at 296 K and average inter atomic distance $\langle \text{Na...O} \rangle$ again decreases to its initial value of 2.4 Å. The average inter atomic distance between the C=O groups is same even at higher temperature runs as depicted with the green line in Figure 7.1. The structural fluctuation in terms of

dihedral angles is first noted at 290K where the gauche is present at the middle of the γ alkyl chain. Extending the run of 290K up to 15ps shows that the gauche present at the middle is retained.

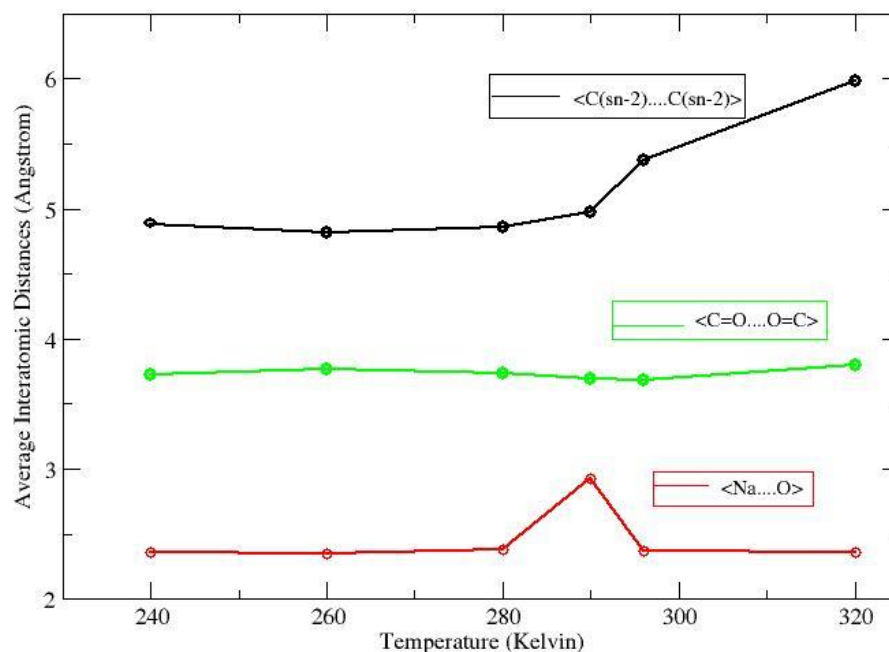


Figure 7.1 Average interatomic change in bond distances of lowest energy conformer.

Distortion of the structure is mainly characterized by the change in trans to gauche dihedrals as a consequence of that the inter atomic distance between the C...C bonds of alkyl chains increased. The distortion of the alkyl chains at 296K is shown in Figure 7.2. At higher temperature of 296 K we noted more than one kink at the alkyl chains. Therefore, one can observe more distortion of the molecule.

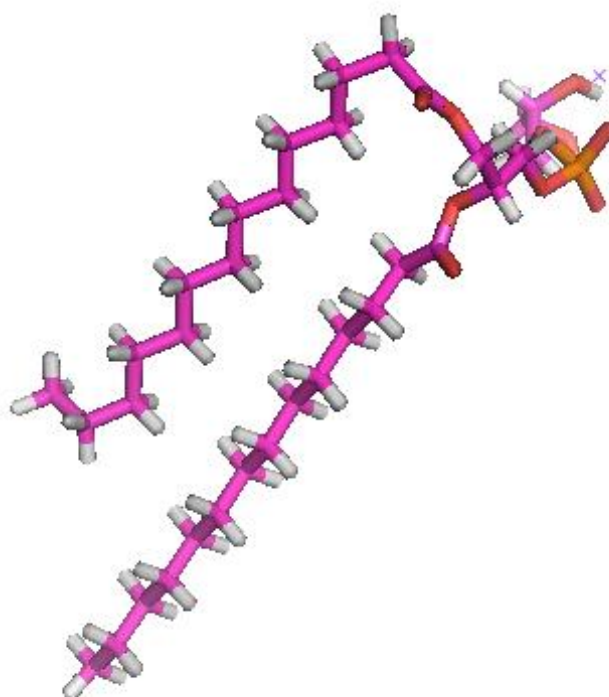


Figure 7.2. The distortion of the alkyl chains at 296K

The transformation of all trans to gauche at higher temperatures is noted in this chapter. This behaviour of distortion of the alkyl chains is noted at 320 K also in addition to the bending of the head group towards the alkyl chains. However the similar behaviour was not seen in DMPC at higher temperature [29]. The reason for the same is the presence of counterion and the displacement of this counterion towards the tail region at 320 K. The change in the dihedral angles of the distorted conformations at 320K is shown in Table 7.1. As depicted in Table 7.1 there is significant change noticed in the dihedral angles of the head group region in addition to the alkyl chains at 320 K. The transformation of

trans to gauche is noted at extremity and middle of the alkyl chains. The change in the particular dihedral angles at three specific temperatures with the initial starting structure of the molecular dynamics runs is depicted in Table 7.1. The dihedral angles which are quite off from the initial starting structure in all three mentioned structure with respect to time and temperature are shown in Table 7.1.

Table 7.1 Distorsions in dihedral angles of lowest energy conformer at different temperatures of simulations.

Dihedral angles	Initial structure	Structure at 290 K after 10 ps	Structure at 296 K after 10 ps	Structure at 320 K after 10 ps
α_1	-66	-81	-57	-71
α_2	90	89	84	<u>74</u>
α_3	116	99	107	123
α_4	87	97	101	89
α_5	-69	-76	-72	-80
θ_1	134	136	140	<u>159</u>
θ_2	-105	-103	-95	<u>-76</u>
θ_3	174	<u>-172</u>	<u>-172</u>	<u>-162</u>
θ_4	54	60	50	73
β_1	-179	<u>174</u>	<u>165</u>	<u>121</u>
β_2	-125	-135	176	-168
β_3	68	65	81	<u>-154</u>
β_4	-175	-170	-178	<u>64</u>
γ_1	84	84	82	79
γ_2	-176	-179	<u>169</u>	-163
γ_3	-59	-64	<u>154</u>	<u>134</u>
γ_4	-177	-157	-174	-168

7.3.2 Disorder parameter for the alkyl chains

In order to understand the above discussed trans to gauche transformation which starts at 290 K we have calculated the Δ RMS value. Berry et al first introduced this parameter of distance fluctuation for demonstrating molecular melting. Therefore the temperature versus Δ RMSD has been plotted as shown in Figure 7.3. As clearly shown in the graph the distortion of the alkyl chains starts at 290 K. The Δ RMS value varies from 0.045 to 0.095 as the temperature varies. There is smooth increase in Δ RMS value starting from 240 K to 320 K.

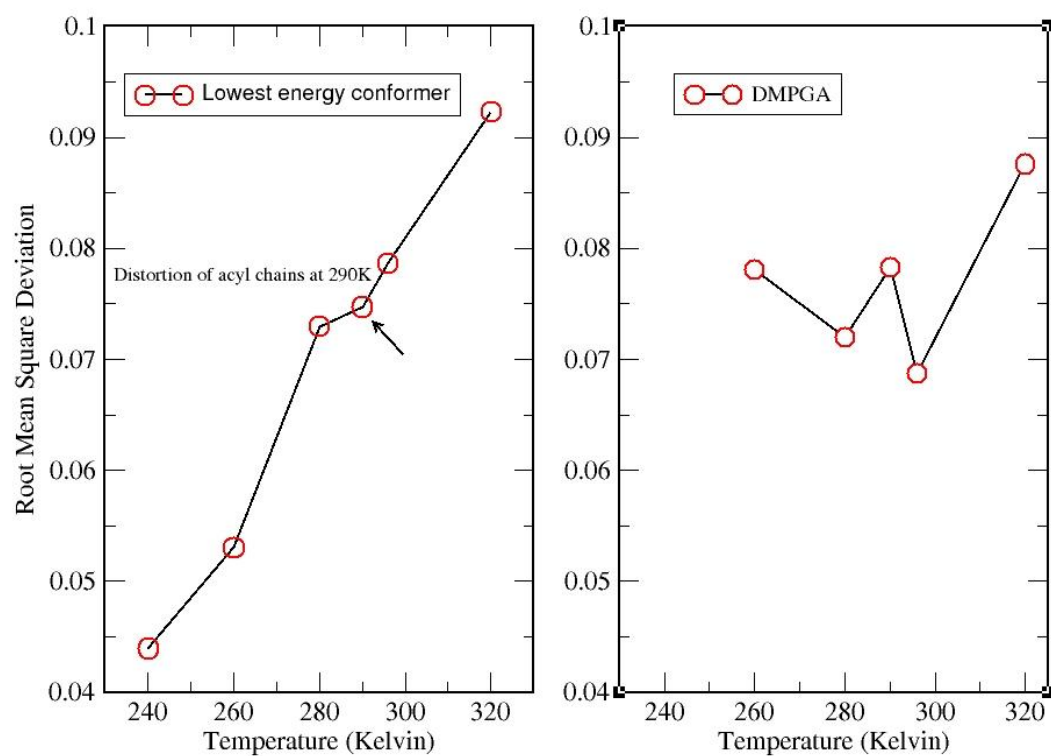


Figure 7.3 Temperature versus Δ RMS value of two different conformers of DMPG.

We have observed the different distortion behaviour for two different conformers of DMPG which opens up the gate of further research on this particular area of molecular melting.

7.4. Conclusion and Future Scope

The dynamical behaviour of two different conformers of DMPG, studied with BOMD and DFT-D methods, reveals several substantial differences from that of DMPC [29]. Such a conformational dependent behaviour of distortion was not observed in the dynamics of DMPC. In addition to this while comparing with DMPC molecular dynamics the DMPG conformers Δ RMS graph as a function of temperature shows different behaviour. The reason for the same is different conformation and hence different interaction towards the counter ion which makes their melting behaviour different. These results lead to the conclusion that the substantially different dynamical behaviour observed experimentally for the DMPG and DMPC bilayers originates in the different intra molecular dynamical behaviour of the different head group orientation of the conformers of lipid molecules. Moreover, they allow one to propose that BOMD/DFT studies of complex molecule can help in the understanding of some dynamical properties of their ensembles.

The peculiar behaviour of two different conformers of DMPG, while distorting at higher temperature, opens up the way to understand the intra molecular interaction involved in biomolecules. Therefore in addition to classical dynamics quantum based molecular dynamics also answers many hidden questions in biomolecules.

7.5 References

- [1] Petty H R, *Molecular biology of membranes: structure and function*, Plenum, New York (1993).
- [2] Silver B L, *The physical chemistry of membranes: an introduction to the structure and dynamics of biological membrane* Solomon Press, Jamaica, (1985) NY.
- [3] Lehninger A L, Nelson D L, Cox M M, *Principles of Biochemistry*, Worth Publishers, (1993) New York.
- [4] McFarland B G, Mc Connell H M, Proc Natl Acad Sci U.S.A. (1971) 68.
- [5] Kusumi, A., Subczynski, W.K., Pasenkiewicz-Gierula, M., Hyde, J.S. & Merkle, H. Biochim. Biophys. Acta 854,(1986) 307-317
- [6] Koynova R, Caffrey M, BBA Rev Biomembranes 1376 (1998) 91–145.
- [7] Thürk M, Porschke D, Biochim Biophys Acta 26;1067(2) (1991) 153-8
- [8] Ruthven N. A. H. Lewis, Nanette Mak, Ronald N. McElhaney Biochemistry 26 (1987) 6118
- [9] Ebel H, Grabitz P, Heimbourg T, J Phys Chem B 105 (2001) 7353–7360.
- [10] Heerklotz H, Seelig J, Biophys J 82 (2002) 1445–1452.
- [11] Heerklotz H, Biophys J 83 (2002) 2693–2701.
- [12] Kharakoz D P, Panchelyuga M S, Tiktopulo E I, Shlyapnikova E A, Chem Phys Lipids 150 (2007) 217–228.
- [13] Stouch T R, Mol Simul 10 (1993) 335–362.
- [14] Ilkka S S, Kari K E, Jorma A V, Paavo K J, Kinnunen Biochim Biophys Acta 982 (1989) 205-215,
- [15] Fernandez R M, Riske K A, Amaral L Q, Itri R, Lamy M T, Biochem Et Biophys Acta 1778 (2007) 907-916.
- [16] Riske K A, Amaral L Q, Döbereiner H-G, Lamy M T, Biophys Journal, 86 (2004) 3722-3733.
- [17] Tyäuble H, Teubner M, Woolley P, Eibl H Biophys Chem 4 (1976) 319-342.
- [18] Karin A R, Roberto M F, Otaciro R N, Barney L B, M. Teresa Lamy-Freund Chem. and Phys. of Lipids 124 (2003) 69-80.
- [19] Karin A R, Mário J P, Wayne F R, M.Teresa Lamy-Freund Chem and Phys of Lipids 89 (1997) 31-44.

- [20] Van Dijck P W M, Ververgaert P H J Th, Verkleij A J, Van Deenen L L M, De Gier J, *J Biochim Biophys Acta* 406 (1975) 465–478
- [21] Earl J. F, Peter G. B, *Biochemistry* 17 (1978) 2400– 2405.
- [22] Pandit S A, Berkowitz M L, *Biophys J* 82 (2002) 1818–1827.
- [23] Bloom T, *J Biol* 2 (2003) 1–5.
- [24] Böckmann R A, Hac A, Heimburg T, Grubmüller H, *Biophys J*, 85 (2003) 1647–1655
- [25] Pedersen U R, Leidy C, Westh P, Peters G H, *BBA* 1758(5) (2006) 573–582.
- [26] Goursot A, Mineva T, Krishnamurty S, Salahub D R, *J Can Chem* 87 (2009) 1261.
- [27] Krishnamurty S, Stefanov M, Mineva T, B_egu S, Devoisselle J M, Goursot A, Zhu R, Salahub D R, *J Phys Chem B* 112 (2008) 13433.
- [28] Mishra D, Pal Sourav, Krishnamurty S, *Mol Simul* 37 (11) (2011) 953–963
- [29] Krishnamurty S, Stefanov M, Mineva T, B_gu S, Devoisselle J M, Goursot A, Zhu R, Salahub D R, *Chem Phys Chem* 9 (2008) 2321 – 2324.
- [30] Mineva T, Krishnamurty S, Salahub D R, Goursot A, 113(5) (2013) 631–636.
- [31] Pascher I, Sundell S, Harlos K, Eibl H, *Biochim Biophys Acta* 896 (1987) 77–88.
- [32] Koster A M, Calaminici P, Casida M E, Flores-Moreno R, Geudtner G, Goursot A, Heine T, Ipatov A, Janetzko F, Martin del Campo J, Patchkovskii S, Reveles J U, Salahub D R, Vela A, The deMon Developers; Cinvestav: Mexico, (2006)
- [33] Zhang Y, Yang W, *Phys Rev Lett* 80 (1998) 890.
- [34] Lee C, Yang W, Parr R G, *Phys Rev B: Condens Mater Phys* 37 (1988) 785.
- [35] Goursot A, Mineva T, Kevorkyants R, Talbi D, *J Chem Theory Comput* 3 (2007) 755.
- [36] Wu Q, Yang W, *J Chem Phys* 116 (2002) 515.
- [37] Godbout N, Salahub D R, Andzelm J, Wimmer E, *Can J Chem* 70 (1992) 560.

- [38] Calaminici P, Janetzko F, Koster A M, Mejia-Olvera R, Zuniga-Gutierrez B, J Chem Phys 126 (2007) 044108.
- [39] Koster A M, Flores-Moreno R, Reveles J U, J Chem Phys 121 (2004) 681.
- [40] Berry R S, Beck T L, Davis H L, Jellinek J, Adv Chem Phys 70B (1988) 75.
- [41] Frantz D D, J Chem Phys 102 (1995) 3747.
- [42] Bartell L S, Dulles F J, J Phys Chem 99 (1995) 17107.
- [43] Wales D J, Ohmine I, J Chem Phys 98 (1993) 7245.